Magnetism in solid ^{3}He: Confrontation between theory and experiment

M. C. Cross* and Daniel S. Fisher

AT&T Bell Laboratories, Murray Hill, New Jersey 07974

A summary of the current understanding of nuclear magnetic ordering in solid ^{3}He is presented. The main emphasis is a critical review of what is known from the experiments along with a critique of various theoretical models. Unanswered questions are raised about both the macroscopic phenomena and the microscopic origins of the magnetism. Several experiments are proposed which should help advance our understanding of the magnetic behavior of solid ^{3}He.

CONTENTS

I. INTRODUCTION

Five years ago, experimental technique finally became powerful enough to allow direct probes of the magnetically ordered phases of solid ^{3}He. In particular, nuclear magnetic resonance experiments incontrovertibly showed the low-field phase to have a structure with only tetragonal symmetry (Osheroff, Cross, and Fisher, 1980—hereafter OCF), a result not evident in previous experiments (Dundon and Goodkind, 1974; Halperin *et al.*, 1974,1978; Kummer *et al.*, 1975; Prewitt and Goodkind, 1977). Quantitative measurements on the ordered phase now yield a whole new set of constraints on models which might describe the system. For the first time there is the immediate prospect of sufficient experimental data to severely test any proposed model for which quantitatively reliable theoretical predictions are made. It is now abundantly clear that solid ^{3}He provides an exceedingly complex magnetic system—a surprising fact, considering the simple nature of ^{3}He itself. It is therefore particularly important in this system to compare theoretical work with experimental results. The purpose of this paper is to review critically the recent work in this area. In addition, we hope to propose fruitful directions for further experiment to investigate specific features of solid ^{3}He that are not yet understood.

The nuclear spins of solid ^{3}He provide a fascinating and challenging magnetic system. On the one hand, there is every expectation that the magnetic properties may be understood from first principles. On the other hand, we have direct experimental evidence for very rich magnetic behavior. The optimistic outlook for a microscopic understanding largely derives from the dramatic separation of energy scales that exists in the system.

First there are the vast differences between the basic interaction energies: the excitation energy of the closed-shell electronic structure is of order 10^5 K; the residual van der Waals atomic interaction potential is characterized by an energy of order 10 K; and the only direct interaction between the nuclear spins, the magnetic dipole interaction, is of order 10^{-7} K. Thus it is an *extremely* good approximation to treat the solid as a collection of balls with an interaction potential known from atomic collision experiments and with a residual degree of freedom $S^z=\pm\frac{1}{2}$ of the nuclear spin. As far as the spatial structure of the system is concerned, the spin acts only as a label distinguishing otherwise indistinguishable particles:[1] thus a collection of "red" and "blue" particles would act in an almost identical way.

*Present address: Department of Physics, California Institute of Technology, Pasadena, CA 91125.

[1]It is a remarkable consequence of the broken symmetry that in the ordered phases the coherent sum of the tiny dipole energies leads to sufficiently large energies to determine the overall orientation of the ordered spins even at 1 mK. In the ordered phases the spin nature of the degree of freedom plays an important role in determining the orientation of the state, but not its energy at the level of mK/atom.

There is a second, more approximate separation of energy scales that appears in considering the exchange interaction between the nuclear spins. The characteristic energy E_0 of the formation of the solid lattice is, as we have seen, of order 10 K. The highly *quantum* nature of solid ^{3}He is reflected in the fact that both the potential energy and the zero-point kinetic energy of the atomic motion are roughly of this same size. Thus the characteristic zone-boundary phonon frequency $\hbar\omega_0$ is also set by the scale E_0. The spin-exchange interaction results from the empirically rare event of a cluster of atoms changing lattice sites by some mechanism. Experimentally this energy J is of order 1 mK.[2] Thus one finds a second, empirical separation of scales

$$J:\omega_0 \equiv 10^{-3}:1 \ . \tag{1.1}$$

This ratio is crucial in allowing the discussion of solid ^{3}He to be separated into two parts: first a solution of the lattice problem, neglecting statistics, and then the use of an effective spin Hamiltonian to yield the small spin splitting of otherwise degenerate states and hence the low-temperature ($\lesssim$100 mK) thermodynamic behavior. As we shall see, due to the strong dependence of exchange rates on lattice distortions, this separation may not be as well justified as suggested by this small ratio: if agreement between a simple spin Hamiltonian and experiment is not ultimately forthcoming, this assumed separation may be brought into question. We should also remark that the empirical separation Eq. (1.1) is not well understood from a theoretical point of view, since solid ^{3}He is indeed very highly quantum. This is quantified by the de Boer parameter $\Lambda=\hbar/\sigma(m\varepsilon^{1/2})$, with σ the characteristic length, ε the strength of the interaction potential, and m the atomic mass. For solid ^{3}He at melting pressure $\Lambda=0.5$. It is not then clear what small number yields the approximate separation of energy scales, although presumably the hard-core nature of the potential is important. Indeed, we believe that understanding this point is probably the crux of theoretical progress in this subject.

Understanding solid ^{3}He should yield considerable insights into other physical systems. Atomic exchange in the sister solid ^{4}He is presumably controlled by the same physics, but is much harder to investigate experimentally since the nuclei carry no spin as a label. If infinitely large exchange loops were important in the solid, one would presumably have an example of a superfluid solid. Understanding the *multiple* exchange processes in solid ^{3}He may yield some insights into this question. Another system in which quantum exchange effects might lead to interesting collective behavior, including magnetic phases, is a two-dimensional Wigner crystal of electrons at densities just below its quantum melting point. This may soon be accessible experimentally. The exchange might be more important in this system than in solid ^{3}He because of the absence of steric impedance to motion. At the other extreme, solid ^{3}He may provide an example of the tunneling of local atomic clusters with geometrical constraints, such as also occurs in metallic glasses and solid hydrogen and deuterium. The ^{3}He problem may be easier to investigate experimentally, since the tunneling can be measured via the resulting collective effects. Solid ^{3}He also provides an example of a highly quantum three-dimensional magnet. Most three-dimensional localized magnetic systems, even if spin $\frac{1}{2}$, show only small quantum effects that are well accounted for by spin-wave perturbation theory (Anderson, 1952; Kubo, 1952). There is good evidence that the quantum effects in the effective spin Hamiltonian of solid ^{3}He are large, for example, amounting to 50—100% corrections to the ground-state energy (Iwahashi and Masuda, 1981; Usagawa, 1982; Roger *et al.*, 1983). It is one of the challenges on the theoretical side to find methods to treat such a highly quantum spin system. One intriguing possibility is that the ground state may have a structure that has no classical analog, so that the usual Néel description of the ground state would not even be a qualitative guide to the structure. (This is discussed in Appendix B.)

Thus solid ^{3}He provides a nontrivial, highly quantum localized spin system that potentially may be understood from first principles starting from the atomic Schrödinger equation. In this paper we will discuss how close we are to reaching some understanding of the magnetic properties of this system.

Although we do not aim for this review to be a pedagogical first introduction, we have attempted to make it self-contained, and have at least schematically developed the main ideas from their inception. More details can be found in earlier review articles referenced at appropriate points. A number of reviews already exist on the magnetic properties of solid ^{3}He. We have found an article by Guyer (1974) to be a nice introduction to the basic phenomenology of the system, and a second one (Guyer, 1978) accounts for pre-1979 experimental work and its failure to agree with contemporary theories. McMahan (1972) discusses the early variational calculations of exchange rates. The revolutionary developments in the past five years have been experimental work on the low-temperature phases and the theoretical realization that previous exchange calculations were probably totally unreliable, together with the development of descriptions based on empirical multiple exchange Hamiltonians. This recent work has been compiled in a review by Roger *et al.* (1983). An interesting review of early work on exchange and on subjects peripheral to our main thrust, such as phonon dynamics, is that of Varma and Werthamer (1976). A provocative view of the quantum solid problem is given by Anderson (1984, pp. 130—158): such a picture has not had immediate impact on most of the topics we discuss, but may be important in future developments.

The purpose of the present paper falls into three parts. First, we believe that a careful discussion is needed of ex-

[2]We shall use the symbol J to denote the order of magnitude of the rate of exchange of ^{3}He atoms; its use does not necessarily imply two-particle exchange.

actly what is learned from various experiments, and what constraints are put on possible theoretical models by the data. For example, the reservations noted in the original paper (OCF) on the identification of the structure of the ground state from the nuclear magnetic resonance experiments are not often mentioned in the subsequent literature; we feel it is important to point out first what is unambiguously deduced from this experiment, and then what is guessed. Second, we believe that further progress requires a more critical review of the successes and failures of various theories than given in previous articles, particularly the derivation of and consequences of multiple exchange Hamiltonians. Finally, we would like to present suggestions for new experiments to probe some of the outstanding questions.

It is of course too easy to present a negative view of progress—no subject is completely uncontroversial until the physics it displays is completely understood, and it is no longer interesting. However, there has been a tendency in the literature on solid ^{3}He to focus on qualitative successes of theories and to ignore problems. Microscopic theories are sometimes "adjusted" to give answers consistent with experiment, so that the applicability of the original model is not tested. Thus, for example, both high-density and low-density descriptions of the exchange process, relying on quite different physics, apparently give good agreement with experiment, and one is left with no idea which physics is operating. There is therefore a need, in our opinion, for a more critical account of the work. In fact, we will raise more questions than we answer. Perhaps it will turn out that our point of view is too cautious—and it is certainly partly a response to previous articles in the subject that we believe err in the opposite direction. The multiple exchange models (Roger *et al.*, 1983) may in the long run turn out to account for all of the data, once their consequences are calculated more accurately. This hypothesis does, however, need further experimental tests and microscopic justification. We hope that our critical review will help to stimulate this process.

The rich magnetic behavior of solid ^{3}He that is the focus of our attention is dramatically displayed by the magnetic field (H) —temperature (T) phase diagram, Fig. 1(a) (Osheroff, 1982). The first observation of a magnetic phase transition in solid ^{3}He was made by measuring the melting curve and showed a strongly first-order transition with a large entropy change ΔS, of almost $0.5 k_B \ln 2$ per spin at a temperature T_c of 1.0 mK (Halperin *et al.*, 1974). This temperature was somewhat lower than would be expected from the high-temperature data then available. Even now, susceptibility measurements (see Sec. II.B) indicate that the Curie-Weiss constant θ is about -2 mK, or larger, which would suggest a transition at above 1.5 mK for a nearest-neighbor bcc spin-$\frac{1}{2}$ Heisenberg antiferromagnet. In addition to the latent heat, the entropy measurements showed an anomalously small specific heat for temperatures between 1 and 2 mK (Halperin *et al.*, 1974). Thus the paramagnetic phase appeared to be stable to a surprisingly low temperature, perhaps indicating

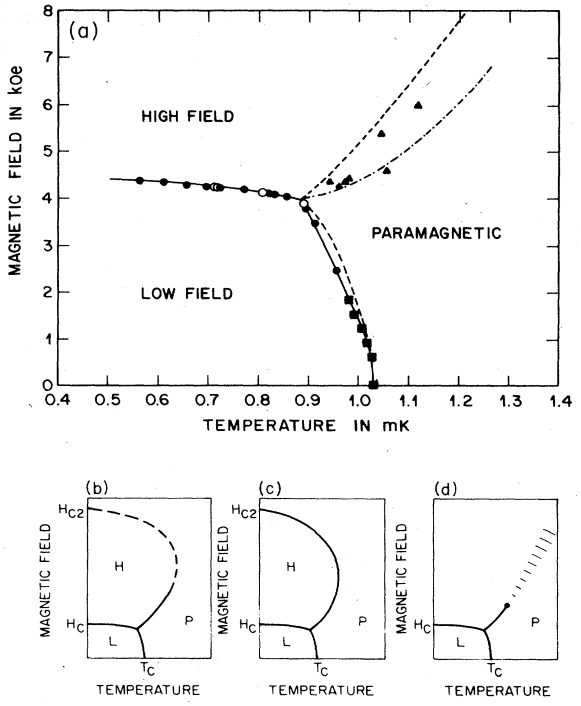

FIG. 1. (a) Magnetic phase diagram of solid ^{3}He [from Osheroff (1982)]. Solid lines are a fit to the data of Osheroff (1982); dashed lines are from Adams *et al.* (1980), and the dotted line is the phase boundary of Prewitt and Goodkind (1980) translated downward in temperature by 0.09 mK. The squares and circles are data for which the NMR frequencies in the low-field ordered phase were used as a thermometer, while for the triangles, Pt NMR thermometry was used. The low-field to paramagnetic and low-field to high-field transitions are definitely first order, but there is some uncertainty concerning the order of the high-field to paramagnetic transition. (b), (c), and (d) Schematics of possible phase diagrams showing the low-field phase (L), paramagnetic phase (P), and putative high-field phase (H), which exists in (b) and (c) up to an upper critical field H_{c2}. The solid lines indicate first-order transitions and the dashed lines second-order transitions. In (d), the high-field first-order line ends in a critical point and there is no distinct high-field phase. In this case, a Schottky-type specific heat anomaly will occur in the shaded region which might be confused experimentally with a smeared-out transition.

competing interactions. A sharp kink in the transition temperature as a function of field was observed at 4 kG by Kummer *et al.* (1975), suggesting a different ordered phase at high fields. The unusual nature of the transition was finally confirmed in 1980 by the NMR data of Adams *et al.* (1980) and OCF; the latter showed that in small magnetic fields the system orders into an unexpected phase: an antiferromagnet with tetragonal symmetry.

The antiferromagnetic phase occupies an anomalously small part of the phase diagram. Thus at a very low field H_c of 4.4 kG (corresponding to $\mu H \sim 0.3$ mK with $\mu = \gamma\hbar/2$ the magnetic moment) there is a first-order transition (Prewitt and Goodkind, 1980) to a phase with no NMR shifts (Osheroff, 1982), implying cubic symme-

try. At the transition the magnetization jumps to about 60% of its saturation value, showing strong ferromagnetic tendencies in the system, and then has only a weak field dependence extrapolating to saturation at much higher fields of order 150—200 kG ($\mu H \sim 10$ mK) (Prewitt and Goodkind, 1977,1980). The lower critical field H_c is almost independent of temperature (Osheroff, 1982). Similarly the low-field dependence of the paramagnet to tetragonal phase boundary given by

$$\frac{d^2T_c}{dH^2} = \frac{\Delta\chi}{\Delta S} \tag{1.2}$$

is very small on the expected scale of 1 mK/(14 kG)^2, and seems to have an anomalous behavior with increasing field (Osheroff, 1982). Thus there is considerable evidence for more than one energy scale.

The part of the currently accessible phase diagram about which there is most uncertainty is the high-field regime. Several authors (Prewitt and Goodkind, 1980; Adams *et al.*, 1980) have reported evidence for a *second*-order line between the high-field phase and the paramagnetic phase. The interpretation of these experiments is considerably clouded, however, by questions of thermal equilibrium. Indeed, Osheroff's (1982) data indicate a triple point with a *first*-order boundary intersecting the boundaries to the tetragonal antiferromagnetic phase. This transition is presumably smeared out in earlier experiments because of equilibration difficulties. Recent data of Uhlig *et al.* (1984) in sinter show a very narrow but finite width to the transition at 4.5 kG; this is probably due to the effects of the confined geometry. The data on the high-field state therefore remains consistent with three hypotheses at this stage: (i) a first-order line becoming second order at a tricritical point and then extending up to high temperatures before, presumably, bending back around to a large critical field H_{c2} at zero temperature; (ii) a first-order line encircling the high field phase; or (iii) a first-order line ending at a critical point with no transition at higher fields, but instead with a Schottky-like entropy anomaly at high fields. These possible phase diagrams are illustrated schematically in Figs. 1(b), 1(c), and 1(d), respectively. If (i) turns out to be correct, and also almost certainly if (ii) is correct instead, then the high-field phase is some kind of canted antiferromagnet with cubic symmetry as shown by the NMR. If (iii) is correct, on the other hand, the high-field phase is just paramagnetic with no spontaneously broken symmetry.

The thermodynamic data are clearly inconsistent with the simple model of a nearest-neighbor Heisenberg Hamiltonian resulting from nearest-neighbor exchange. Much of the behavior, in particular the complicated phase diagram with apparently several different energy scales, and the surprising nature of the low-field ordered phase, suggest that the magnetic properties in solid ^{3}He are governed by a rather delicate balance between several competing magnetic interactions. In apparent contradiction to this is the weak effect of pressure found experimentally. In experiments to date the effect of pressure appears to be merely to shift *all* the energy scales down by a uniform factor, leaving the thermodynamic behavior unchanged up to a common rescaling of temperature and field. This is in striking contrast to the reasonable expectation that for competing interactions even small differences in the pressure dependence of magnetic interaction strengths would have large effects on the phase diagram. The effect of pressure on H_c would thus provide a stringent test. We will return to this puzzle later in the paper.

Since very rich magnetic behavior is displayed by solid ^{3}He, the effective magnetic Hamiltonian will be much harder to understand than initially anticipated. However, this also means that a careful comparison of theory and experiment will yield a great deal more information on the truly microscopic description of the system. The spin dynamics of a nearest-neighbor Heisenberg system are characterized by a single exchange, J, and its volume dependence; this is the only information learned from the magnetic properties that may restrict possible models of the *microscopic* dynamics. On the other hand, it is not even known how many parameters are needed to account for all the observed properties of magnetic solid ^{3}He. Clearly the dividends of understanding the behavior are correspondingly larger.

II. EXPERIMENTAL CONSTRAINTS

It is important to analyze what experiments can yield *model-independent* constraints on the spin Hamiltonian of solid ^{3}He. In principle, given any candidate Hamiltonian involving a few adjustable parameters, experimentally relevant quantities can be calculated and compared with the data. In this section, however, we will discuss experiments which can be analyzed or usefully parametrized in a way that is independent of the specific Hamiltonian. In this way definite constraints are placed on possible models. The experiments we will discuss either yield qualitative information, such as the *symmetry* of the ground state, or quantitative information that can be rigorously and usefully parametrized in a model-independent way, such as high-temperature data fit to a $1/T$ expansion. Such quantitative information is most useful if the parameters are easy to calculate with sufficient accuracy from a proposed Hamiltonian. We will discuss this latter question in relation to using data at *low* temperatures in the *ordered* phases to put quantitative constraints on models.

A. Symmetry of the antiferromagnetic phase

Nuclear magnetic resonance (NMR) experiments provide a direct probe of the rotational symmetries of the spin structure. Until neutron scattering experiments are done to probe the actual spatial arrangement of the spins, NMR must suffice to tell us as much as possible about the symmetry of the ground state.

1. Equations of motion

In the absence of any knowledge of the structure of the ground state the common method (Kittel, 1971) of analyzing antiferromagnetic resonance by writing n dynamical equations for n "sublattice" spin variables fails. In any case, this method is not rigorous and gives only approximate answers. A better approach is to use the weakness of the anisotropy energy to write down quasihydrodynamic equations for the variables relevant in the low-frequency dynamics of a NMR experiment.

A NMR experiment probes the resonant frequency of the precession of the total magnetization of the sample $\mathbf{M}=\gamma\mathbf{S}$ in a magnetic field $\mathbf{H}$. This is simply the Larmor precession perturbed by the weak magnetic dipolar anisotropy: the much larger spin exchange interaction commutes with the total spin operator $\mathbf{S}$ and so cannot lead to *any* frequency shifts. Thus we will arrive at a *model-independent* analysis of these experiments. In addition to the quasiconserved spin variable, the variables corresponding to the spontaneously broken spin rotational symmetry of the antiferromagnetic ordering also relax on long time scales and must be included in the equations for the slow dynamics. For a general antiferromagnet without large external fields or anisotropies there are three such variables, corresponding to the three broken spin rotational symmetries. To investigate the dynamics it is convenient to use the variables $\delta\boldsymbol{\eta}=(\delta\eta_x,\delta\eta_y,\delta\eta_z)$ describing infinitesimal rotations of all the spins about three orthogonal axes $(\hat{x},\hat{y},\hat{z})$. The coupled equations of motion are then

$$\begin{aligned}\dot{\mathbf{S}}&=\gamma\mathbf{S}\times\mathbf{H}-\partial E_D/\partial\boldsymbol{\eta}\ ,\\ \dot{\boldsymbol{\eta}}&=\gamma\mathbf{H}-\gamma^2\overleftrightarrow{\chi}^{-1}\mathbf{S}\ ,\end{aligned}\tag{2.1}$$

where the first equation is the usual torque equation,[3] and the second is a kinematic relation between angular velocity ($\dot{\boldsymbol{\eta}}$) and angular momentum.

It is important to point out that these equations (2.1) are model independent and valid in a well-defined approximation. They are best derived along the lines of Halperin and Saslow (1977), although they are also familiar in the literature of other systems with broken spin rotational symmetry (Graham, and Pleiner, 1976; Brinkman and Cross, 1978). The basic approximation used is that the system is always near to the equilibrium defined by $\mathbf{S}$ and the orientation of the broken symmetry. This requires that all the microscopic coordinates are relaxed essentially to their local equilibrium values, and that the motion of $\mathbf{S}$ and $\delta\boldsymbol{\eta}$ indeed relaxes on a much longer time scale. Typical microscopic relaxation times are expected to be of order $\hbar/J$ with J a characteristic exchange rate. At very low temperatures thermal magnons become scarce, and their relaxation times become longer as some power of the temperature. On the other hand, their importance in determining reactive responses correspondingly decreases and it is likely that the criterion $\omega\ll J$, with ω a characteristic frequency of the dynamics, remains useful down to arbitrarily low temperatures. More concretely, we would expect additional dissipative terms in Eq. (2.1) of order $\tau_m\Omega_0^2$ and $\tau_m(\gamma H)^2$, with $\Omega_0^2=\gamma^2E_D/\chi$ and $\tau_m^{-1}\sim J$ a microscopic relaxation rate. The inclusion of the term proportional to H^2 accounts for the fact that in an applied field H (or effective field $H-M/\chi$ from a spontaneous magnetization M) the transverse symmetry is externally broken, so that the transverse rotation coordinates relax more rapidly to minimize the susceptibility anisotropy. Equations (2.1) result when these dissipative terms are negligible.

Without the dissipation terms, which both *a priori* (since Ω_0/J is of order 10^{-2} to 10^{-3} in ^{3}He) and experimentally are small, the dynamical equations are very simple, and can indeed be understood using Poisson brackets for the variables $\mathbf{S}$, $\delta\boldsymbol{\eta}$:

$$\begin{aligned}\{S_i,S_j\}&=\varepsilon_{ijk}S_k\ ,\\ \{S_i,\delta\eta_j\}&=\delta_{ij}\ ,\\ \{\delta\eta_i,\delta\eta_j\}&=0\ ,\end{aligned}\tag{2.2}$$

and the equation of motion $dO/dt=\{O,\mathscr{H}\}$ together with the effective Hamiltonian

$$\mathscr{H}=E_D(\boldsymbol{\eta})+\tfrac{1}{2}\mathbf{S}\overleftrightarrow{\chi}^{-1}\mathbf{S}-\mathbf{S}\cdot\mathbf{H}\ .\tag{2.3}$$

The NMR response is given by solving Eqs. (2.1) for small oscillations about the value of $\mathbf{S}$ and the orientation of the sublattice structure which minimize the total energy $\mathscr{H}$. The equations can also be used to study large-angle tipping experiments, providing dissipation may be neglected (Brinkman and Smith, 1975; Hu and Ham, 1981; Fishman, 1982).

2. Analysis of the NMR spectrum

The equations of motion for a general antiferromagnet, Eqs. (2.1), are six equations for the variables $\mathbf{S}$ and $\delta\boldsymbol{\eta}$. These in general lead to three pairs of modes for each field, with frequencies $\omega=\pm\omega_i$ for $i=1,2,3$. Typically there will be a complicated dependence on the field, since the equilibrium orientation given by minimizing the total energy will change with increasing field as the magnetic energy begins to dominate the dipole energy. This may be seen by the following analysis of the low- and high-field limits.

At zero field the triad of axes defining the orientation of the spin ordering orients to minimize the dipole energy. The squares of the resonant frequencies are then given by the eigenvalues of $\overleftrightarrow{\tau}\overleftrightarrow{\chi}^{-1}$, where $\overleftrightarrow{\tau}$ is the real symmetric matrix defined by

$$\frac{\partial E_D}{\partial\eta_i}=\tau_{ij}\delta\eta_j\tag{2.4}$$

[3] The derivative $\partial E_D/\partial\boldsymbol{\eta}$ must be interpreted at constant entropy if E_D is the internal energy, but at constant temperature if E_D is the free energy.

for small rotations $\delta\eta$ from the equilibrium orientation minimizing E_D.

On the other hand, at high magnetic fields (along the z direction) the modes are

$$\omega^2=H^2 \ [S_x,S_y] , \tag{2.5a}$$

$$\omega^2=H^2(1-\chi_{zz}/\chi_{yy})(1-\chi_{zz}/\chi_{xx}) \ [\eta_x,\eta_y] , \tag{2.5b}$$

$$\omega^2=0 \ [S_z,\eta_z] , \tag{2.5c}$$

where the quantities in brackets denote the variables involved, and χ_{zz} is the least principal value of the susceptibility tensor. Note that here the susceptibility tensor determines the triad orientation. The dipole energy may now be included by perturbation theory. The third mode of Eqs. (2.1) and (2.5) gains a finite frequency

$$\omega^2=\tau_{zz}\chi_{zz}^{-1} , \tag{2.6}$$

the longitudinal resonant frequency, and the first two modes become mixed, with frequencies perturbed by $O(\tau^2/H)$. Notice that because of the reorientation Eq. (2.6) is in general not equal to any of the frequencies at zero field: the matrix $\overleftrightarrow{\tau}$ is defined with respect to the equilibrium orientation, which now minimizes the magnetic energy. Typically there will be a complicated intermediate field dependence interpolating between the low- and high-field limits that can be trivially calculated numerically for a given $\overleftrightarrow{\chi}$ and E_D.

This general picture should be contrasted with the experimental NMR spectrum for solid ^{3}He (Fig. 2). These spectra are fully explained by the assumptions of two modes per crystal domain,[4] rather than the general three, and have a very simple field dependence. (We follow here the analysis of OCF.) This suggests that, at least for the NMR response, the antiferromagnetic spin arrangement may be characterized by a unique axis $\hat{d}$ (i.e., by two variables rather than the three needed for a general phase). In particular, the dipole energy and susceptibility tensor must show this uniaxial symmetry, i.e.,

$$E_D=-\tfrac{1}{2}\hat{\mathbf{d}}\cdot\overleftrightarrow{\mathbf{A}}\cdot\hat{\mathbf{d}} , \tag{2.7}$$

$$\chi=\chi_0(\overleftrightarrow{1}+\delta\hat{\mathbf{d}}\hat{\mathbf{d}}) , \tag{2.8}$$

with $\overleftrightarrow{\mathbf{A}}$ a second rank tensor reflecting the symmetry of the dipole energy under rotations of the lattice, and δ a parameter giving the susceptibility anisotropy. The form Eq. (2.7) follows, since the dipole energy, evaluated without perturbations due to the dipole energy itself, consists of the contraction of a *second*-rank tensor in spin space reflecting the spin rotational symmetries of the antiferromagnetic state, with a *second*-rank tensor in real space. Note that had we allowed dipole energy-induced perturbations in the state, a more complicated form would have resulted.

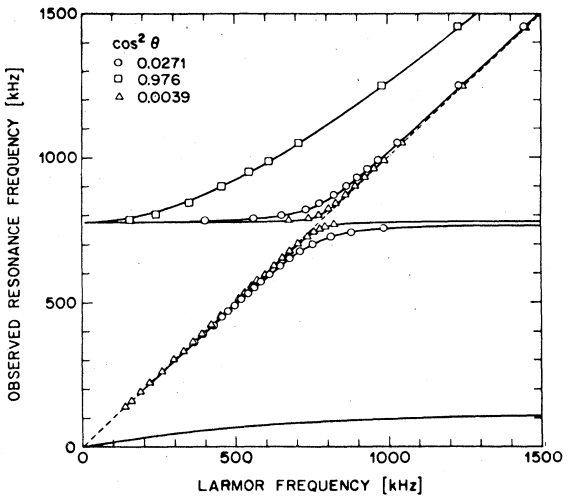

FIG. 2. NMR spectra from Osheroff *et al.* (1980) on a single crystal of solid ^{3}He containing three domains. The pairs of modes for each domain are denoted by the same symbols. The solid lines are theoretical fits to Eq. (2.13), with $\Omega_0/2\pi=777.7$ kHz and the values of $\cos^2\theta$ as shown. The dashed line is the Larmor frequency, γH.

It should of course be admitted that the assumption of a symmetry based on the observation of fewer modes than generally possible should not be made lightly: it is certainly conceivable that an additional mode might be missed or be in a frequency range not scanned. However, in the experiments analyzed here, the absence of a third mode for the many different crystal orientations studied and a wide range of magnetic fields, coupled with the very simple field dependence of the observed modes, seems sufficient evidence to justify this assumption. Again, the final justification must be the excellent fit eventually obtained based on this assumption. It should also be emphasized that uniaxiality of the second rank tensors in Eqs. (2.7) and (2.8) does not require that the state itself be uniaxial: as we will see, lesser symmetries may be sufficient to guarantee these results, although higher rank tensor properties may then not be uniaxial.

Since the variable $\hat{\mathbf{d}}$ defines the orientation of the spin ordering globally, it is now convenient to rewrite the dynamical equations (2.1) in this variable. Using the expression for an infinitesimal change $\delta\hat{\mathbf{d}}=\hat{\mathbf{d}}\times\delta\eta$ gives

$$\begin{aligned}\dot{\mathbf{S}}&=\gamma\mathbf{S}\times\mathbf{H}-\hat{\mathbf{d}}\times\overleftrightarrow{\mathbf{A}}\cdot\hat{\mathbf{d}} ,\\ \dot{\hat{\mathbf{d}}}&=\hat{\mathbf{d}}\times(\gamma\mathbf{H}-\gamma^2\chi_0^{-1}\mathbf{S}) .\end{aligned} \tag{2.9}$$

The susceptibility anisotropy δ does not appear directly in the equations of motion, but will be involved in determining the equilibrium configuration. These equations in

[4]As the reader can see, typically three modes were seen in the field scans for each single crystal. These were associated with three domains of each single crystal. The original evidence suggesting two modes for each of three domains was similarities in strengths and shapes of pairs of peaks (associated with each symbol in Fig. 2). Confirming evidence is the final excellent fit to the data based on this assumption.

general have two pairs of finite frequency modes $\omega=\pm\omega_{1,2}$ consistent with experiment, together with a single mode at zero frequency corresponding to the identity

$$\frac{d}{dt}(\hat{\mathbf{d}}\cdot\mathbf{S})=0\ . \tag{2.10}$$

This last mode is not seen in NMR. It becomes the spin-diffusion mode at nonzero wavevectors.

Analysis of the high-field dependence immediately shows that $\delta<0$: i.e., $\hat{\mathbf{d}}$ tends to lie perpendicular to an applied field. In the opposite case the high-field asymptotes for ω are γH and $\delta\gamma H$ corresponding to Eqs. (2.5a) and (2.5b), the second result conflicting with experiment. For $\delta<0$ Eqs. (2.5a) and (2.5c) apply, leading to one mode asymptotically flat and another approaching the Larmor frequency, as observed.

The other information learned from the NMR is the form of the tensor $\overleftrightarrow{A}$. In general, $\overleftrightarrow{A}$ is characterized by its principal values $\lambda_1\geq\lambda_2\geq\lambda_3$ with respect to three orthogonal principal axes. The NMR spectrum then depends just on differences, e.g., $\lambda_1-\lambda_2$, $\lambda_1-\lambda_3$. A typical spectrum for arbitrarily chosen values is shown in Fig. 3. In particular, the zero-field frequencies are given by

$$\omega_1^2=\gamma^2(\lambda_1-\lambda_2)/\chi_0\ ,$$
$$\omega_2^2=\gamma^2(\lambda_1-\lambda_3)/\chi_0\ . \tag{2.11}$$

The zero frequency observed for the lower mode at zero magnetic field shows that $\overleftrightarrow{A}$ has planar symmetry, i.e., $\lambda_1=\lambda_2$, and that we may then write

$$E_D=\tfrac{1}{2}\lambda(\hat{\boldsymbol{l}}\cdot\hat{\mathbf{d}})^2\ , \tag{2.12}$$

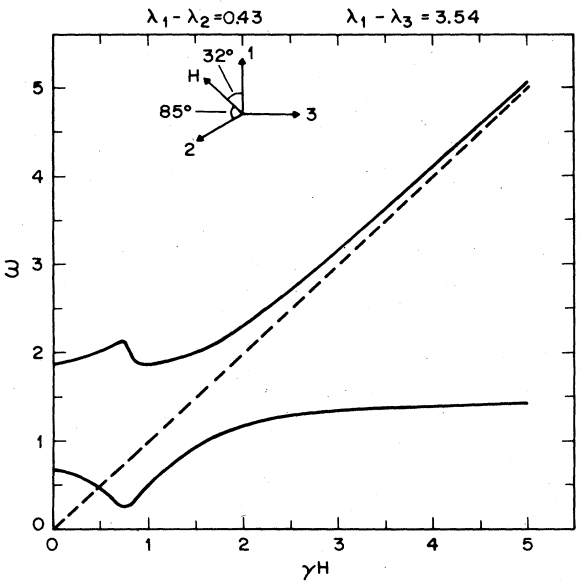

FIG. 3. Typical NMR spectrum for a uniaxial spin structure with nonuniaxial dipole energy with eigenvalues $\lambda_1,\lambda_2,\lambda_3$ related as shown. The inset indicates the direction of the magnetic field, and the dashed line the Larmor frequency. Note the remanent of the spin-flip transition at $\gamma H\approx 0.7$.

with $\lambda=\lambda_1-\lambda_3>0$, and $\hat{\boldsymbol{l}}$ the unique axis normal to the plane of degeneracy for $\hat{\mathbf{d}}$. [Note: $\lambda<0$ would correspond to axial symmetry and two degenerate modes at zero field split linearly by the field. This is the case in liquid ^{3}He A (Brinkman and Cross, 1978).] This result is also suggested by the complete absence of spin-flop effects, such as those evident in Fig. 3 at $\gamma H\approx 0.7$, when the $\hat{\mathbf{d}}$ vector reorients from primarily minimizing E_D to primarily minimizing the magnetic energy. In the case of planar symmetry an orientation of $\hat{\mathbf{d}}$ perpendicular to both $\hat{\boldsymbol{l}}$ and $\mathbf{H}$ minimizes both E_D and the magnetic energy for all values of the field, and no reorientation occurs.

The resonant frequencies from Eqs. (2.9) are

$$\omega^2=\tfrac{1}{2}\{\omega_L^2+\Omega_0^2\pm[(\omega_L^2-\Omega_0^2)^2+4\omega_L^2\Omega_0^2\cos^2\theta]^{1/2}\}\ , \tag{2.13}$$

where $\Omega_0(T)$ is given by

$$\Omega_0^2=\gamma^2\lambda/\chi_0\ , \tag{2.14}$$

with ω_L the Larmor frequency γH and $\cos\theta$ the angle between the magnetic field and the lattice anisotropy axis $\hat{\boldsymbol{l}}$, which must be obtained from a best fit to the data for each pair of modes. In addition, for each run, Ω_0 must be fitted. As can be seen, the resulting agreement is excellent (and Ω_0 is indeed then found to be a function only of temperature and not crystal orientation). A careful analysis of deviations of the low-frequency modes from Eq. (2.13) at small magnetic fields shows that any deviation from the planar symmetry of $\overleftrightarrow{A}$ is characterized by an energy

$$(\lambda_1-\lambda_2)/\lambda<10^{-3}\ . \tag{2.15}$$

For practical purposes this may be taken as evidence of planar symmetry for $\overleftrightarrow{A}$ in the undistorted antiferromagnetic state.

To summarize, the entire evidence learned from NMR is the following:

(i) The uniaxial symmetry of the dipole energy and susceptibility tensors, given by an axis $\hat{\mathbf{d}}$ in spin space.

(ii) A susceptibility anisotropy $\delta<0$.

(iii) The form of the dipole energy Eq. (2.12), implying uniaxial symmetry of $\overleftrightarrow{A}$ in real space, together with a measurement of λ/χ_0 as a function of temperature.

(iv) Some information (via the fitted $\cos\theta$) on the orientation of the domains.

Clearly this evidence is insufficient to determine uniquely a possibly complex microscopic spin arrangement. We can, however, make definite statements on some rotational symmetries this structure must show. These symmetries turn out to be rather unexpected, and lead us to a plausible suggestion for a possible structure.

3. Symmetry requirements on the antiferromagnetic state

The anisotropic part of the dipole energy per unit volume leading to the NMR shifts can be written

$$E_D = -\frac{3}{2}\left\langle \sum_{\mathbf{r}} \frac{r^\alpha r^\beta}{|r|^5} C^{\alpha\beta}(\mathbf{r}) \right\rangle_{\mathbf{r}} , \tag{2.16}$$

where the spin correlation function is

$$C^{\alpha\beta}(\mathbf{r}) = V^{-1} \sum_{\mathbf{r}'} \langle S^\alpha(\mathbf{r}') S^\beta(\mathbf{r}+\mathbf{r}') \rangle , \tag{2.17}$$

with $\mathbf{r}$ the distance between spins, and where the average in Eq. (2.17) is over the spin fluctuations. In (2.16) we sum over the neighbors and average over lattice fluctuations. Notice that in general $C^{\alpha\beta}$ will depend on fluctuations in $\mathbf{r}$ through the dependence of the exchange energy on separation, but since the exchange is invariant under rotations in spin space, this will not affect the symmetries of $\overleftrightarrow{C}$ under spin rotations. We may thus consider the dipole energy to be the contraction

$$E_D = A^{\alpha\beta} E^{\alpha\beta} , \tag{2.18}$$

where $\overleftrightarrow{A}$ is a second-rank lattice tensor reflecting the spatial symmetry, and $\overleftrightarrow{E}$ is a second-rank spin tensor reflecting the spin rotational symmetries.

Two different rotational symmetries are important. [Because of the sum over $\mathbf{r}'$ in Eq. (2.17) it is clear that we are interested in point groups not space groups.] The first is the spin point group, consisting of the rotations of the spin coordinates that together with optional translations (but not rotations) of the lattice leave the state unchanged.[5] The second is the set of lattice rotations that, again with optional lattice translations but now no change in the spin degrees of freedom, leave the state unchanged.[6] This new lattice point group may be reduced from the original cubic symmetry. For a spin state described by a single plane wave $\mathbf{k}$ in the spin density the lattice point group is the group of $\mathbf{k}$. The symmetries are easily visualized in the classical description of the antiferromagnetic state: the spin point group acts on the "arrows" representing the spin directions; the lattice point group changes the lattice sites of the arrows, but leaves the directions unchanged.

We have argued that the NMR spectra lead to the conclusion

$$E^{\alpha\beta} \propto \hat{\mathbf{d}}^\alpha \hat{\mathbf{d}}^\beta , \tag{2.19}$$

$$A^{\alpha\beta} \propto \hat{l}^\alpha \hat{l}^\beta , \tag{2.20}$$

with $\hat{\mathbf{d}}$ and $\hat{l}$ anisotropy axes for spin and lattice rotations, respectively. The symmetries (i.e., spin and lattice point groups) of the antiferromagnetic state must be sufficient to reduce second-rank tensors to these forms.

Let us first consider the spin tensor. A possible symmetry leading to Eq. (2.19) is obviously complete uniaxial symmetry about the axis $\hat{\mathbf{d}}$. Any state with all the spins up or down along this direction satisfies this criterion.[7] However, the state may show lesser symmetry, but continue to satisfy Eq. (2.19), since discrete rotational symmetries of order $n \geq 3$ about some axis are sufficient to guarantee complete isotropy about this axis for a second-rank tensor. One class of states satisfying this symmetry is the helicoidal state, in which $\langle \mathbf{S}(\mathbf{r}) \rangle$ spirals about the axis $\hat{\mathbf{d}}$ with some wave vector $\mathbf{k}$ as $\mathbf{r}$ passes through the lattice. An incommensurate $\mathbf{k}$ leads to a spin point group invariant under rotations about $\hat{\mathbf{d}}$. Any $\mathbf{k} = n^{-1}\mathbf{G}$, with n an integer greater than two and $\mathbf{G}$ a reciprocal lattice vector, leads to a point group with discrete rotational symmetry. (Note here that the lattice translations are needed to return the rotated state to the original configurations.) In either case the dipole energy will be uniaxial, consistent with experiment. Since the susceptibility tensor is also of second rank, these same symmetries guarantee uniaxial symmetry here also, although in the helicoidal states higher rank tensors will not in general be uniaxial.

For the lattice symmetry Eq. (2.20) we may simply argue that the sublattice structure must preserve one of the threefold axes or one of the fourfold axes of the original cubic point group. Such an axis is necessary to make the second-rank lattice tensor uniaxial about $\hat{l}$, with $\hat{l}$ along this axis. (Of course the full cubic symmetry cannot be preserved, since this leads to no NMR shifts.) In fact, from the observation of domains we may conclude that $\hat{l}$ must be one of the fourfold symmetry axes. This would then imply the possibility of *three* domains for each single crystal with orthogonal directions of $\hat{l}$ corresponding to the three [100] directions. (If $\hat{l}$ were along a threefold axis, there would be four possible domains, with the various $\hat{l}$ at angles of 109°.) A quantitative test of this result, confirming that no domains were missed, is provided by the values obtained by fitting the spectra with θ_i for $i = 1,2,3$, which are the angles between the possible $\hat{l}$'s and the field direction. To a very good approximation (better than 2% in each case) these satisfy

$$\sum_{i=1}^{3} \cos^2\theta_i = 1 , \tag{2.21}$$

as required for orthonormal axes.

To summarize, the analysis of the NMR spectra im-

[5]This is the set $\{R_s \mid 0\}$, where the operations $\{R_s \mid \mathbf{t}\}$, with R_s a rotation acting on the spin degrees of freedom and $\mathbf{t}$ a lattice translation, leave the state unchanged.

[6]The set $\{R_l \mid 0\}$, where $\{R_l \mid t\}$, with R_l a lattice rotation, leaves the state unchanged.

[7]This is a classical Néel description of a spin-$\frac{1}{2}$ system for which quantum corrections are likely to be large. We may then define a state with this kind of uniaxial symmetry by imagining turning on quantum effects and supposing no change in symmetry during this continuous process. It cannot be entirely ruled out that in a highly quantum system a state with a uniaxial $C^{\alpha\beta}$ might exist but with $\langle \mathbf{S}_i \rangle = 0$. One obvious example is the A phase of superfluid ^{3}He. This would not correspond to a conventional quantum antiferromagnet, and we shall not consider this possibility further.

plies an antiferromagnetic structure with a spin point group containing a symmetry axis of order $n \geq 3$ (i.e., a spin rotation of $2\pi/n$ plus a lattice translation leaves the state invariant), and a new lattice point group retaining one of the original fourfold axes of the cubic symmetry. For a state with $\langle \mathbf{S}_i \rangle$ consisting of a single plane wave, the wave vector $\mathbf{k}$ must lie along a [100] direction (cube edge).

4. Quantitative analysis

It is not surprising that a qualitative analysis of the NMR spectra can lead only to rather global symmetry requirements on the antiferromagnetic state. In particular, point symmetries are determined, but many spatial structures are consistent with each point symmetry. Any further conclusions concerning the microscopic spin arrangement must involve first some guesses as to likely possible states and then a quantitative comparison, through $\Omega_0^2=\gamma^2\lambda/\chi_0$, with the experiment. A source of uncertainty in the comparison is that although λ may be easily calculated for any Néel-type antiferromagnetic state (i.e., each $\mathbf{S}$ aligned with known magnitude along some direction in a rigid lattice), both zero-point spin fluctuations and lattice fluctuations may significantly affect the result. Particularly serious for a spin-$\frac{1}{2}$ system will be the zero-point spin fluctuations. An estimate of the resulting change in λ depends on the microscopic spin exchange Hamiltonian, and so is not model independent. Thus, although the magnitude of the frequency shift Ω_0 may ultimately provide a quantitative test for a proposed microscopic Hamiltonian and its consequent ground state, it does not provide a definite constraint on the antiferromagnetic state without knowledge of the microscopic Hamiltonian. Experimental uncertainty in the measurement of χ_0 leads to further uncertainty at present.

As a first approximation to calculate the NMR frequencies for some possible structures we make the mean-field factorization

$$\langle S_i^\alpha S_j^\beta \rangle \Longrightarrow \langle S_i^\alpha \rangle \langle S_j^\beta \rangle \tag{2.22}$$

and then suppose $\langle S_i^\alpha \rangle$ to be given by the classical description—usually we will suppose that then all $|\langle \mathbf{S}_i \rangle|$ are equal—but with a magnitude reduced from $\frac{1}{2}\hbar$ by a factor of ψ to roughly take into account the zero-point spin fluctuations. The evaluation of E_D then reduces to the calculation of dipole sums in classical states—a straightforward calculation.

It is instructive to explicitly calculate $\overleftrightarrow{A}$ using this mean-field approximation for uniaxial spin states described by a single plane wave $\mathbf{k}$

$$\langle \mathbf{S}_i \rangle = \tfrac{1}{2}\hbar\psi \,\mathrm{Re}[\boldsymbol{\sigma} \exp(i\mathbf{k}\cdot\mathbf{r}_i)] \,. \tag{2.23}$$

This class includes (with $\mathbf{G}$ a reciprocal lattice vector)

(a) all two sublattice "up-down" states ($k=\frac{1}{2}\mathbf{G}$, $\boldsymbol{\sigma}=\hat{\mathbf{d}}$),

(b) states with ferromagnetic planes arranged in the sequence up-up-down-down ($\mathbf{k}=\frac{1}{4}\mathbf{G}$, $\boldsymbol{\sigma}=\sqrt{2}e^{i\pi/4}\hat{\mathbf{d}}$),

(c) helicoidal states with the spin spiralling in the plane normal to $\hat{\mathbf{d}}$ ($\boldsymbol{\sigma}=\boldsymbol{\Delta}_1+i\boldsymbol{\Delta}_2$ with $\boldsymbol{\Delta}_1,\boldsymbol{\Delta}_2$ unit vectors and $\boldsymbol{\Delta}_1\cdot\boldsymbol{\Delta}_2=0$, $\boldsymbol{\Delta}_1\times\boldsymbol{\Delta}_2=\hat{\mathbf{d}}$, $\mathbf{k}\neq\frac{1}{2}\mathbf{G}$), and

(d) planar spin-density waves in which not all $|\langle \mathbf{S}_i \rangle| = \frac{1}{2}\hbar\psi$ ($\boldsymbol{\sigma}=\hat{\mathbf{d}}$, $\mathbf{k}\neq\frac{1}{2}\mathbf{G}$, including incommensurate wave vectors).

It seems unlikely that the last class is physically relevant at low temperatures where one would expect a tendency towards a state without spins of anomalously low expectation values. For each of these classes $\overleftrightarrow{A}$ is given by

$$A_{\alpha\beta}(\mathbf{k}) = 3(\gamma\hbar/2)^2\rho^2\psi^2 F S_5^{\alpha\beta}(\mathbf{k}) \,, \tag{2.24}$$

where

$$S_5^{\alpha\beta}(\mathbf{k}) = \left[\rho^{-1}\sum_i \exp(i\mathbf{k}\cdot\mathbf{r}_i) r_i^\alpha r_j^\beta / |r_i|^5\right] \tag{2.25}$$

is the dimensionless lattice sum, which is tabulated for a mesh of points in the bcc reciprocal cell by Cohen and Keffer (1955), ρ is the number density, and the numerical factor F is $+1$ for classes (a) and (b), $-\frac{1}{2}$ for (c), and $+\frac{1}{2}$ for (d). Diagonalizing the matrix $S_5^{\alpha\beta}$ then confirms the result of the general analysis, that in order to have a degenerate pair of eigenvalues of $\overleftrightarrow{A}$, $\mathbf{k}$ must lie along a [111] or [100] direction. Out of the physically reasonable classes (a), (b), and (c) it turns out that only two sets of states are consistent with the requirement $\lambda>0$. These are a state in class (b) with $\mathbf{k}=2\pi/d\,(1,0,0)$ with d the cubic lattice constant [this is denoted $(\frac{1}{4},0,0)$ by Cohen and Keffer (1955) hereafter referred to as CK], and helicoidal states based on the F points of the bcc reciprocal zone [represented in CK by $(\frac{3}{8},\frac{1}{8},\frac{1}{8})\equiv(\frac{3}{8},\frac{3}{8},\frac{3}{8})$]. The elimination of other states from consideration does of course depend on the assumption that the mean-field factorization is sufficiently accurate to give the sign of λ correctly. [If the unphysical seeming states (d) are also allowed, then wave vectors $\mathbf{k}=(\alpha,0,0)$ and $\mathbf{k}=(\beta,\beta,\beta)$ with $0<\beta<\frac{1}{4}$ also give the correct sign of λ.] The helicoidal states would be likely, however, to yield the wrong sign of the susceptibility anisotropy, δ.

Taking into account the symmetry arguments given above shows that out of the large class of states (a), (b), and (c) only the one in class (b), consisting of [100] planes of ferromagnetically aligned spins arranged in the sequence up-up-down-down (and the two other symmetry related directions of $\mathbf{k}$ corresponding to the other domains) is consistent with both the symmetry implied by the NMR and the sign of λ, as calculated with the mean-field factorization. This state, which we call u2d2, is shown in Fig. 4.

Before discussing the quantitative comparison with experiment we may consider other possible states suggested by this structure. Although states in class (d) with $k=(\alpha,0,0)$ are consistent with the symmetry requirements and the sign of λ, a physically more likely set of states based on other [100] wave vectors is given by arranging the ferromagnetically aligned [100] planes in

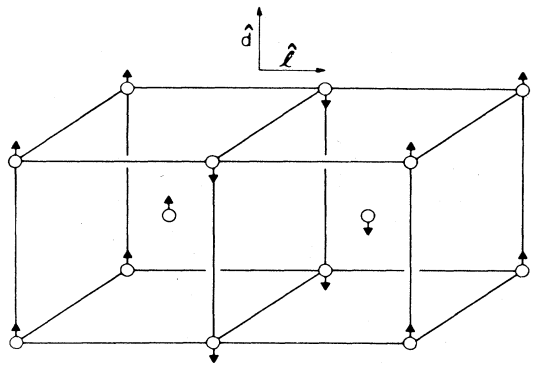

FIG. 4. A schematic representation of the u2d2 structure showing the spin and real-space anisotropy axes $\hat{\mathbf{d}}$ and $\hat{l}$, respectively.

longer sequences, for example, u3d3 (where u stands for "up" planes, d for "down" planes with respect to the spin anisotropy axis).

A straightforward comparison of the dipole sums in various umdm structures is given by noticing that the dipole interaction between the ferromagnetically aligned sheets decreases exponentially with separation. Consequently we may write in the same mean-field approximation as before

$$\lambda = 3(\gamma\hbar/2)^2\rho^2\psi^2\lambda_s \ , \tag{2.26}$$

with the numerical factor

$$\lambda_s = \left\langle \sum_{-\infty}^{\infty} f_p(\pm 1) \right\rangle \ , \tag{2.27}$$

where f_p gives the dipole interaction between sheet zero and sheet p, the (± 1) factor is for parallel or antiparallel sheets, and the average is over all ferromagnetic sheets in the crystal. The interaction f_p decreases very rapidly with p. In terms of the first few f_p we find the following results for λ_s in Eq. (2.27):

$$\text{u2d2: } \lambda_s = f_0 - 2f_2 + 2f_4 + \cdots = 2.42 \ ,$$

$$\text{u3d3: } \lambda_s = f_0 + \tfrac{2}{3}f_1 - \tfrac{2}{3}f_2 - 2f_2 + \cdots = 3.01 \ ,$$

$$\text{u4d4: } \lambda_s = f_0 + f_1 - f_3 + \cdots = 3.30 \ ,$$

$$\lim_{m\to\infty} \text{u}m\text{d}m\text{: } \lambda_s = f_0 + 2f_1 + 2f_2 = 4.19 \ .$$

The first result agrees with the value calculated by Cohen and Keffer (1955). As can be seen, λ_s gets progressively larger as m increases, but saturates at $4\pi/3$ for $m\to\infty$ corresponding to planar ferromagnetic domains, only 70% larger than for $m=2$. (Of course for $m\to\infty$ we would expect quite different static and dynamic properties on application of a magnetic field; this limit is evaluated only to show the trends in the dipole energy.) Notice that the values depend mainly on the fraction of nearest planes that are parallel: further neighbors give only small corrections.

To compare with experiment, we find at melting pressure

$$\Omega_0/2\pi = 1910\lambda_s^{1/2}\psi(T_m/1\ \text{mK})^{-1/2}\ \text{kHz} \ , \tag{2.28}$$

where T_m is the magnetic temperature defined by $T_m = (\gamma\hbar/2)^2\rho\chi^{-1}$ and we have introduced λ_s as in Eq. (2.26). Note that the numerical prefactor is density dependent.

The best estimate at present for T_m at low temperatures comes from measurements by Osheroff (1981). He finds a value of T_m near the transition temperature roughly consistent with the early measurement of Prewitt and Goodkind (1977), but with a considerable (and rather unexpected) increase as the temperature is lowered, leading to an extrapolated zero-temperature value of $T_m = 5.8$ mK. This is larger than the value used in OCF, which corresponded to the knee near T_c of the low-field measurements of Prewitt and Goodkind (1977).

For the u2d2 structure we therefore estimate

$$\Omega_0/2\pi \simeq 1230\psi\ \text{kHz} \ , \tag{2.29}$$

compared with the experimental extrapolation

$$(\Omega_0/2\pi)_{\text{expt}} = 825\ \text{kHz} \ . \tag{2.30}$$

For agreement we need a large renormalization due to zero-point spin fluctuations $\psi \sim 0.67$. This should be compared with a value $\psi \sim 0.85$ that might be guessed from previous spin wave calculations on simple antiferromagnetic states (Anderson, 1952; Kubo, 1952). However, a larger value may be reasonable in this system, although it is hard to calculate (see Sec. IV.B). In view of these uncertainties, the quantitative agreement with experiment for the u2d2 state must be considered an open question. Note that longer sequences umdm make the agreement progressively worse (e.g., u3d3 gives 12% worse agreement), although perhaps not significantly so for small m, considering the large discrepancy for $m=2$.

Roger and Delrieu (1981) have suggested that the zero-point lattice motion may improve the agreement with experiment by smearing out the effective magnetic moments and so reducing the dipole anisotropy. It seems very unlikely that this would yield a large correction in the u2d2 state, since uncorrelated, spherically symmetric fluctuations lead to *no* change in the dipole energy, as follows from elementary magnetostatics. Such a description should be good in the u2d2 state, where nearest neighbors, whose motion might be significantly correlated, do not contribute to the dipole sums in the Néel approximation.

We (OCF) have suggested a simple phase based on a [100] wave vector—the u2d2 phase—that is consistent with the symmetry requirements imposed by the analysis of the NMR spectrum. The quantitative agreement with experiment is uncertain, because zero-point spin fluctuation corrections are not reliably known. Consistency apparently requires an anomalously large correction, based on our expectations from analyses of simpler systems. Larger sequences umdm give worse agreement. Similar structures based on a [100] wave vector, but in which $|\langle \mathbf{S}_i \rangle|$ is modulated appear unlikely from physical grounds at low temperatures but cannot be ruled out by experiment [and, in fact, because of the factor $F = \frac{1}{2}$ in

Eq. (2.24) may give rather good numerical agreement with $\psi \approx 1$]. It is certainly true, however, that other phases exist consistent with the symmetry, but with more complicated spatial structures.

B. High-temperature series

Very few experiments other than NMR provide information on the effective spin Hamiltonian that is independent of detailed model assumptions. Fitting measurements of thermodynamic quantities to the terms of a high-temperature expansion of the spin Hamiltonian (i.e., a series in J/T for measurements well above T_c) in principle provides such information. There remains considerable controversy concerning the values of the coefficients produced by this analysis. It seems to us that a careful exploitation of this approach, involving precise measurements of specific heat, magnetic susceptibility, and the pressure $P(T,H)$, together with a proper calibration of the temperature scale, is essential to provide reliable numbers that can constrain proposed model Hamiltonians.

The development of the high-temperature series for thermodynamic quantities is straightforward. The free energy is given by the series

$$F = T \ln \sum_{n=0}^{\infty} \mathrm{Tr} \frac{\langle (\mathscr{H} + \gamma S^z H)^n \rangle}{n! T^n} \tag{2.31}$$

with $\mathscr{H}$ the effective spin Hamiltonian and S^z the total spin along the direction of the magnetic field assumed to be in the z direction. Although for a given model Hamiltonian $\mathscr{H}$ this series may in principle be developed to high orders to compare with experiment, the reliable experimental *constraints* to be imposed on possible models are probably restricted to measurements of the first one or two coefficients. In particular, in the series for the susceptibility χ per unit volume,

$$\chi^{-1} = \left[\frac{\gamma \hbar}{2} \right]^{-2} \rho^{-1} \left[T - \theta + \frac{B}{T} + \cdots \right] \tag{2.32}$$

the specific heat

$$C_V = \frac{\rho}{4} \left[\frac{e_2}{T^2} + \cdots \right] \tag{2.33}$$

and the pressure

$$P(T,H) = P_0 + \frac{1}{8} \frac{e_2'}{T^2} + \cdots + \left[\frac{\gamma \hbar H}{2} \right]^2 \left[\frac{1}{T^2} \theta' + \cdots \right] + O(H^4) \tag{2.34}$$

(where the prime denotes the volume derivative), we will restrict our discussion to the first nontrivial corrections θ, e_2 and their volume derivatives. Here ρ is the number density. These coefficients are given by moments of the spin Hamiltonian

$$e_2 = \frac{4}{N} \langle \mathscr{H}^2 \rangle \Longrightarrow 12 J^2 \quad \text{for nearest-neighbor exchange},$$
$$\theta = \frac{4}{N} \langle (S^z)^2 \mathscr{H} \rangle \Longrightarrow 4J \quad \text{for nearest-neighbor exchange}, \tag{2.35}$$

where the expectation value $\langle\ \rangle$ is taken with respect to the high-temperature disordered density matrix (i.e., all states weighted equally) and N is the number of spins. The only assumption involved in deriving these expressions is that the temperature is high compared to characteristic magnetic energies of $\mathscr{H}$. Thus the temperature must be *high* compared to the exchange energies (typified by the Néel temperature) but *low* enough so that the lattice degrees of freedom such as vacancies and phonons are not excited.

For the specific heat there is a rather wide range of temperature, at least at the larger molar volumes, where the magnetic T^{-2} term gives the dominant specific heat: the phonon contribution becomes comparable only at 100–200 mK. Thus e_2 is rather well known near the melting curve (Fig. 5) with $e_2^{1/2} \approx 2.4$ mK at a molar volume $V = 24.2$ cm^3/mole. Panczyk and Adams (1970) measured the temperature dependence of the pressure in zero field, leading to values of $e_2' = de_2/dV$. We would like to stress that there is *no* way of deducing $e_2(V)$ from this data without further assumptions, since an arbitrary constant added to

$$e_2(V) = \int e_2' dV \tag{2.36}$$

obviously leads to the same e_2'. This problem is surmounted in practice by continuing the measurements to high enough densities, where the exchange rate is expected to be small, so that small bounds may be placed on the additive constant. The actual numbers derived by Panczyk and Adams (1970) are consistent with a very small value < 0.1 (mK)^2 assumed for e_2 at 21 cm^3/mole. The nature of the assumption involved should, however, be remembered whenever pressure measurements are used

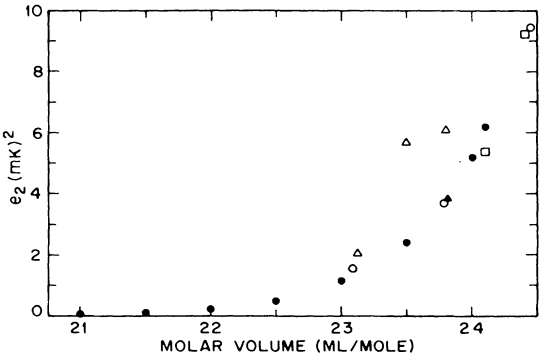

FIG. 5. Leading coefficient of the high-temperature expansion of the specific heat ($C_v \sim e_2/T^2$) as a function of molar volume. The open points are from direct measurements: ○, Greywall (1977); □, Castles and Adams (1975); △, Dundon and Goodkind (1974). The solid points (●) are derived indirectly from pressure measurements (Panczyk and Adams, 1970).

to derive exchange constants. An alternative method sometimes used is to assume a particular form for the logarithmic derivative (Gruneisen parameter)

$$\gamma(V) \equiv \partial \ln e_2 / \partial \ln V , \tag{2.37}$$

typically a constant. This is not reliable: the system is sufficiently complicated and the theoretical understanding is poor enough that any such assumption that such a form is obeyed over a wide range of volumes is completely arbitrary.

Deriving reliable estimates from experiment for the Curie-Weiss constant θ is more difficult, and there has been considerable controversy over its value for the past twenty years. Recent more precise measurements have heightened this controversy, with values quoted for θ near the melting pressure a factor of 2 lower than previous values. The basic difficulty is that the term required is a small correction to the "trivial" Curie susceptibility of noninteracting spins. Thus at high temperatures, θ is given by a very small fractional change in the susceptibility and the statistical errors are large. The size of the interaction corrections may be made larger by going to lower temperatures, but then the approximation of retaining only the lowest-order term in the high-temperature series is less good and the systematic errors become larger.

The experimentally deduced values of $\theta(V)$ fall into two classes. Direct measurements of $\chi(T)$ have led to values shown as open points in Fig. 6 which rise to a value of about 3 mK at melting pressure. A second class of measurements are shown as solid points: these are derived from pressure measurements which yield directly values for θ', and the comparison technique mentioned above, which yields $\theta(V)-\theta(V_0)$, with V_0 a reference volume. This second class of measurements is undoubtedly more precise; they, however, suffer from the problem encountered above that an unknown constant offset may be added to $\theta(V)$. Kirk and Adams (1971) and Van Degrift *et al.* (1982) use assumptions about the expected volume dependence to fix this constant. We find this method unsatisfactory for the reasons noted previously. Kirk *et al.* (1983) try to place bounds on the offset [more precisely, on $\theta(V_0)$, with V_0 the lowest volume measured—21 cm^3/mole in the published data] by a less precise *direct* measurement of $\theta(V_0)$ using cerium magnesium nitrate (CMN) and lanthanum CMN (LCMN) thermometry. They estimate $\theta(V_0)=0.11$ mK and conclude that almost certainly $\theta(V_0)<0.22$ mK, although this estimate remains somewhat uncertain due to possible offset effects in the thermometry scales. Extending the measurements down to a volume of 19 cm^3/mole leads to similar values for $\theta(V)$ (Kirk, 1983) and adds further weight to their estimates.

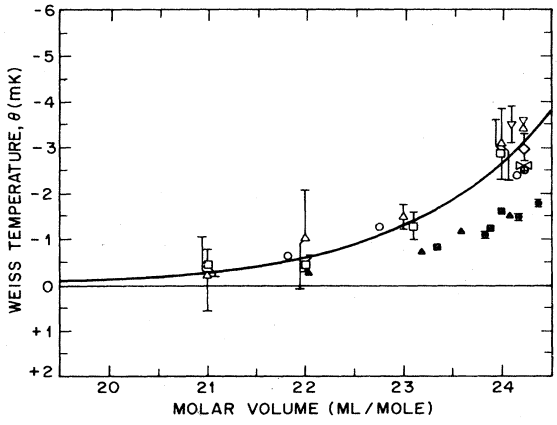

FIG. 6. Curie-Weiss temperature θ as a function of molar volume. The open points are from direct measurements. ⧖, Bakalyar *et al.* (1977); ⋈, Prewitt and Goodkind (1977); ⊕, Morii *et al.* (1978); △, Bernat and Cohen (1973); ▽, Johnson and Wheatley (1970); ◇, Sites *et al.* (1969); □, Kirk *et al.* (1969); ○, Hata *et al.* (1981). The solid points are indirect or comparison measurements as discussed in the text: ●, Van Degrift *et al.* (1982); ■, Kirk and Adams (1971); ▲, Kirk *et al.* (1983).

One is then left with the problem of reconciling the two sets of data. The greatest discrepancy is at melting pressure (24.2 cm^3/mole), where the comparison measurements yield θ of about 1.6 mK, and the direct measurements yield a systematically larger θ of about 3 mK, with typically ± 0.5 mK error bars in the latter. Two options seem open at this stage. One is to obtain consistency of all the *measured* data by adding a constant offset of about 1 mK to the value derived from pressure and comparison measurements. This requires a value of θ at 21 cm^3/mole of about 1 mK, much larger than expected from the volume dependence $\theta \sim V^{18}$ typically observed for other quantities. However, in a system where evidence for competing ferromagnetic and antiferromagnetic interactions is strong, it is an intriguing possibility that the decrease in θ with volume could lessen, or even that θ begins to increase with decreasing volume as the ferromagnetic part of the interaction becomes relatively less important. Against this argument is the apparent inconsistency of the value of 1 mK at 21 cm^3/mole with the direct measurement of Kirk *et al.* (1983).

The second option seems to be to suppose that the analysis of the less precise measurements at melting pressure for some reason systematically lead to too large a value of θ. Except for the data of Sites *et al.* (1969), these experiments were all analyzed by plotting χ^{-1} against T with the intercept on the T axis giving θ. The ranges of temperatures used in the various measurements differ widely, yet all yield similar values of θ. It is particularly hard to understand why the results of Prewitt and Goodkind (1977), Bakalyar *et al.* (1977), Morii *et al.* (1978), and Hata *et al.* (1981) obtained from temperatures below 15 mK should lead to too *large* a value of θ: if the enhancement in the susceptibility at lower temperatures shown in these data may be ascribed to the next term in the high-temperature expansion (i.e., $B<0$) the estimation of θ at too low temperatures should lead to too *small* a value. On the other hand, Kirk *et al.* (1984) have recently measured an anomalous *decrease* in χ at around 50 mK in samples very near melting that would be consistent with the idea that a χ^{-1} vs T fit to the direct measure-

ments yields too large a value of θ.

It is clear that at the present stage this question requires further experimental work, entailing precise direct measurements of $\chi(T)$ over a wide temperature range. Kirk *et al.* (1984) have demonstrated the danger of graphical fits to measurements without a careful analysis of the weights to be given each data point. Plotting $(\chi T)^{-1}$ or χT against T^{-1} displays deviations due to higher-order terms in the expansion more clearly, better showing over what range in temperature the lowest-order fit is reasonable. At the same time this plot gives larger weight to the low-temperature region where the higher-order terms are important. On the other hand, plotting χ^{-1} against T weights more strongly the high-temperature region where the expansion is best, yet masks deviations at lower temperatures. Since the signs of the higher-order terms are not known, neither method is *a priori* more likely to minimize their effect. A least-squares fit to either form with consistent weighting of the data points according to the experimental uncertainty would eliminate differences due to these different treatments. An inspection of the residuals from either fit to examine whether the deviations appear systematic or truly statistical would then answer the question of whether the data is extending into regions where the assumed high-temperature form is no longer adequate.

C. Low-temperature thermal properties and spin waves

In the previous two sections we have shown that there are severe qualitative constraints on the symmetry of the low-temperature ordered phase imposed by the NMR data and somewhat less stringent quantitative constraints from the high-temperature thermodynamic data. In addition to this information, there is a considerable amount of thermodynamic data at low temperatures in the ordered phase which it might be hoped would provide additional constraints on possible theories.

For $T \ll T_c$ the temperature dependences of thermodynamic quantities are determined by the low-energy elementary excitations of the system, i.e., the antiferromagnetic spin waves. Except at extremely low and currently inaccessible temperatures, the dipolar anisotropy can be ignored and the spin-wave frequencies will be linear in the wave vector $\mathbf{k}$ in the absence of a magnetic field. For states with tetragonal spatial symmetry like the zero-field phase, the low-frequency spin wave modes have a spectrum

$$\omega_\alpha^2(\mathbf{k}) = c_{\alpha\|}^2 k_z^2 + c_{\alpha\perp}^2 (k_x^2 + k_y^2) , \tag{2.38}$$

where we have chosen the spatial anisotropy axis $\hat{l}$ to be in the $\hat{\mathbf{z}}$ direction. For general structures there will be a different spin-wave mode, labeled by the index α, for each of the broken spin symmetries. However, for uniaxial (in spin space) spin structures which the NMR indicates for ^{3}He, two of the spin-wave modes must be degenerate. For up-down structures, such as the u2d2 structure, only two of the spin rotation symmetries are broken and only two modes exist: there will thus be a unique spin-wave velocity in each direction. For helicoidal and other structures which break all three spin symmetries but are still uniaxial, there will be three modes, two of them degenerate. In addition to the acoustic spin-wave modes, there will generally be optic spin-wave modes; however, because of the Bose occupation factors, the *thermal* effects of these modes will be exponentially small at low T. All the modes will, however, contribute to the zero-point suppression of, for example, the dipole energy and the order parameter.

The characteristic magnitude of the spin-wave frequencies will be $T_c/\hbar$ and hence the velocities will be of order $T_c a/\hbar$ which is very small (of order cm/sec) due to the weak magnetic interactions. An experimental determination of a combination of the spin wave velocities can be obtained from the low-temperature specific heat per unit volume

$$C_V = \frac{1}{V} \sum_{k\alpha} \left[\frac{\hbar\omega_\alpha(\mathbf{k})}{T} \right]^2 n' \left[\frac{\hbar\omega_\alpha(\mathbf{k})}{T} \right] , \tag{2.39}$$

where $n(x) = (e^x - 1)^{-1}$ is the Bose distribution function, the prime denotes differentiation, and the sum runs over wave vectors in the antiferromagnetic Brillouin zone and the number of acoustic modes. Using the linear dispersion for small k which will dominate the sum for low temperatures, we have the usual result

$$C_V = \frac{2\pi^2 T^3}{15\hbar^3} \sum_\alpha \left\langle \frac{1}{c_\alpha^3(\mathbf{k})} \right\rangle , \tag{2.40}$$

where the average is over angles which for the tetragonal case is given by

$$\left\langle \frac{1}{c_\alpha^3} \right\rangle = \frac{1}{c_{\alpha\perp}^2 c_{\alpha\|}} . \tag{2.41}$$

Experimentally (Osheroff and Yu, 1980) it is found that the specific heat behaves as T^3 almost up to T_c with

$$\sum_\alpha \left\langle \frac{1}{c_\alpha^3} \right\rangle = 3.34 \times 10^{-3} \ (\text{sec/cm})^3 . \tag{2.42}$$

For an up-down structure, this implies that the geometric mean spin-wave velocity is 8.4 cm sec, which is of roughly the expected magnitude.

Other low-temperature properties will depend on both the spin-wave velocities *and* their eigenvectors. The form of the latter will depend on the structure of the ordered phase and so for the rest of this section we will assume the u2d2 structure.

For three-dimensional antiferromagnets, it is generally a relatively good approximation to consider the ground state to be close to a classical Néel state and to treat quantum fluctuations in terms of noninteracting spin waves (Anderson, 1952). The spin-wave frequencies and eigenvectors are determined from expanding about the Néel state and neglecting terms of order higher than quadratic. The zero-temperature suppression of the order parameter and the concomitant reduction of the dipolar anisotropy

can then be attributed to zero-point fluctuations of all the spin waves. The leading low-temperature dependence of these quantities and the $T=0$ susceptibility will come from only the long-wavelength acoustic modes. In this section we will introduce a combination of measured quantities which, once one has assumed the u2d2 ordered state, depends *only* on the assumption that interactions between the spin waves can be ignored and *not* on the details of the microscopic Hamiltonian. This quantity gives us model-independent information about the accuracy of the noninteracting spin-wave calculations of low-temperature properties. (The details of the calculations, which are somewhat tedious, are contained in Appendix A.)

The zero-temperature transverse susceptibility is found to be, from Eq. (A13),

$$\chi(0)=\rho\frac{\gamma^2\hbar^2}{16\Upsilon}\ , \tag{2.43}$$

with ρ the number density. The energy Υ is a combination of the exchange constants in the Hamiltonian which can be evaluated for any specific candidate Hamiltonian and is related simply to the long wavelength limit of the acoustic spin-wave eigenvectors Eq. (A11). As described in Appendix A, all the important properties of the long-wavelength spin waves in the noninteracting approximation are contained in their velocities and the single parameter Υ, so that the other low-temperature thermal properties can be directly related to the spin-wave velocities and the susceptibility. In particular, we find that the suppression of the order parameter is given by Eq. (A29):

$$2\langle S^z(0)\rangle-2\langle S^z(T)\rangle=\frac{4}{3}\frac{T^2\Upsilon}{\hbar^3\rho}\left\langle\frac{1}{c^3}\right\rangle\ , \tag{2.44}$$

where $\langle 1/c^3\rangle=1/c_\perp^2 c_\parallel$ is the same combination as that which enters the specific heat. The order parameter is not directly measurable except with neutron scattering, but another quantity, the thermal suppression of the dipolar anisotropy exhibits related behavior and is measurable. The dipolar anisotropy, as discussed in Sec. II.A, can be most conveniently expressed in terms of the difference $\lambda=\lambda_1-\lambda_3$ between the largest and smallest eigenvalues of the dipole energy tensor $A^{\alpha\beta}$. The thermal depression of λ is found to be, from Eq. (A28),

$$\Delta(T)=\lambda(T)-\lambda(0)$$

$$=-7.26(\gamma\hbar)^2\frac{T^2\Upsilon\rho}{\hbar^3}\left\langle\frac{1}{c^3}\right\rangle\ , \tag{2.45}$$

where the numerical factor is obtained from the dipolar sums discussed in Sec. II.A. We note that $\frac{2}{3}$ of this suppression, $\Delta(T)$, arises from the order-parameter suppression Eq. (2.44) and the remainder from the spin correlations transverse to the broken symmetry direction $\hat{\mathbf{d}}=\hat{\mathbf{z}}$.

The low-T temperature dependence of the zero-field NMR frequency Ω_0 is expressible in terms of $\Delta(T)$ and other measured quantities:

$$\Omega_0^2(T)-\Omega_0^2(0)=\Omega_0^2(0)\left[\frac{\chi(0)}{\chi(T)}-1\right]+\gamma^2\frac{\Delta(T)}{\chi(0)}\ . \tag{2.46}$$

If we use the value $\Upsilon=1.4$ mK obtained from Eq. (2.43) and the measured low-T susceptibility

$$\chi(0)=\left[\frac{\gamma\hbar}{2}\right]^2\frac{\rho}{5.8\ \text{mK}}\ , \tag{2.47}$$

$\langle 1/c^3\rangle$ from the specific heat, and the measured temperature-dependent susceptibility, then the predicted value for the right-hand side of Eq. (2.40) is

$$\Omega_0^2(T)-\Omega_0^2(0)\,|_{\text{pred}}=-1.2T^2\left[\frac{2\pi\ \text{MHz}}{\text{mK}}\right]^2\ . \tag{2.48}$$

This should be compared with the experimentally measured

$$\Omega_0^2(T)-\Omega_0^2(0)\,|_{\text{expt}}=-0.33T^2\left[\frac{2\pi\ \text{MHz}}{\text{mK}}\right]^2\ , \tag{2.49}$$

which is a factor of almost 4 smaller.

The theoretical expression Eq. (2.48) is based only on the assumption of the u2d2 state and the neglect of interactions between the spin waves. It is possible that the large discrepancy is primarily due to errors in the measured quantities, particularly the susceptibility which enters the result squared; however, the estimated errors are far less than would be required for consistency.

A more likely, and certainly more interesting, possibility is that the discrepancy is due either to the incorrect identification of the ordered phase or to the strong effects of the spin-wave interactions in changing their frequencies and eigenvectors from their noninteracting form. If the latter is true, then all the properties of the ordered phase will be strongly affected by quantum fluctuations. Thus, although the low-temperature experimental data can be used in principle to constrain possible theories, it will be difficult to calculate the low-T behavior of candidate Hamiltonians well enough for detailed quantitative comparisons to be made. We will return to this question in Sec. IV in connection with difficulties of obtaining useful predictions from candidate models.

III. POSSIBLE THEORETICAL EXPLANATIONS

The ground-state energy of solid ^{3}He is almost independent of the fermionic nature of the atoms and the spin degrees of freedom of the nuclei. The lattice energy may be very well calculated, at the fraction of a Kelvin level, by assuming each atom is confined to the vicinity of a particular lattice site. At this level of approximation fermions, bosons, or distinguishable particles of identical mass have the same energy.

For ^{3}He atoms each localized to a lattice site there are 2^N degenerate configurations corresponding to the possible spin arrangements. This degeneracy is split by any process that leads to atoms exchanging their lattice sites.

Empirically these processes are rare, corresponding to a frequency of order 1 mK/atom, a factor of 10^4 less than the vibrational frequencies. Because of the total antisymmetry of the fermionic wave function under pairwise permutations, there is a correspondence between the symmetry of the spatial wave function under permutations and the spin state. A spatial wave function that is not even under all permutations implies the existence of nodes in the wave function with a corresponding increase in the kinetic energy. Thus the residual quantum processes exchanging atomic sites lead to interesting phenomena at energies of order mK that are manifest in the magnetic properties of the system. The theoretical task is to understand the nature of these quantum processes from the rich experimental properties discussed in the preceding section and the Introduction. The general properties of exchange in solid ^{3}He were first discussed by Thouless (1965), following ideas of Herring (1962,1966) for magnetic insulators.

The most obvious exchange process is the pairwise exchange of nearest-neighbor atoms. If these events are rare, they may be treated in isolation. It is then immediately clear that the contribution to the energy from any pair of atoms is lower for the nodeless symmetric spatial wave function (associated via the Pauli principle with the antisymmetric spin state) than for the antisymmetric spatial wave function (associated with the symmetric spin state). Thus the total contribution to the energy from the pairwise exchange process is

$$\mathscr{H}=J_1\sum_{\langle ij\rangle}P_{ij}\ , \tag{3.1}$$

where the sum runs over nearest neighbor pairs $\langle ij\rangle$ with P_{ij} the spin permutation operator acting at sites i,j and J_1 a positive energy equal to one-half the splitting of symmetric and antisymmetric spatial states.[8] Physically, J_1 gives the rate of occurrence of the process in which two neighbors change position. Writing the permutation operators in terms of the spin-$\frac{1}{2}$ operator $\mathbf{S}_i$

$$P_{ij}=\tfrac{1}{2}+2\mathbf{S}_i\cdot\mathbf{S}_j \tag{3.2}$$

yields

$$\mathscr{H}=2J_1\sum_{\langle ij\rangle}\mathbf{S}_i\cdot\mathbf{S}_j+\text{const}\ , \tag{3.3}$$

the well-known nearest-neighbor Heisenberg spin Hamiltonian.

It is worth reflecting a little on the procedure leading to this result. The original problem of finding the "most nodeless" spatial wave function (with the dynamics of nearest-neighbor exchange) consistent with the Pauli principle amongst two sets of indistinguishable fermions (spin up and spin down) is replaced by the problem of diagonalizing a lattice spin Hamiltonian. A good approximation to the ground state of Eq. (3.3) for the bcc lattice is the Néel antiferromagnet with $S^z=+\frac{1}{2}$ on the body centers (for example) and $S^z=-\frac{1}{2}$ on the body corners, known as the NAF (for normal antiferromagnet) phase. This state corresponds to one in which the exchange process does not operate, i.e., in which each atom remains localized at its lattice site—a result that is much less obvious from the original statement of the problem. (The result is of course approximate, and zero-point corrections will correspond to some atomic exchange.)

Although simple, the spin Hamiltonian Eq. (3.3) is remarkably inconsistent with nearly all the experimental data on solid ^{3}He. If any doubt remained, the NMR experiments on the antiferromagnet phase are by themselves sufficient to show that Eq. (3.3) requires drastic modification, since the ground state of the near-neighbor Heisenberg antiferromagnet is strongly believed to have cubic symmetry, leading to no shifts of the resonance from the Larmor frequency. In fact, the u2d2 ground state proposed by OCF which is consistent with the NMR would, if correct, rule out any spin Hamiltonian involving *only* pairwise exchange even if it included further neighbor pair exchange: such a Hamiltonian would give a degeneracy in the ground state in which the spins in alternate planes could be rotated uniformly with respect to the other spins. The thrust of the work since the inadequacy of Eq. (3.3) was realized has been to find the proper description of the system to replace the hypothesis of only pairwise exchange.

A. Multiple exchange (general)

If pairwise exchange is not sufficient to describe the system, it is natural to consider more complex exchange processes involving a larger number of atoms. This idea received initial impetus from the paper of McMahan and Wilkins (1975). These authors attempted a microscopic calculation of various exchange rates. Although their method is now thought not to capture the features essential in determining the overall rates, the physics favoring multiple exchange is perhaps as well documented in that original work as anywhere else. The basic point is that steric effects of neighboring atoms are much more serious for two-particle exchange than for higher-order ring exchange processes. Thus the steric suppression of two-particle exchange may be more important than the suppression of multiple exchange due to the larger number of particles involved.

The derivation of the effective spin Hamiltonian resulting from multiple exchange proceeds essentially as before. Again, since the exchange processes are rare, each one may be considered in isolation, and the total Hamiltonian will be the sum of individual exchange terms. Thus for an exchange process corresponding to a permutation $P^{(R)}$ of the sites of the atoms we write the splitting in the energy between the approximate eigenfunctions

$$\psi\simeq\psi_0\pm P^{(R)}\psi_0 \tag{3.4}$$

[8]Note that we have gone from particle spin coordinates to site spin coordinates. This is valid in the small exchange limit.

as $2J(P)$, where ψ_0 is an approximation to the spatial wave function in which each atom is confined to the neighborhood of one lattice site [the "home base wave function" of Herring (1962)]. Again, by general arguments the symmetric, nodeless combination [the + sign in Eq. (3.4)] has the lower energy so that $J(P)$ is positive. Thus the energy splitting is given by

$$\Delta E\psi = -J(P)P^{(R)}\psi \ . \tag{3.5}$$

Now, using the fact that the wave function must be antisymmetric under an odd number of interchanges of spin and spatial coordinates together, so that acting on any fermion wave function

$$P^{(R)}P^{(\sigma)} \equiv (-1)^P \ , \tag{3.6}$$

where $(-1)^P$ is positive for a permutation involving an even number of interchanges and negative for a permutation involving an odd number of interchanges, we can write the energy splittings completely in terms of the spin permutations $P^{(\sigma)}$. Summing over all permutations in the lattice yields the effective spin Hamiltonian

$$\mathscr{H} = -\sum_P (-1)^P J(P) P^{(\sigma)} \ . \tag{3.7}$$

Note that for an even (odd) permutation, the ferromagnetic state of aligned spins with $P^\sigma \equiv 1$ is the lowest (highest) energy state. Thus it is the general rule that even (odd) exchange processes favor ferromagnetism (antiferromagnetism).

Physically $J(P)$ can be thought of as the rate of occurrence of the process in which distinguishable particles undergo a permutation P of their position. We would therefore like to obtain a formal expression for J in terms of paths connecting the two configurations. This is straightforward in a weakly quantum system with the de Boer parameter $\Lambda \ll 1$ in terms of the WKB integral, but is more difficult in the highly quantum case corresponding to solid ^{3}He at low densities. Formally we may generally write the exchange splitting as

$$J(P) = \lim_{U\to\infty} \frac{1}{U} \ln \left[\frac{\int d\mathbf{x}[\rho(\mathbf{x},\mathbf{x},U) - \rho(\mathbf{x},P\mathbf{x},U)]}{\int d\mathbf{x}\,[\rho(\mathbf{x},\mathbf{x},U) + \rho(\mathbf{x},P\mathbf{x},U)]} \right] , \tag{3.8}$$

where the density matrix $\rho(\mathbf{x},\mathbf{x}',U)$ at temperature $\hbar/U$ may be expressed in path integral form

$$\rho(\mathbf{x},\mathbf{x}',U) = \int\int \exp\left[-\frac{1}{\hbar} S(U) \right] \mathscr{D}x(U) \ , \tag{3.9}$$

where $S(U)$ is the imaginary time action for particles at $\mathbf{x}_i(t)$

$$S(U) = \int_0^U dt \left[\tfrac{1}{2} m \sum_i \left[\frac{d\mathbf{x}_i}{dt} \right]^2 + V(\mathbf{x}_i) \right] \tag{3.10}$$

and the path integral is over all paths starting at $\mathbf{x}$ and ending at $\mathbf{x}'$ at "time" U. We have not seen any rigorous development starting from Eq. (3.8). However, it seems that the expression for $J(P)$ can be simplified if we assume that the *empirical* rarity of the exchange events allows, even in the absence of an expansion involving $\hbar \to 0$, a treatment of the path integral in terms of a "dilute gas" of independent to-and-fro exchange events, each one occurring over a time scale small compared with the typical time between events. In this case we find

$$J(P) = \int d\mathbf{x}\, \bar{\rho}(\mathbf{x},P\mathbf{x},U\to\infty) \ , \tag{3.11}$$

where $\bar{\rho}$ is defined as $\rho(\mathbf{x},P\mathbf{x},U)$, but with paths restricted to a single exchange event ($\mathbf{x}\to P\mathbf{x}$).

For a weakly quantum system the usual WKB expansion can be performed to yield

$$J = \omega_a \exp(-S_{\min}/\hbar) \ , \tag{3.12}$$

with $S_{\min}$ the action evaluated over the path minimizing the action, and ω_a a complicated but well-defined quantity that can be interpreted as the attempt frequency and is expected to be of order the frequency of the zero-point motion, ω_0.

For hard-sphere atoms (which may well be a reasonable approximation for ^{3}He) exchange is somewhat more subtle conceptually. Since there is no potential energy (it is either zero or infinity for hard spheres), there is no tunneling in the usual sense. In addition, the atoms fluctuate around lattice positions which are not minima of the potential energy. (Note that this *is* in fact also true for bcc solid ^{3}He.) Thus the "initial" and "final" configurations of the exchange cannot be described as quantum fluctuations about local minima. The boundary conditions due to hard-core constraints do, however, force the wave function to go to zero when any pair of atoms approach to within a hard-core diameter, and the effective potential V_{eff} can be associated with the kinetic energy K_t of the degrees of freedom transverse to the exchange path which will be large because of the small distance δ_t between the atoms: roughly, according to $K_t \propto \hbar^2/m\delta_t^2$. This effective potential, V_{eff}, might possibly be included in the action as a pseudopotential and minimized to give a classical path, but this has not yet been suitably formalized. The exchange would then again be of the form of Eq. (3.12) with V in (3.10) replaced by V_{eff}.

For solid ^{3}He near the melting curve, the exchanges are probably in an even more complicated intermediate regime between the soft potential case and the hard-sphere limit. In the absence of reliable calculations of any exchange rates for ^{3}He, it is useful to make a few general comments here. In order to have $J \sim 1$ mK, the actions in the exponential in Eq. (3.12) determining J's must be relatively large, on the order of $10\hbar$. Twenty-percent variations in the exponential between different P's will yield almost an order of magnitude variation in the corresponding $J(P)$'s. It is thus extremely unlikely that more than a few exchange processes play major roles unless some additional physics (e.g., a common intermediate state) leads to similar actions. Also, if the observed magnetic phases at melting pressure are determined by a delicate balance be-

tween several J's, small increases in pressure might be expected to cause relatively large changes in the phase diagram and thermodynamic properties. To date this does not seem to be the case; this is discussed further in Sec. IV.A. Finally, it is clear that exchange processes P which can be factorized into two simultaneous permutations $P=P_1P_2$ will be negligible if P_1 involves only atoms far from those in P_2 (except for noninstantaneous coupling via phonons discussed in the next section). In addition, permutations involving atoms separated by more than the nearest few neighbors which do not *also* involve the intervening atoms are likely to be negligible.

For a soft interaction potential between atoms, one expects that the exchange integral for a permutation P involving n atoms each moving by, say, one nearest-neighbor separation, will fall off roughly as e^{-n} due to the total mass being proportional to n and from the assumption that the barrier potential per particle is independent of n. In this case, one would expect two-spin exchange to dominate over all others if the sum in Eq. (3.7) is sensibly convergent. For ^{3}He, however, the hard core may cause the two-spin exchange to have an anomalously large effective potential per particle relative to "ring" exchange of nearest (or perhaps next-nearest) neighbors. This is the basic argument behind the proposal for multiple exchange Hamiltonians. Consistency with the data apparently requires competition between three- and four-spin exchange processes; this is described in detail below. However, it is interesting first to consider the possibility of large-n ring exchange.

For large n, the exchange rate for a particular ring of n atoms is roughly

$$J\sim\omega_0\exp[-n(V_b ma^2/\hbar^2)^{1/2}]\,, \tag{3.13}$$

with V_b the effective barrier per particle for the intermediate state between $(1,2,3,\ldots n)$ and $(n,1,2,\ldots,n-1)$. An alternative process might be considered in which an interstitial-vacancy pair forms, followed by the migration of the vacancy around the loop and subsequent recombination. In this case the action in Eq. (3.12) may be split into n parts in which the vacancy hops one lattice space in time t:

$$S\sim -nt\left[\frac{1}{2}m\left[\frac{a}{t}\right]^2+V_v\right]\,, \tag{3.14}$$

where V_v is the sum of the vacancy-interstitial formation energy and the barrier to vacancy hopping (the latter is presumably small). Minimizing with respect to t yields

$$J\sim\omega_0\exp[-n(V_v ma^2/\hbar^2)^{1/2}]\,, \tag{3.15}$$

which has the *same dependence on n* as Eq. (3.13). [Roger (1984) incorrectly finds the n dependence $J\sim\exp(-n^{1/2})$ for the latter case: his error arises from taking the geometric path length in the intermediate configuration to be of length $\sim n^{1/2}$ rather than the "taxi-cab" path of lattice hops made by the vacancy which gives a length $\sim n$.] In either case $J(n)$ decreases exponentially with n. Since, however, the *number* of loops of length n in the lattice increases as $e^{\alpha n}$, with α a number of order one, it is conceivable that

$$\alpha>(Vma^2/\hbar^2)^{1/2}\,, \tag{3.16}$$

so that large (in fact, infinite) loops might dominate. [Note that the right-hand side of Eq. (3.16) is similar to the inverse of the Boer parameter.] What would be the implications for the physical states? One possibility is that Eq. (3.16) is inconsistent with the solid state, and the system becomes liquid. More interesting is the possibility that the system remains solid. It is not clear what large exchange loops would imply for the spin state in the Fermi system of ^{3}He. In a Bose system such as ^{4}He infinite-exchange loops would seem, following the argument of Feynman (1953) for the liquid, to lead to a supersolid state. Understanding of multiple exchange from studying ^{3}He may thus have fascinating consequences in other systems, particularly electron crystals.

B. Three- and four-spin ring exchange

Roger, Delrieu, and Hetherington (1980a,1980b,1983) (RDH) have proposed a specific two-parameter spin Hamiltonian for solid ^{3}He. Since this work has been reviewed in depth recently, we refer the reader to that work for a detailed discussion. The philosophy of their work is to find the Hamiltonian with the fewest exchange processes that is consistent with the data. As we have seen, unless there are as yet unknown mechanisms that yield many exchange processes at comparable rates, it is unlikely that different exchange processes will coincidentally have comparable rates. In fact, RDH are forced to use at least two competing processes. Their simplest Hamiltonian contains no two-spin exchange, but instead consists of a three-spin exchange involving two nearest-neighbor pairs and one next-nearest-neighbor pair, and a particular four-spin ring exchange involving a planar nearest-neighbor ring of four atoms. The Hamiltonian can be written

$$\mathscr{H}=-J_t\sum_{ijk}(P_{ijk}+P_{ijk}^{-1})+K_p\sum_{ijkl}(P_{ijkl}+P_{ijkl}^{-1})\,, \tag{3.17}$$

where the sums run, respectively, over all distinct three-spin rings (of the form mentioned above) and all distinct planar four-spin rings. The permutation operator $P_{ijk}\ldots$ cyclically permutes the spins $i,j,k,\ldots$. As discussed above, general arguments lead, with the sign convention (which is the opposite to that of RDH) in Eq. (3.17), to $J_t>0$ (ferromagnetic) $K_p>0$ (antiferromagnetic).

Since any permutation operator may be expressed as the product of pairwise permutations, which in turn can be written in terms of the spin operators via

$$P_{ij}=\tfrac{1}{2}+2\mathbf{S}_i\cdot\mathbf{S}_j\,, \tag{3.2}$$

Eq. (3.17) may be written directly in terms of a spin representation. The three-spin permutation term leads only to pairwise spin interactions involving both nearest and

next-nearest neighbors

$$P_{123}+P_{123}^{-1}=\tfrac{1}{2}+2(\mathbf{S}_1\cdot\mathbf{S}_2+\mathbf{S}_1\cdot\mathbf{S}_3+\mathbf{S}_2\cdot\mathbf{S}_3)\ , \tag{3.18}$$

while the four-spin permutation gives four-spin interactions, as well:

$$\begin{aligned}P_{1234}+P_{1234}^{-1}=&\tfrac{1}{4}+\mathbf{S}_1\cdot\mathbf{S}_2+\mathbf{S}_2\cdot\mathbf{S}_3+\mathbf{S}_3\cdot\mathbf{S}_4\\&+\mathbf{S}_4\cdot\mathbf{S}_1+\mathbf{S}_1\cdot\mathbf{S}_3+\mathbf{S}_2\cdot\mathbf{S}_4\\&+4[(\mathbf{S}_1\cdot\mathbf{S}_2)(\mathbf{S}_3\cdot\mathbf{S}_4)+(\mathbf{S}_2\cdot\mathbf{S}_3)(\mathbf{S}_4\cdot\mathbf{S}_1)\\&-(\mathbf{S}_1\cdot\mathbf{S}_3)(\mathbf{S}_2\cdot\mathbf{S}_4)]\ .\end{aligned} \tag{3.19}$$

It turns out that for high-temperature series calculations the spin representation is easier to use, essentially because $\langle P\rangle\neq 0$ in the high-temperature limit, whereas $\langle \mathbf{S}_i\cdot\mathbf{S}_j\rangle=0$. For other purposes (e.g., ground states) it is often conceptually simpler to work with the permutation operators.

Three-spin ring exchange favors ferromagnetic rings which are clearly eigenstates of P_{ijk} with eigenvalue 1, the maximum possible value. For four-spin exchange, ferromagnetic rings are *least* favorable, the most favorable four-spin states being eigenstates of P_{1234} with eigenvalue -1, i.e., antisymmetric under P_{1234}, for example,

$$\frac{1}{\sqrt{2}}(|\uparrow\downarrow\uparrow\downarrow\rangle-|\downarrow\uparrow\downarrow\uparrow\rangle)\ .$$

If we restrict consideration to Néel-type states, which may be a reasonable approximation for three-dimensional ground states, then the spin-wave function can be expressed as a product of single spin-wave functions, each giving the direction of one spin. In this case the minimum expectation value of P_{1234} is $-\frac{1}{4}$, which is achieved when all the spins rotate by $\pi/2$ around the ring (or by $-\pi/2$), for example, $|\uparrow\rightarrow\downarrow\leftarrow\rangle$.[9] Any ring, except all spins parallel, described by a Néel state involving *only* up and down spins will give $\langle P_{1234}\rangle=0$.

In principle, the two parameters J_t and K_p in (3.17) could be fitted to the two high-temperature series coefficients θ, e_2 in Eqs. (2.35) and then all other properties could be carefully calculated and compared with experiment. For the Hamiltonian Eq. (3.17), we have

$$\begin{aligned}&\theta=18(K_p-2J_t)\ ,\\&e_2^{1/2}=24(J_t^2-\tfrac{7}{8}K_pJ_t+\tfrac{17}{64}K_p^2)^{1/2}\ .\end{aligned} \tag{3.20}$$

Figure 7, taken from Roger *et al.* (1983), shows this graphically. In practice, because of the current controversy over the value of θ discussed in Sec. II.B, the fitting cannot be done with confidence at this stage. In addition, the parameters accurately measured at low temperatures

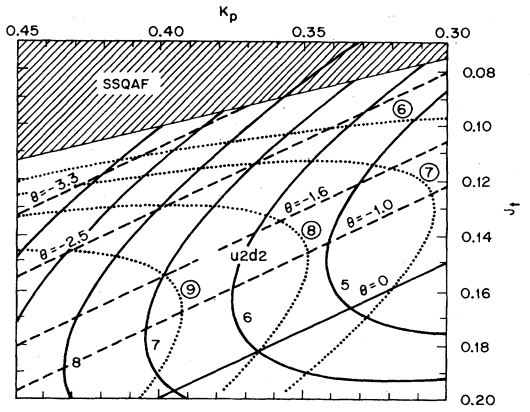

FIG. 7. Calculated quantities for the RDH Hamiltonian [from Roger *et al.* (1983)] with three-spin (J_t) and four-spin (K_p) exchange in mK. The solid lines are contours of constant e_2 [in (mK)^2], the coefficient of the high-temperature $1/T^2$ specific heat; the dashed lines contours of constant Curie-Weiss θ (in mK); and the dotted lines geometric mean spin-wave velocities (in cm/sec) calculated from linear spin-wave theory. In the shaded region the low-field ordered phase in mean-field theory is the SSQUAF phase, while in the rest of the phase diagram it is the u2d2 phase. The best-fit parameters of RDH are $K_p=0.385$ mK and $J_t=0.13$ mK.

have not been *calculated* accurately from the theoretical Hamiltonian (as we have seen in Sec. II.C, zero-point corrections to low-temperature properties seem likely to be very large) and only a qualitative comparison with experiment may be done at this stage. At the end of Appendix A we quote some quadratic spin-wave results for the RDH Hamiltonian.

Roger *et al.* (1983) have recently chosen parameters by fitting to $e_2\simeq 7$ (mK)^2 and to the average spin-wave velocity obtained from the measured T^3 specific heat at low temperatures in Eq. (2.40) and that calculated *without zero-point corrections.* This yields

$$J_t=0.13\text{ mK},\quad K_p=0.385\text{ mK}\ . \tag{3.21}$$

Since the zero-point corrections to the spin-wave velocity may well be large, these may not be the best values to use. RDH have then calculated the phase diagram from Eq. (3.17) using mean-field theory at finite temperatures and the classical Néel approximation to the various ground states. For the parameter values Eq. (3.21) this is shown in Fig. 8. There is certainly a remarkable qualitative agreement with the experimental phase diagram. [See Table I in RDH (1983.)] In particular,

(1) The low-field antiferromagnetic phase below about 1 mK is the u2d2 phase suggested by OCF to be consistent with the symmetry assigned from the NMR.

(2) There is a first-order transition at low temperatures as a function of field from the u2d2 phase to a high-field phase which is cubic (and so consistent with the NMR there) and has a large ($\sim\frac{1}{2}$ saturation at the critical field H_c) weakly field-dependent magnetization. In the RDH

[9] As for two-spin exchange, the classical ground state for a single ring has a considerably higher energy than the quantum ground state.

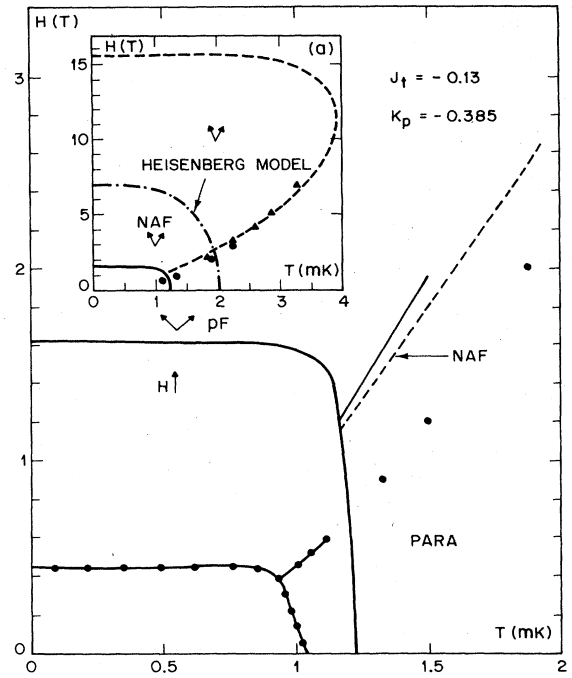

FIG. 8. Mean-field phase diagram for the RDH model with $J_t=0.13$ mK and $K_p=0.385$ mK [from Roger *et al.* (1983)]. The solid lines are predicted first-order transitions and the dashed lines second-order transitions. The circles and triangles are experimental data. The solid lines through the data are guides to the eye. The phase boundary of the spin-$\frac{1}{2}$ nearest-neighbor model is shown as a dot-dashed line for comparison.

model this phase is the NAF phase with a canting of the spins that would persist even in zero field. RDH labeled this phase CNAF (for canted NAF). This state has a broken symmetry transverse to the field and is separated from the paramagnetic phase by a second-order line in RDH's calculation. Whether the high-field phase of solid ^{3}He in fact *has* a spontaneously broken symmetry, and whether a phase boundary (either first order or continuous) *enclosing* the high-field phase exists has not been proven by experiment.

(3) A first-order line ending in a critical point extends upwards from the intersection of the $H_c(T)$ and the $T_c(H)$ lines. The existence of a first-order transition is consistent with the experiments of Osheroff (1982), although it is not known how or whether the line ends.

The greatest discrepancy of Fig. 8 with the experimental phase diagram is that the critical field $H_c(0)$ for the u2d2 to high-field phase transition at zero temperature is predicted (Roger *et al.*, 1983) to be 16 kG—a factor of 4 larger than the experimental value. Although, as we have seen, there may be considerable zero-point fluctuation corrections to the classical approximation (Roger *et al.*, 1983), which yields

$$M_0 H_c \simeq 4(K_p J_t)^{1/2}(2K_p - 3J_t)\ , \tag{3.22}$$

with M_0 the saturation magnetization, it does not seem reasonable that the errors would be so large. The discrepancy is equivalent to an error in the difference in the ground-state energies of the two phases roughly equal to the ground-state energies themselves. Since zero-point corrections lower both energies, it seems unlikely that their inclusion could eliminate the large discrepancy. The first-order spin-wave corrections move the transition field in the wrong direction, to a larger value (Roger *et al.*, 1983). This conclusion is strengthened (as discussed in Sec. IV) by the exact solution of a 16 quantum spin system with the Hamiltonian Eq. (3.17) by Cross and Bhatt (1984); these authors found an H_c very little changed from the classical estimate.

Other details of the phase diagram require further experiment or further theoretical work. For example, the details of the high-field phase to paramagnetic transition warrants additional experimental investigation—even the existence of two transitions cannot confidently be confirmed or ruled out. More accurate calculations of the phase diagram [e.g., a calculation of $T_c(H=0)$ beyond mean-field theory] are also needed to make serious quantitative tests of the model.

As we have said, the choice of values Eq. (3.21) for K_p and J_t is somewhat arbitrary. Some qualitative features of the phase diagram change with fairly small changes in the values. For example, an earlier choice of parameters $J_t=0.1$, $K_p=0.355$ leads to the prediction (Roger *et al.*, 1980a,1980b) of an intermediate helicoidal phase in a magnetic field at about 1 mK. In addition, these values are near to the critical value $K_p/J_t=4$ in the classical approximation to a transition (see Fig. 7) to a different antiferromagnetic ground state of lower symmetry with Roger *et al.* (1980a) labeled SSQUAF for simple square antiferromagnet, a complicated eight sublattice structure. Associated with this proximity is an anomalously soft spin wave, again in the classical approximation, which is too soft to be consistent with the low-temperature experiments. The parameters were, in fact, revised to move the system away from the phase boundary, although the softness of the spin wave at the boundary is actually an artifact of the classical approximation.

To resolve remaining discrepancies, Roger *et al.* (1983) have considered including a third exchange process, although they acknowledge that with each additional parameter the model becomes less attractive—or at least requires a more microscopic justification of the apparently unlikely coincidence necessary to yield several comparable exchange rates. The most promising additional process to include is the two-spin nearest-neighbor antiferromagnetic exchange. This has the effect (Roger *et al.*, 1983; Hetherington and Stipdonk, 1985) of lowering the transition field H_c to the CNAF phase but unfortunately introduces an additional antiferromagnetic phase in zero field at temperatures above T_c (u2d2). This does not seem consistent with experiment (e.g., a susceptibility enhancement is observed in this temperature range rather than a suppression, as might have been expected with antiferromagnetic ordering). Also, the reduction of H_c seems very sensitive to quantum effects (Cross and Bhatt, 1985).

We do not, however, know if H_c can be brought into agreement with experiment while retaining the other qualitatively correct features of the model.

Various authors have studied alternative models with three or more exchange processes. These have a very rich behavior as a function of the relative strengths of the exchanges. Iwahashi and Masuda (1983) have investigated the phase diagram of a model with three-spin (J_t), planar four-spin (K_p), and tetrahedral (folded) four-spin (K_F) exchange and find new "double spiral" states. Other models have been investigated in somewhat less detail. Yosida (1980) investigated possible ground states with large four-spin interactions, $(\mathbf{S}_1\cdot\mathbf{S}_2)(\mathbf{S}_3\cdot\mathbf{S}_4)$, but without maintaining the corresponding two-spin terms in Eq. (3.19); thus this Hamiltonian does not correspond to the permutation processes we have been discussing. Roger *et al.* (1983) have briefly studied four-spin exchange resulting from *rotating* the nearest-neighbor tetrahedron (i.e., two simultaneous pairwise exchanges) rather than permuting them.

C. Coupling of exchange to phonons

An alternative mechanism which goes beyond simple pairwise exchange is to include the coupling of exchange to phonons.

Experimentally it is found that the characteristic exchange energy J has a strong dependence on *static,* long-wavelength volume dilations, quantified by the Gruneisen constant, $\gamma=-d(\ln J)/d(\ln V)$, which is of order 20 in ^{3}He.[10] This has led to the idea that the coupling of spatially separated exchange processes via virtual phonons, leading to more complicated higher-order effective spin couplings, may account for the complex magnetic behavior of ^{3}He. The resulting changes in the high-temperature properties have been investigated by Varma and Nosanow (1970), and some low-temperature effects were considered by Guyer and Kumar (1982). Before we consider the implications of an exchange phonon Hamiltonian, we shall investigate the physical basis of this picture a little further.

Even in the semiclassical limit there remains some controversy over the correct definition of the characteristic time scale for each exchange process as the "barrier residence" time; the best justified value in the semiclassical limit seems to be (Buttiker and Landauer, 1982) the "bounce" time given by $\tau_e\sim l(m/V_{\rm eff})^{1/2}$, with l the path length, m the particle mass, and $V_{\rm eff}$ the barrier potential. With this estimate we find in the semiclassical limit

$$(\omega_0\tau_e)^{-1}\sim(V_{\rm eff}/Kl^2)^{1/2}\ , \tag{3.23}$$

with K the elastic constant per atom, *independent* of $\hbar$. The ratio (3.23) essentially depends on the anharmonicity of the potential, and cannot simply be estimated from the tunneling rate alone. If $\omega_0\tau_e$ turns out to be small, then, as first suggested by Thouless (1965), it may be reasonable to assume that the exchange rate J depends on the instantaneous displacement coordinates of the atoms $\{\mathbf{u}(\mathbf{r})\}$, which are treated in terms of a phonon Hamiltonian. This leads to the Hamiltonian

$$\mathscr{H}=-\sum_{\langle ij\rangle}J_{ij}\{\mathbf{u}(\mathbf{r})\}P_{ij}+\mathscr{H}_{\rm ph}\ , \tag{3.24}$$

where $\mathscr{H}_{\rm ph}$ is the usual phonon Hamiltonian, and the sum in the first term runs over nearest-neighbor pairs.

There are even more difficulties in applying this idea, particularly in the case of solid ^{3}He. There is no doubt that expression (3.24) correctly describes the coupling to *slow,* long-wavelength phonons, leading to a residual power-law interaction between exchange processes at large distances and important consequences for long-wavelength phonon propagation experiments (see Sec. V.B). However, when the phonons are integrated out in the disordered phase, the dominant effect occurs at short distances and comes from the high-frequency, short-wavelength phonons. This introduces two problems. First, at short distances the atomic displacements are necessarily large and a harmonic description would not be expected to be valid. Second, in a highly quantum crystal such as ^{3}He, the short-wavelength phonons are not very well defined excitations, and probably do not describe the fluctuations in the ground state accurately. Furthermore, in the absence of a semiclassical picture for the tunneling, there is no obvious way of deciding if $\omega_0\tau_e$ is in fact small, although a naive estimate evaluating $V_{\rm eff}$ empirically from the ratio J/ω_0 using Eq. (3.13) and using $l\sim a$ and $\omega_0\sim\hbar/ma^2$ leads to the estimate

$$(\omega_0\tau_e)^{-1}\sim\ln(\omega_0/J)\simeq 10\ . \tag{3.25}$$

Despite these difficulties, it remains true that the coupling to lattice fluctuations may be an important effect. This may occur at two levels. First, on the microscopic scale, it may be possible to understand the similarity of many different exchange rates in terms of a common intermediate state of a particular lattice distortion. Second—and this is the main topic of this section—on a macroscopic scale the coupling to a *static* lattice distortion may be the energy driving the magnetic ordering. In the absence of any better description, we shall follow previous authors in using the instantaneous, harmonic approximation to investigate the latter possibility.

Before proceeding with a discussion of the possible ground states of a Hamiltonian of the form Eq. (3.24), we briefly digress to discuss an equivalent spin Hamiltonian. If the coupling of the exchange to phonons is *linear,* i.e.,

$$J_{ij}\{\mathbf{u}(\mathbf{r})\}=\tilde{J}\left[1+\sum_{\mathbf{r}}\mathbf{\Gamma}(\mathbf{r}_i-\mathbf{r},\mathbf{r}_j-\mathbf{r})\cdot\mathbf{u}(\mathbf{r})\right]\ , \tag{3.26}$$

then the phonons can be explicitly integrated out (Varma, 1970) to yield an effective spin Hamiltonian which will

[10] Note that, as pointed out by Thouless (1965), even this Gruneisen constant may be the difference between two larger effects: as the lattice constant is decreased, the distance the atoms must move decreases, increasing J. On the other hand, the volume available for exchange decreases, and hence $V_{\rm eff}$ goes up, *decreasing J,* and dominating the distance effect.

include terms of the form $\mathbf{S}_i\cdot\mathbf{S}_j\mathbf{S}_k\cdot\mathbf{S}_l$, where $\langle ij\rangle$ and $\langle kl\rangle$ are nearest-neighbor pairs and the interaction will be retarded at large enough distances. These are similar, but not identical, to terms generated by four-spin ring exchange. While for calculating certain properties, e.g., at high temperatures, it is convenient to work with an effective four-spin Hamiltonian, for discussing ground states it is more convenient to work with Eq. (3.24), in which the phonons appear explicitly.

The sign of $J_{ij}\{\mathbf{u}(\mathbf{r})\}$ is given by the usual arguments, now considering the *spatial* dependence of the atomic many particle wave functions appropriate to a given set of phonon coordinates. The wave functions *even* under two particle exchange will be lower energy than the odd ones. The overall antisymmetry of the wave functions imposed by the fermionic character of ^{3}He then implies that $J_{ij}\{\mathbf{u}(\mathbf{r})\}<0$ for *all* $\{\mathbf{u}(\mathbf{r})\}$. The same result applies to the effective exchange constant in the disordered phase, which can be thought of as the exchange averaged over the zero-point motion of the phonons: $\tilde{J}=\langle J_{ij}\{\mathbf{u}(\mathbf{r})\}\rangle$. In the presence of a *static* distortion $\{\mathbf{u}_s(\mathbf{r})\}$ (or equivalently a strain) the effective exchange, now depending on position, will be $\tilde{J}_{ij}\{\mathbf{u}_s\}=\langle J_{ij}\{\mathbf{u}_s(\mathbf{r})+\delta\mathbf{u}_s(\mathbf{r})\}\rangle$, where the average is over the zero-point motions $\{\delta\mathbf{u}_s(\mathbf{r})\}$ about the distorted state.

The logarithmic derivatives $\tilde{J}_{ij}$ with respect to a local fractional static distortion $\mathbf{u}_s(\mathbf{r}_i)/a$ will have a characteristic magnitude[11] Γ which is of order γ_J. In an antiferromagnetic ground state, there will be a *static* phonon distortion with displacements $\mathbf{u}_s\simeq\Gamma\tilde{J}a/K$, where $K\sim 20$ K is a characteristic elastic constant per atom of solid ^{3}He. The reduction in ground-state energy per atom, ΔE, due to the lattice distortion will be of order

$$\Delta E\sim-\frac{1}{2}\frac{(\Gamma\tilde{J})^2}{K}\ . \tag{3.27}$$

It is possible that the dependence of the exchange rate on a zone-boundary distortion will be considerably larger than on a uniform compression. The appropriate coefficient Γ entering Eq. (3.27) might thus be larger than γ_J. If, for definiteness, we take $\Gamma\simeq 100$ and $\tilde{J}\simeq 1$ mK, we obtain $\Delta E\simeq -0.5$ mK, which is of the order of $\tilde{J}$. It thus appears just possible, in principle, that the coupling of exchange to phonons might lower the energy of an antiferromagnetic ground state other than NAF by enough to give it the lowest total energy. As we shall see, however, this is unlikely to be the case.

We first consider the possible classical Néel ground state of Eq. (3.24), i.e., we ignore quantum spin-wave fluctuations. In this approximation the spins $\mathbf{S}_i$ are just vectors with magnitude $\frac{1}{2}$, and hence the permutation operators P_{ij} become numbers $\bar{P}_{ij}$ with $0\le\bar{P}_{ij}\le 1$. It is now simple to compare the ground-state energies of the NAF state with another state, S, in which the $\bar{P}_{ij}$ assume values $\bar{P}^S_{ij}$. The energy, E_S, of state S will be the ground-state energy, with corresponding phonon wave function ψ_S of the purely phonon Hamiltonian

$$\bar{\mathscr{H}}_S=-\sum_{\langle ij\rangle}J_{ij}\{\mathbf{u}(\mathbf{r})\}\bar{P}^S_{ij}+\mathscr{H}_{\rm ph}\ , \tag{3.28}$$

with $\bar{P}^S_{ij}$ the fixed numbers. In the NAF state, all the nearest-neighbor pairs are antiferromagnetically aligned and hence all $\bar{P}_{ij}$ are zero. In the classical spin approximation, the NAF energy, $E_{\rm NAF}$, is thus the (trivial) ground-state energy of

$$\bar{\mathscr{H}}_{\rm NAF}=\mathscr{H}_{\rm ph}=\bar{\mathscr{H}}_S+\sum_{\langle ij\rangle}J_{ij}\{\mathbf{u}(\mathbf{r})\}\bar{P}^S_{ij}\ , \tag{3.29}$$

where we have substituted Eq. (3.28). A lower bound for E_S can be established variationally by noting that

$$\begin{aligned}E_{\rm NAF}&\le\langle\psi_S\,|\,\bar{\mathscr{H}}_{\rm NAF}\,|\,\psi_S\rangle\\&=E_S+\left\langle\psi_S\left|\sum_{\langle ij\rangle}J_{ij}\{\mathbf{u}(\mathbf{r})\}\bar{P}^S_{ij}\right|\psi_S\right\rangle\\&<E_S\ ,\end{aligned} \tag{3.30}$$

where the second inequality follows by observing that $\bar{P}^S_{ij}J_{ij}\{\mathbf{u}(\mathbf{r})\}$ is strictly negative for some pairs $\langle ij\rangle$, and zero for the rest. We thus conclude that in the classical spin approximation the NAF state will always have the lowest energy.

Lieb and Fisher (1981) have gone on to prove that for the *quantum* spin-$\frac{1}{2}$ case, a similar result holds: for Hamiltonians of the form (3.25) with all $J_{ij}\{\mathbf{u}(\mathbf{r})\}$ negative, all the body-centered spins will be antiferromagnetically correlated with all the body corner spins and ferromagnetically correlated with each other at all temperatures. This implies the desired result that phonon coupling of nearest-neighbor exchanges cannot give rise to the u2d2 antiferromagnetic state.

Guyer and Kumar (1982) have got around this result by invoking an "effective" distortion-dependent nearest-neighbor exchange which can be either ferromagnetic or antiferromagnetic. However, since this effective exchange must result from a combination of other more complicated exchange processes, and since we have seen that the u2d2 phases arise naturally from just two competing exchange processes, it does not appear necessary at this stage to invoke both phonon coupling and multiple-exchange processes in order to explain only the nature of the low-field phase.

We have just argued that distortion-dependent nearest-neighbor exchange cannot yield the phase suggested by OCF. It is natural to ask whether another phase which has the observed symmetries could be induced by such couplings. From the Lieb-Fisher result, we know that the *sign* of the spin correlations must be the same as for NAF, i.e., positive for all pairs on the same cubic sublattice and negative between the sublattices. This leaves

[11] We shall use capital Γ's to denote Gruneisen constants defined as derivative with respect to strains and small γ's those with respect to volume.

open the possibility that the *magnitude* of the correlations for different originally equal spaced pairs varies in such a way that the phase does not have the cubic symmetry of the NAF phase. In Appendix B we discuss a novel phase of this kind which is based on the spin analogy of a Peierls instability of a uniform antiferromagnetic chain and we call this the SPNAF (for spin-Peierls NAF) phase.

D. Zero-point vacancies

An alternative explanation that has been proposed for the anomalous magnetic properties of solid ^{3}He invokes the existence of "zero-point vacancies," that is, a finite concentration of vacancy defects such that in the ground-state wave function the number of lattice sites is not equal to the number of atoms. Note that this is *not* the same as a ground state containing fluctuations of vacancy-interstitial pairs: such a fluctuation conserves the total particle number; the vacancy-interstitial fluctuation may facilitate the exchange processes but is not intrinsically a separate process. The possibility of zero-point vacancies was suggested by Andreev and Lifshitz (1969), who argued that the decrease in energy (zt, with z the number of nearest neighbors and t the hopping matrix element) of the vacancy due to quantum hopping (the banding energy) could overcome the "classical" activation energy of a localized vacancy, E_v. For the bcc lattice this requires

$$8t > E_v \ . \tag{3.31}$$

Estimates of E_v from activated thermal processes suggest $E_v \sim 10$ K, but perhaps it could be as low as 1 K or less near the melting curve. Estimates of t from nuclear-spin relaxation rates suggest $t \sim 20$ mK, so that the inequality Eq. (3.31) is not totally unreasonable. The nature of the system if Eq. (3.31) is satisfied is much less clear, however.

The properties of an isolated vacancy in a fermion lattice have been studied in considerable detail (Nagaoka, 1966; Brinkman and Rice, 1970). It is easy to see that the passage of a vacancy around an even (odd) ring in the lattice leads to an odd (even) permutation of the spins on the occupied sites of the ring. Thus, following the argument of Thouless (1965) given in Sec. III.A for conventional exchange, if all the rings are even, the vacancy leads to a *ferromagnetic* tendency in the lattice. (The lowest energy vacancy wave function has $\mathbf{k}=0$ and does not introduce additional sign changes.) This is the case for the bcc ^{3}He lattice if the hops are restricted to nearest neighbors, which seems a reasonable first guess in the absence of the steric effects which suppress nearest-neighbor exchange in the absence of vacancies. The energy of the ferromagnetic state is lowered due to the vacancy hopping by exactly the banding energy $8t$/vacancy. A transition to the ferromagnetic state would therefore be expected when this ferromagnetic tendency exceeds any competing antiferromagnetic tendencies due to direct exchange, i.e., for a vacancy concentration x_v (assumed small) given by

$$zx_v t \gtrsim J \tag{3.32}$$

or for temperatures given by the competition between the energy reduction and the ln2 entropy per spin of the otherwise degenerate spin system:

$$zx_v t \gtrsim T \ln 2 \ . \tag{3.33}$$

For smaller vacancy concentrations Andreev (1976) suggested the existence of magnetic polarons, namely, regions of ferromagnetically aligned spins in which each vacancy is bound and in which the vacancy hops. The radius of the polaron, given roughly by minimizing the total free energy, is

$$R \sim \left[\frac{\pi t}{\theta + 2T \ln 2} \right]^{1/5} .$$

Montambaux *et al.* (1982) have studied more sophisticated versions of such a theory.

[The situation in a lattice containing odd-membered nearest-neighbor rings, or when further neighbor hopping of the vacancy is allowed, is much more complicated. In this case, since the contribution of large rings and small rings alike is $O(t)$, only a detailed combinatoric analysis can determine the ground state.]

The attractive feature of the zero-point vacancy model in accounting for the magnetic properties of solid ^{3}He is the natural introduction of a ferromagnetic tendency into the system. Thus for $T \lesssim t$ the formation of easily aligned magnetic polarons may be used to explain the anomalous tendency (beyond the simplest exchange models) towards ferromagnetism apparent in the observed magnetic susceptibility (Prewitt and Goodkind, 1977) and the excess specific heat (Halperin *et al.*, 1974) below 20 mK. On the other hand, the theoretical analysis and predictions of the model are far from complete. In particular, no prediction of an ordered state below 1 mK consistent with the symmetries deduced from the NMR has been made from the model. Also, no reasonable explanation has been given for the very small concentration $x_v \sim 10^{-4}$, needed to fit the energy scale of the magnetic anomalies. On the basis of the competition between the two large energies introduced in (3.30) it is very hard to see why the concentration of the weakly interacting vacancies should remain so small. The magnetic interactions between the polarons are weak, but attractive, and the repulsive kinetic energy is small. The elastic interaction of the vacancies is also weak at these concentrations, although perhaps comparable to the magnetic interactions. Thus there seems to be no repulsive interaction strong enough to lead an equilibrium concentration as small as 10^{-4}. In fact, the interaction may well be attractive, leading to phase separation. On the other hand, the properties of a system with a much larger number of vacancies are extremely uncertain: it is not at all clear that such a system would in fact be a solid. No anomalous dependence of the ordering transition on density near the melting curve, where the concentrations of vacancies might be anomalously large, is seen, nor does the magnetic behavior depend on whether the ordered solid is grown from the liquid or cooled from a

high-temperature solid. Thus the suggestion of metastable trapped spin polarons is untenable as an explanation of most of the magnetic properties.

It is conceivable that vacancies may explain some of the anomalous results that do not seem to fit in with other general frameworks [e.g., the specific-heat anomaly seen in some samples at around 100 mK (Castles and Adams, 1975) or the susceptibility anomaly of Kirk *et al.*, 1984] for small ranges of parameters near melting or in poor samples. The nature of the solid near the minimum of the melting curve where the concentration of thermally activated vacancies apparently grows considerably may be particularly interesting to investigate further. (For example, a sudden proliferation of vacancies should affect the plasticity of the crystal due to the additional dislocation motion.) However, we do not see any indication that the concept of zero-point vacancies is likely to explain the bulk of the magnetic properties of solid ^{3}He.

IV. THEORETICAL PROSPECTS

In this section, we discuss the current level of understanding and explore the prospects for advances in the theoretical understanding both of the microscopic exchange rates and the behavior of candidate quantum spin Hamiltonians.

A. Calculation of exchange rates

1. General comments

Although a considerable amount of effort has been put into the calculation of exchange rates, there remains no method that is *a priori* convincing at a fundamental level. Quite good accounts of experimental trends have been displayed using simple approximations that approach the problem from dramatically opposite points of view—for example, simple estimates based on a hard-sphere model in which all the energy is kinetic, or conventional WKB calculations in which the kinetic energy is assumed small compared with the repulsive potential energy. Both have yielded ordering of the various exchange rates consistent with experimental deductions, and reasonable results for the density dependence of the exchange (Roger *et al.*, 1983; Roger, 1984). Yet neither of these approaches, at least in their present forms, is reasonable at the densities in the bcc phase or even at somewhat higher densities. It seems to us that the important physics involved in a quantitative determination of the exchange rates has not yet been elucidated. The rough agreement (either obtained directly or by further adjustments to the calculation) between theories using opposite approximations and the experimental trends simply does not help in this quest.

The great difficulty in calculating exchange rates in solid ^{3}He arises from the fact that ^{3}He forms a highly quantum solid, but one in which the exchange rate is very small ($J/\omega_0 \sim 10^{-4}$ with ω_0 the attempt frequency, of order of the local oscillation frequency). Thus in terms of the de Boer quantum parameter $\Lambda = \hbar/\sigma(m\varepsilon)^{1/2}$ the estimates for the potential energy E_P, oscillation frequency ω_0, and exchange rate J would be (cf. Anderson, 1984)

$$E_P : \omega_0 : J \sim 1 : \Lambda : \Lambda e^{-c/\Lambda} , \tag{4.1}$$

with the constant c naively expected to be $O(1)$. The highly quantum nature of ^{3}He is demonstrated by the equality over a wide density range between the potential and kinetic energy in the ground state. This is consistent with the estimate $\Lambda \sim 1$. The small value of J compared with the value then given by Eq. (4.1) is probably a real effect due to the additional reduction in J arising from the strong steric impedance caused by the hard core of the repulsive interaction, which is not adequately described by the single parameter Λ. The upshot of this is that exchange cannot be calculated in terms of small quantum fluctuations about a well-defined classical ground state (which would in any case be locally unstable at densities corresponding to the melting pressure), yet a full quantum calculation is extremely hard since knowledge of the wave function is required in regions where it is very small and to which most approximate calculational schemes (e.g., variational) are completely insensitive.

Rather good accounts of the *lattice* properties of solid ^{3}He are given by variational methods with trial functions involving Gaussian fluctuations of each atom about a lattice site together with a Jastrow correlation between neighboring atoms. It is now abundantly clear, however, that calculations of the exchange rates based on the variational wave function, although historically important in suggesting the importance of higher-order exchange process (McMahan and Wilkins, 1975), are not correct: the method is insensitive to the form of the tail of the wave function that is critical in calculating exchange rates. We will not discuss further these variational calculations of the lattice properties, since this subject has been well reviewed (Varma and Werthamer, 1976; McMahan, 1972). It will, however, be useful to consider two phenomenological, highly approximate treatments, to investigate which features of the system are important in the large probability configurations determining the lattice properties, and also perhaps in the low probability configurations of the exchange "barriers."

Perhaps the most appealing caricature is that the solid can be understood as a collection of hard spheres. This has been discussed in some detail by Guyer (1974). The important energy is then the kinetic energy of zero-point motion, which might be estimated as the kinetic energy of an atom in a spherical free volume of radius $a-b$, with a the nearest-neighbor spacing and b the hard-sphere radius:

$$E_k \simeq \frac{\hbar^2}{2m}\frac{\pi^2}{(a-b)^2} . \tag{4.2}$$

This energy then competes with the externally applied pressure P—the lack of binding at low pressures is of little consequence, since the solid becomes unstable to the

liquid phase there. With suitable choices of the hard-sphere radius b and with a different numerical proportionality constant in E_k, Guyer finds reasonable agreement for the lattice parameter $a(P)$. In this vein, it is interesting to note that for $(a-b)/a$ small Eq. (4.2) leads to the volume dependences for the pressure and compressibility κ:

$$\gamma_P=\frac{\partial \ln P}{\partial \ln V}\sim\frac{a}{a-b}$$
$$\gamma_\kappa=\frac{\partial \ln \kappa}{\partial \ln V}\sim\frac{4}{3}\frac{a}{a-b}\ . \tag{4.3}$$

Taking the radius b to be the Lennard-Jones parameter σ gives $\gamma_\kappa\sim 4$ at melting pressure and $\gamma_\kappa\sim 5$ at a volume of 21 cm^3/mole, in rough agreement with experiment.

A more stringent test of this picture is given by the calculations of Kalos *et al.* (1974). These authors divide the potential $V(r)$ up into a repulsive core

$$V_r(r)=\begin{cases} V(r)-\varepsilon_0, & r<r_0 \\ 0, & r>r_0\ , \end{cases} \tag{4.4}$$

with ε_0 the energy minimum at radius r_0, and an attractive part

$$V_a(r)=\begin{cases} +\varepsilon_0, & r<r_0 \\ V(r), & r>r_0\ . \end{cases} \tag{4.5}$$

They then suggest that the repulsive part $V_r(r)$ can be replaced by a hard sphere of radius equal to the zero-energy scattering length $b=0.84\sigma$. Futhermore, they propose that the wave function at a fixed density is rather insensitive to the slowly varying attractive potential, which can then be included in lowest-order perturbation theory, i.e., as the expectation value $\langle\psi_0|\,V_a(r)\,|\psi_0\rangle$ with ψ_0 the hard-sphere wave function. These suggestions are then tested by comparison with variational calculations using the full potential on the fcc phase of solid ^{4}He for densities 24 to 16 cm^3/mole; similar conclusions would be expected for ^{3}He. Their results are displayed in Table I. Interesting points to note are that the kinetic energy, as pointed out by Roger (1984), agrees quite well with the simple expression Eq. (4.2), with the prefactor differing only by 20% and varying by less than 10% as the kinetic energy varies over a factor of 4. However, the attractive part of the potential provides a large canceling contribution not only to the ground-state energy at one volume, but also to the *volume dependence* of this energy. Thus the agreement between a pure hard-sphere model neglecting the attractive potential and experimental trends in the lattice properties seems to be spurious.

An alternative, less attractive picture that has been put forward by Avilov and Iordansky (1982) and by Roger (1984) is that the high-density limit, where the energy is dominated by the detailed form of the repulsive part of the potential

$$V(r)\simeq+4\varepsilon\left[\frac{\sigma}{r}\right]^{12}, \tag{4.6}$$

has some relevance to the properties at experimentally accessible densities. Since quantum fluctuations are small in this limit, calculations based on this model are very much more straightforward. This intrinsically unlikely model is given some credence by the observed scaling of various lattice quantities with volume in rough agreement with predictions based on the r^{-12} form, e.g., P, $\kappa\propto V^5$, and the Debye temperature $\theta_D\propto V^{-7/3}$. However, this model requires a remarkably exact cancellation of the other, larger, energies in the problem, and in view of the alternative explanation of these scalings in terms of the hard-sphere model, we are inclined to view these successes as pure coincidences.

It is instructive to attempt to estimate the range of validity of the high-density limit. We shall do this by comparing the potential energy with the zero-point kinetic energy. The latter is estimated as the harmonic-oscillator energy $\frac{1}{2}\hbar\omega_0$ for the one-dimensional motion of an atom along a line to two of its nearest neighbors that are assumed fixed. The high-density approximation should be good if the zero-point kinetic energy is small compared with the potential energy. For a displacement x the potential is taken to be

TABLE I. Energies calculated for fcc solid ^{4}He by Kalos *et al.* (1976). E_H is the energy for hard spheres, with radius $b=0.84\sigma$, with σ the Lennard-Jones parameter. $\langle V_a\rangle$ is the expectation value of the attractive part of the potential Eq. (4.5) in the hard-sphere ground-state wave function. E_p is the sum $E_H+\langle V_a\rangle$, which is the estimate of the ground-state energy of the Lennard-Jones potential. It agrees well with the calculation on the full potential, E_v. All calculations are based on variational Jastrow wave functions.

Nearest-neighbor spacing a (Å)	Vol/mole (cm^3)	E_H (K)	$\langle V_a\rangle$ (K)	E_p (K)	E_v (K)	$\frac{E_H}{\hbar^2/m}(a-b)^2$
3.85	24.2	23.3	−28.4	−5.1	−4.9	5.6
3.72	21.8	27.9	−32.7	−4.8	−4.8	5.7
3.59	19.6	33.4	−36.5	−3.1	−3.9	5.8
3.41	16.8	44.2	−44.6	−0.4	−1.4	5.9
3.26	14.7	57.7	−54.9	2.9	3.2	6.0
3.03	11.8	93.5	−66.0	27.5	22.8	6.1

$$V(x)=4\varepsilon\left[\left[\frac{\sigma}{a-x}\right]^{12}+\left[\frac{\sigma}{a+x}\right]^{12}\right], \tag{4.7}$$

where we are neglecting the contribution from other neighbors. This gives the ratio

$$\frac{\frac{1}{2}\hbar\omega_0}{V(0)}\simeq 2\Lambda\left[\frac{a}{\sigma}\right]^5, \tag{4.8}$$

where $\Lambda=0.5$ is the de Boer parameter. Thus the zero-point kinetic energy is comparable to the potential energy up to $a\sim\sigma$, corresponding to densities of 8 cm^3/mole.

Applying either of these simple pictures to the low probability configurations important in exchange is more problematical.

To consider the validity of the hard-sphere model we should first estimate the energies involved in the exchange configuration. From the WKB expression for the tunneling rate we would estimate the maximum energy of an exchanging particle to be (cf. Sec. III.A)

$$V_{\text{eff}}\sim\left[\frac{\hbar^2}{ma^2}\right]\left[\frac{1}{n}\ln\left[\frac{\omega_0}{J}\right]\right]^2, \tag{4.9}$$

where N is the order of the exchange process. Since the first quantity in large parentheses is a few degrees, and $\ln\omega_0/J$ is of order 10, we see that the energy in the barrier configuration per particle for multiple-exchange processes is not enormously greater than the ground-state energies. This suggests that the penetration into the hard sphere may not be an important effect. Again, the role of the attractive part of the potential is harder to estimate. The rather flat attractive potential might be expected to have a relatively small effect on the motion of a single particle in the static field of its neighbors. If, however, as seems likely, exchange involves the collective motion of a small cluster, the energy may be significantly changed—for example, by changing the local density.

The range of validity of the semiclassical high-density approximation to the exchange configuration should be easier to assess. For example, for the four-particle exchange barrier in the bcc lattice Roger (1984) finds in this approximation a change from the ground-state repulsive potential, given in dimensionless form by

$$\delta\left[\sum_{i<j}\left[\frac{a}{r_{ij}}\right]^{12}\right]\simeq 40, \tag{4.10}$$

with a the equilibrium lattice spacing. Simply dividing this by four, corresponding to the four exchanging particles, leads to an upper bound for the minimum separation r in the exchange configuration

$$\left[\frac{a}{r}\right]<1.2. \tag{4.11}$$

We may compare the transverse kinetic energy of localization with the potential energy in the exchange configuration, again using the harmonic oscillator approximation. Then replacing a by r in Eq. (4.8) would suggest that the semiclassical approximation to the exchange barrier is reasonable only for $a\lesssim 1.2\sigma$, corresponding to densities certainly less than 13 cm^3/mole. It therefore seems that towards melting pressure, a semiclassical description of even part of the tunneling path will not be adequate for multiple exchange.

2. Specific calculations

The early work based on the Gaussian variational wave function has been reviewed by a number of authors. In a number of papers Roger, Delrieu, and Hetherington (see Roger *et al.*, 1983, and references therein) have pointed out the inadequacy of the early work, and have attempted to go beyond the estimates based on these correlated Gaussian wave functions. It seems to us that the only approach discussed there that potentially goes beyond an illustrative level is a one-dimensional variational calculation.

The idea of the one-dimensional variational calculation (Roger *et al.*, 1980b) is to use as a variational trial function

$$\psi(r)=\varphi_G(\mathbf{r})f(\tau(\mathbf{r})), \tag{4.12}$$

where $\varphi_G(\mathbf{r})$ is the Jastrow-correlated Gaussian wave function for the $3N$-dimensional coordinate $\mathbf{r}$ chosen to describe the lattice dynamics and $f(\tau)$ is the variational function, with $\tau(\mathbf{r})$ the projection along an "exchange path" between the two configurations connected by the exchange process. The wave function φ_G may either be the "home-based" wave function, as introduced by Herring (1962), or a wave function symmetrized between the two configurations connected by the exchange. The idea is that the function $f(\tau)$ corrects the Gaussian falloff of φ_G in the tails of the wave function into a form more appropriate for a tunneling problem. The function $f(\tau)$ is determined by minimizing the total energy. No algorithm is given by Roger *et al.* (1980b) for choosing the best $\tau(\mathbf{r})$. Instead they specialize immediately to a straight-line path, which implies that the function

$$\bar{f}=f\langle\varphi_G^2\rangle_\perp \tag{4.13}$$

satisfies a one-dimensional Schrödinger equation with an effective potential

$$U(\tau)=\frac{\langle V\varphi^2\rangle_\perp}{\langle\varphi^2\rangle_\perp}-\frac{1}{2}\frac{\langle\varphi^2\nabla^2\ln\varphi\rangle_\perp}{\langle\varphi^2\rangle_\perp}+\frac{1}{4}\frac{\partial^2}{\partial t^2}\ln\langle\varphi^2\rangle_\perp, \tag{4.14}$$

where V is the interatomic potential and $\langle\ \rangle_\perp$ signifies the average over the coordinates transverse to $\tau(\mathbf{r})$. This potential has the appealing feature of adding to the tunneling barrier a contribution from the transverse kinetic energy due to the particle localization. However, as a practical calculational scheme this method would be expected to suffer the same problems as all direct variational methods, namely, the insensitivity of a variational calculation based on the total energy to the tails of the wave

function. Thus, although Eq. (4.13) is certainly a better approximation than the Gaussian part φ_G, the important corrections to the energy will again come from the regions where the wave function is moderately large, and the determination of $f(\tau)$ will be dominated by these regions. The tails of the wave function will be better given, but, since the energy scale of the total energy is of order 10 K, there is no reason to expect an accuracy of better than 2 or 3 orders of magnitude in the exchange energy. In addition, different exchange processes will, due to the different choice of the coordinate $\tau(\mathbf{r})$, lead to different corrections to φ_G in the moderately large probability regions; thus comparisons of various exchange rates are not likely to be even approximately valid.

Delrieu and Sullivan (1981) suggest an estimate of the exchange barrier as the extra elastic energy due to the local compression in the exchange configuration. Although this effect may well be important, their calculation of this elastic energy involves arbitrary renormalizations, so that their calculations cannot be considered quantitative.

More recently there have appeared semiclassical calculations valid in a very-high—density limit. Although there is no reason to believe that these approaches are valid at low densities (as discussed earlier), a number of interesting points do come out of this work. In an asymptotically high-density limit the usual WKB method for calculating tunneling rates becomes a good approximation. The tunneling path is the path that minimizes the action. Since that is given by a classical dynamical problem in the inverted potential, with modern computing powers the minimum action can, with sufficient effort, be calculated as accurately as desired, even including many-particle correlations in three-dimensional systems. Roger (1984) has pursued this program. In the hcp phase expected in the high-density limit he finds that triple exchange in the basal plane dominates, followed closely by triple exchange out of this plane. Roger (1984) also investigates the bcc phase in the high-density limit. He finds in an approximate calculation of the asymptotic limit

$$\begin{aligned} K_p &\cong \exp(-8.47 g^{-1}) , \\ J_t &\cong \exp(-9.27 g^{-1}) , \\ J &\cong \exp(-9.78 g^{-1}) , \end{aligned} \tag{4.15}$$

with J the nearest-neighbor exchange and

$$g = \Lambda (a/\sigma)^5 / 2\sqrt{2} . \tag{4.16}$$

(His exact calculation for J_t in which 9.27 is replaced by 9.09 gives some idea of the validity of the particular approximation.) Thus the ordering of exchange constants is consistent with the experimental deductions at melting pressure, although we reiterate that by any reasonable criteria the high-density limit should not be valid at these densities.

Avilov and Iordansky (1982) have attempted to extend the WKB approach to lower densities by matching the WKB calculation of the tunneling path in the repulsive r^{-12} potential that becomes more important near the barrier configuration to a phenomenological elastic description in the high-probability regions. Thus the small displacements from the initial configuration are supposed to be determined by the harmonic force matrix, derived by inverting the phonon spectrum. Clearly for the atoms actually exchanging, the harmonic approximation breaks down at large displacements; here Avilov and Iordansky suppose that the repulsive part of the potential dominates. It seems to us that there are two flaws in this interesting approach that warrant further attention. The first is a conceptual problem: the phonon theory describes the oscillations of some effective atom smeared out by the rapid, short-length scale zero-point motion, and it is not obviously trivial to match this to the semiclassical tunneling of the atoms at large displacements. Second, it is clear that the anharmonic corrections are not simply an increase in the repulsive force for particles at *small* separations, but also a reduction of the attractive forces for particles that have separated to large distances from their initial neighbors. This can be seen best by considering a harmonic lattice consisting of particles connected by springs: an exchange process clearly requires the cutting of some springs that are stretched too far and a reconnection of others to return the lattice to the original topology after the exchange process. The phenomenological harmonic force matrix for solid ^{3}He will typically couple many neighbors with effective springs, requiring a complicated "reconnection" process at the exchange configuration which is not adequately taken into account by Avilov and Iordansky.

3. Effects of pressure

The idea that the magnetic properties of solid ^{3}He result from a delicate competition between antiferromagnetic and ferromagnetic interactions leads to the obvious suggestion that varying the density of the solid may, by changing the relative strengths of the interactions, lead to dramatic effects. It seems conceivable that the small antiferromagnetic region of the phase diagram might be suppressed altogether, or replaced by an alternative antiferromagnetic phase. For example, in the competing three-spin four-spin multiple-exchange Hamiltonian of RDH the SSQUAF phase is predicted to occur at slightly larger values of K_p/J_t [Roger *et al.* (1980a); see Fig. 7] such as might be expected on increasing the density.

Although the detailed structure of the phase diagram has not yet been investigated as a function of molar volume, a large number of parameters that have been measured show a remarkably similar volume dependence (Pancyzk and Adams, 1970; Mamiya *et al.*, 1981; Hata *et al.*, 1981,1983; Devoret *et al.*, 1982; Shigi *et al.*, 1983), with no evidence of a relative change in competing parameters. The experimental results can be summarized as

$$J_{\text{eff}} \propto V^{\gamma} , \tag{4.17}$$

with

$$\gamma = 18 \pm 2 , \tag{4.18}$$

where J_{eff} is a quantity with the dimensions of frequency. The power-law dependence is assumed *a priori*— the data do not usually provide a precise test. The range of values we quote for γ include the error bars for each fit, and the range of values derived for different quantities: the two ranges are quite comparable. The range of volumes used is typically about 22–24 cm^3/mole, corresponding to a range in J_{eff} of about a factor of 5. Quantities varying in this way include the nuclear relaxation times T_1 and T_2, the first two parameters derived from the high-temperature expansion of $P(T,V)$, the Néel temperature T_N, and the susceptibility at T_N. In addition, a direct scaling of the magnetization $M(T)/M(T_N)$ with T/T_N has been demonstrated more precisely but over a smaller range of volumes 23–24 cm^3/mole (Hata *et al.*, 1983; Shigi *et al.*, 1983). The variation of the Curie-Weiss constant over a wide range of volume is not clear at this stage because of the discrepancies discussed in Sec. II.B. As discussed there, one possible resolution of the discrepancy involves assuming a quite different form for $\theta(V)$. This is a very important question to resolve, since of all quantities the Curie-Weiss constant may be expected to be the most sensitive to the change in the relative strengths of ferromagnetic and antiferromagnetic interactions. The pressure dependence of the transition field H_c to the high-field phase has not been measured—it might also be expected to be rather sensitive to competing exchanges.

How does the result Eq. (4.17) agree with theoretical expectations? If we assume, for example, a relationship

$$J_{\text{eff}} = \alpha J_1 + \beta J_2 , \tag{4.19}$$

with J_1 and J_2 the basic interactions, we obviously find

$$\gamma_{\text{eff}} = \frac{\left[\frac{\alpha J_1}{\beta J_2}\right]\gamma_1 + \gamma_2}{\left[\frac{\alpha J_1}{\beta J_2}\right] + 1} , \tag{4.20}$$

where γ_i is the power law volume dependence of J_i. Thus for quantities involving both processes with comparable strengths ($\alpha J_1 \sim \beta J_2$), if γ_1 and γ_2 were significantly different as would be naively expected, then the γ_{eff} for different quantities should vary widely. [The same conclusion of course holds for more complicated relationships than Eq. (4.19).] We are thus forced to conclude either that only one process is involved in all the magnetic interactions, or that the two (or more) different processes must for some reason have a rather similar volume dependence, i.e., γ_1/γ_2 is unity to within 20%.

It is interesting to consider the multiple-exchange model from this point of view. At first sight three- and four-spin exchange would be assigned quite different volume dependence: naively one supposes that the greater steric impedance effects on the three-spin exchange are compensated, at melting pressure, by the larger number of particles involved in four-spin exchange. At higher densities four-spin exchange would be expected to dominate. If, however, only one part of the interatomic energy dominates the exchange process, one might expect that

$$J_i \sim \omega_i e^{-\mu_i / g(V)} , \tag{4.21}$$

where ω_i and the barrier parameter μ_i are different for different processes, but the volume dependence of the barrier factor $g(V)$ is the same for all processes. Then one roughly finds (for $J_i \sim 1$ mK, $\omega_i \sim 10$ K)

$$\frac{\gamma_1}{\gamma_2} = \frac{\mu_1}{\mu_2} \simeq 1 + \zeta \ln\left[\frac{J_1}{J_2}\frac{\omega_2}{\omega_1}\right] , \tag{4.22}$$

where

$$\zeta = [\ln(\omega/J)]^{-1} \sim 0.1 . \tag{4.23}$$

Thus the Gruneisen constants $\gamma_{1,2}$ would be similar to within 10% for $J_{1,2}$ roughly comparable. The validity of Eq. (4.21) is therefore an interesting conjecture. It is valid in the very-high–density limit, where only the repulsive part of the potential is important. Then

$$g(V) = (\hbar/m\sigma^2\varepsilon)^{1/2}(a/\sigma)^5 2\sqrt{2} , \tag{4.24}$$

where the first factor is the de Boer quantum parameter, a is the nearest-neighbor spacing, and σ is the Lennard-Jones length parameter. The μ_i are then pure numbers for the different processes. In the hard-sphere model all energies are kinetic

$$E_k \sim \frac{\hbar^2}{2m}\frac{1}{(\Delta x)^2} , \tag{4.25}$$

but since different lengths Δx may be identified that involve different combinations of the lattice parameter a and the hard-core radius b the simple expression Eq. (4.21) is not obvious.

The unexpectedly similar volume dependence of many quantities leads (subject to further experimental work) to the following conclusion: The complicated magnetic properties observed at melting pressure are probably *not the result of a fortuitous competition at only one density.* There is, however, no real understanding of the mechanism behind the rough equality over the range of volumes of interest.

One possible mechanism which might yield this rough equality of exchanges for a range of volumes involves rare large fluctuations of the neighboring atoms of those exchanging. If the dominant contribution to the actions which control exchange rates is caused by a shell of neighboring atoms collectively expanding to allow the exchanges, then it is possible that the action for *one* such event could control several exchange processes. For example, if the effective volume of four neighbors was increased to that characteristic of the liquid, then several exchange processes could take place among the four particles. This qualitative idea may well be worth pursuing.

B. Solution of effective spin Hamiltonians

In the preceding section, some of the difficulties associated with deriving a spin Hamiltonian from first principles were discussed. We now go to the next level, and assume that the spin Hamiltonian is known and then ask what macroscopic properties can be reliably derived from the candidate quantum spin Hamiltonian.

In Sec. III.B we argued that for the RDH Hamiltonian with competing three- and four-spin exchange, the only hard theoretical numbers were a few terms in the high-temperature series expansions for thermodynamic properties. The quantitative phase diagram and low-temperature thermodynamic properties, which in principle should provide much more stringent quantitative tests of the applicability of the Hamiltonian are difficult to calculate reliably. This is due almost entirely to the strongly quantum nature of the spin system. For a classical spin Hamiltonian, high- and low-temperature series combined with Monte Carlo simulations analyzed by renormalization-group methods can yield reasonably accurate thermodynamic properties. For conventional three-dimensional antiferromagnets such as nearest-neighbor exchange for the bcc lattice, the quantum corrections to the classical behavior are relatively small even for spin $\frac{1}{2}$. For example, the order parameter $\langle S^z \rangle$ at zero temperature is suppressed by only about 15% due to quantum spin fluctuations (Anderson, 1952). There are several indications, however, that for Hamiltonians rich enough to yield the ^{3}He phase diagram, quantum effects will be much larger. For the purposes of this discussion, we will assume that the zero—field-ordered phase is the u2d2 structure.

From the discussion in Sec. II we know that the dipole anisotropy at $T=0$ must be reduced by a factor of 2 from its Néel value due to quantum fluctuations. If this were primarily due to the reduction of the order parameter, then $\langle S^z \rangle$ would have to be less than 70% of its saturation value, i.e., a factor of 2 larger suppression than for typical three-dimensional antiferromagnets. With zero-point fluctuations as large as 30%, the approximation of noninteracting linear spin waves is likely to be rather poor.

Further evidence for the importance of spin-wave interactions comes from the large (factor of 4) Hamiltonian-independent discrepancy between the coefficient of the T^2 temperature dependence of the dipolar anisotropy calculated from linear spin wave theory and the measured value from the NMR as discussed in Sec. II.C.

With the value of the parameters of Eq. (3.21), RDH (Roger *et al.*, 1983) find the order parameter suppression from zero-point fluctuations calculated in the noninteracting spin wave approximation to be 26%, which is roughly the right magnitude to account for the dipolar anisotropy. However, with an effect this large, the neglect of spin-wave interactions is unlikely to be justifiable. It is natural to try to improve the spin-wave calculations by treating interactions between spin waves. This has been done by Iwahashi and Masuda (1981), who treat the interactions self-consistently in the Holstein-Primakoff (1940) formalism. They find that the energy and the T^3 coefficient in the specific heat have very large corrections from the linear spin-wave results and that the instability of the u2d2 phase to the SSQUAF phase is suppressed.

In addition to general difficulties associated with treating spin-wave interactions within the Holstein-Primakoff formalism (Dyson, 1956a,1956b), it is hard to judge whether the errors in the self-consistent calculation are smaller than the effects calculated, especially since the corrections to the noninteracting approximation are so large. At this stage it is an open theoretical question whether interacting spin-wave calculations for the RDH Hamiltonian can be performed in a controlled manner. In the absence of controlled approximations for calculating low-temperature properties of the ordered state, Monte Carlo calculations would in principle be very useful. However, because of the commutation relations for the spins and the antiferromagnetic interactions, none of the existing stable methods for performing quantum Monte Carlo simulations can be used for nonbipartite lattices due to problems with negative weights in evaluation of the necessary $(3+1)$-dimensional effective statistical mechanical problem. Advances in quantum Monte Carlo methods might perhaps resolve this difficulty in the future.

Another numerical approach to the problem, which is unfortunately rather limited, is the exact diagonalization of the Hamiltonian for small systems. Cross and Bhatt (1984) have performed such a calculation for a 16-spin bcc cube with periodic boundary conditions ($2\times2\times2$ plus body centers), which is the largest cube for which this method is feasible. Their results, while somewhat difficult to draw conclusions from, do yield some insight into the effects of the quantum fluctuations. The ground-state wave energy as a function of $\kappa=K_p/J_t$ in zero field shows a surprisingly sharp change in slope at a κ_c which it is tempting to associate with the u2d2 to SSQUAF transition. This occurs at a value of κ_c slightly *smaller* than found in mean-field theory, so that the quantum fluctuations tend to favor the SSQUAF phase.

For a fixed value of $\kappa<\kappa_c$ the transition to what is presumably a canted NAF phase as a function of magnetic field appears as a large jump in the ground-state magnetization at a field H_c. This critical field H_c appears to be rather insensitive to quantum fluctuations, a surprising result, since this quantity might be expected to be particularly sensitive to changes in the competition between ferromagnetism and antiferromagnetism.

Within the range of K_p and J_t allowed by the high-temperature data, Cross and Bhatt (1984) found that H_c for this 16-spin system cannot be decreased to below 10 kG, still more than a factor of 2 larger than the experimentally measured $H_c\simeq4.4$ kG. If the critical field of this small system is reasonably close to that for an infinite system, as might be expected for such a strongly first-order transition, this is probably the most serious

discrepancy between the RDH Hamiltonian and experiment.

Reliable theoretical treatments of the RDH Hamiltonian, which are likely to be rather difficult, are crucially needed to test the validity of this multiple exchange model.

We end this section with a remark concerning the order of the transition in zero field, assuming the low-field phase has the u2d2 structure. Bak and Rasmussen (1981) have performed a renormalization-group expansion near four dimensions for a Ginzburg-Landau-Wilson effective Hamiltonian appropriate to the symmetry of the u2d2 phase which should be valid independent of the microscopic Hamiltonian. They argue that even if the transition were second order in mean-field theory, fluctuations below four dimensions would drive it into a regime where it is first order. Although this argument is probably correct, it is likely to be somewhat moot, since for the range of models studied by RDH, the transition to the u2d2 phase is strongly first order already in mean-field theory.

V. FUTURE EXPERIMENTS

We now consider various experiments which might shed additional light on the nature of the microscopic exchange dynamics, the effective spin Hamiltonian, and the identification of the various observed phases.

Several authors (Goodkind, 1983; Roger *et al.*, 1983) have suggested that it should be possible to investigate the long-wavelength *optic* spin waves by their resonant coupling to phonons at the same frequency. This would yield important additional information on the structure of the antiferromagnetic phase. For example, the number of long-wavelength optic modes tells us about the *number* of sublattices, distinguishing between the various u*m*d*m* phases. In fact, as we shall argue below, the coupling is extremely *small* for the u2d2 structure because of symmetry restrictions, although it may be much larger for other structures. Observation of a large direct coupling would therefore tend to rule out the u2d2 structure. Unfortunately, higher-order spin-wave couplings (e.g., one phonon to two spin waves) will make it difficult to observe the direct coupling clearly through phonon experiments.

The resonant coupling of the phonons to the uniform acoustic spin modes will not yield information about the symmetry of the phase—the frequencies of these modes are well known from the NMR experiments. However, little is yet known about the coupling of the ordered phases to strains, and nothing at all is known about the effects of *shear* on the magnetic properties, since the linear effects are absent in the paramagnetic phase, although, as we shall see, they will be present in the antiferromagnetic phase. Increased knowledge of the effects of strain on the magnetic behavior, which can be derived from the mixing of phonons with almost-uniform spin-wave modes and from shifts in the sound velocities, may therefore yield additional insight into the microscopic nature of the exchange processes. Measurements of the sound velocities may also yield additional symmetry restrictions on the ordered phases.

Finally, we consider the measurement of the specific heat of the various phases in a magnetic field. The T^3 contribution contains information on the number of broken symmetries. Such a contribution in the high-field phase, for example, would convincingly confirm the suggestion of a transverse broken symmetry.

A. Coupling of phonons to optic spin waves

If we neglect dipolar interactions, spin conservation prevents mixing of phonons and spin waves in zero magnetic field for any structure with only two broken spin symmetries. This is because the component of spin parallel to $\hat{\mathbf{d}}$ (which we take to be in the $\hat{\mathbf{z}}$ direction) will still be conserved in the ordered phase. The spin waves are excitations with $S^z=\pm 1$ and cannot mix with spinless phonons. In a field, however, mixing is generally possible. The magnitude of the coupling for up-down structures can be estimated as follows.

Let us consider an optic spin-wave mode with frequency $\omega_0 \sim J/\hbar$ and creation operator $\alpha_0^\dagger$ in the absence of a field. A field will induce an expectation value of each spin transverse to $\hat{\mathbf{d}}$ and hence generally an expectation value of α_0 of the same magnitude:

$$\langle \alpha_0 \rangle \sim \frac{\hbar\gamma H}{J} . \tag{5.1}$$

This can be shifted away simply by defining $\alpha=\alpha_0-\langle\alpha_0\rangle$, to make the Hamiltonian quadratic in α. However, since a strain will alter J, it will induce an extra linear coupling to the optic mode of the form

$$\delta\mathscr{H} \sim \hbar\omega_0(\alpha+\alpha^\dagger)\left[\frac{\hbar\gamma H}{J}\right]\Gamma u/a , \tag{5.2}$$

with u the atomic displacement and Γ the appropriate Gruneisen constant for J. Near the crossing of a phonon with wavelength q and a sharp optic mode, this coupling will induce a splitting, Δ, of the degeneracy of order

$$\frac{\Delta}{\omega_0} \sim \Gamma\left[\frac{\hbar\gamma H}{J}\right]\left[\frac{\hbar q^2}{m\omega_0}\right]^{1/2} \sim \Gamma\left[\frac{\hbar\gamma H}{J}\right]\left[\frac{J}{K}\right]^{1/2} , \tag{5.3}$$

where the last factor is the strain (m is the atomic mass) associated with a single phonon with elastic constant per atom $K\sim 20$ degrees. Since $\Gamma(\hbar\gamma H/J)$ can be made of order one in the low-field phase, this relative splitting will be of order 10^{-2}. [Note that for coupling via the dipole interactions in the absence of a field, the factor $\Gamma(\hbar\gamma H/J)$ would be replaced by something of the order of the dipole energy divided by J, which is much smaller.] Unfortunately, for symmetry reasons this simple estimate

is not correct for the optic modes in four-sublattice u2d2 structure.

As discussed in Appendix A, for the u2d2 structure there are two degenerate acoustic modes (with $S^z=\pm 1$ and frequencies $\pm\omega$) and two degenerate optic modes. The uniform acoustic modes, like the structure itself, are *even* under a real-space inversion about a point midway between a spin-up body corner and a spin-up body center. The optic modes, on the other hand, are *odd* under inversion. Since the dipole energy, all the spin parts of the Hamiltonian, and uniform strains are all even under inversion, the odd optic modes cannot couple to them linearly at $q=0$ (Goodkind, 1983). At nonzero q coupling is possible, but there will be an extra factor qa (with a the lattice spacing) appearing in the coupling Hamiltonian Eq. (5.2) and Δ/ω_0 will be reduced from Eq. (5.3) by this factor. At the crossing point of a phonon and the optic mode, this suppression factor is roughly the ratio of J to the zone boundary frequency of order 10 K, so that

$$\frac{\Delta}{\omega_0}\sim 10^{-6} \tag{5.4}$$

for the u2d2 structure, and the splitting is thus very unlikely to be observable.

For a more complicated up-down structure—for example, u3d3—there will be optic modes which are odd (under inversion about one of the middle up spins) which will couple very weakly, and also optic modes which are even which can couple much more strongly as given by Eq. (5.3).

Structures which break all three spin rotational symmetries can in principle couple even more strongly to phonons, since there will be no factor $\gamma\hbar H/J$ appearing in these cases. Thus the coupling to some of the modes in a helicoidal structure (such as discussed in Sec. II.A) could result in splitting of the degeneracy by an amount of order 10% of the frequency. Observation of a nonnegligible mixing of phonons with an optic spin wave would strongly suggest that the simple u2d2 structure is not correct.

In practice, optic spin wave modes are likely to be quite broad, with a width τ_S^{-1} arising from spin-wave interactions which is a significant fraction of their frequency. In this case mixing of phonons with these modes will result in a broad peak in the phonon attenuation with width τ_S^{-1} and maximum phonon attenuation rate

$$\frac{1}{\tau_P}=\frac{\Delta^2\tau_S}{4}\ , \tag{5.5}$$

which is appreciable if $\Delta\sim 10^{-2}\omega_0$.

Unfortunately, there are other phonon attenuation processes which are likely to obscure the resonant effects discussed above. Even in the absence of a magnetic field, phonons couple to spin waves quadratically and thus can decay into two spin waves of opposite helicity provided the phonon frequency is not too large. Because the phonon velocity is much larger than the spin-wave velocity, in order to conserve energy, the spin-wave momenta will be much larger than the phonon momentum, and hence of roughly equal magnitude but opposite direction. A phonon with frequency ω_P of the order of the optic spin-wave frequency at zero momentum (which is $\sim$180 MHz for the RDH Hamiltonian in the quadratic spin wave approximation) will decay into two spin waves near the zone boundary with frequencies of order of $J/\hbar$. The matrix element W for this process is of order

$$W\sim J\Gamma\left[\frac{\hbar q^2}{m\omega_P}\right]^{1/2}\ , \tag{5.6}$$

where q is the phonon wave vector and the factor involving the atomic mass m is again the strain associated with the phonon. The coupling is proportional to some Gruneisen constant Γ. Fermi's golden rule gives the phonon attenuation rate at low temperatures

$$\frac{1}{\tau_P}=\frac{2\pi}{\hbar}W^2\frac{dn}{dE}\ , \tag{5.7}$$

where dn/dE is the density of states per unit cell, which is of order $1/J$. We thus find a decay rate for the phonon with frequency ω_P equal to the optic spin-wave frequency, a phonon decay rate

$$\frac{1}{\tau_P}\sim\omega_P\frac{J}{K}\Gamma^2\ , \tag{5.8}$$

with $K\sim m\omega_P^2/q^2$ an elastic constant of order 20 K. For phonons at lower frequencies, phase-space and matrix element factors will cause the rate to decrease as ω_P does (for $\hbar\omega_P$ smaller than T the rate from this process goes as ω_P^4), and the attenuation will thus increase very sharply as ω_P is increased. Putting in numbers more carefully with parameters from Eq. (3.4) yields for ω_P equal to the optical spin-wave frequency,

$$\frac{1}{\tau_P}\sim 10^{-3}\omega_P\Gamma^2\ . \tag{5.9}$$

Naively, if Γ were a typical Gruneisen constant of order 20, this damping rate would be enormous. However, the appropriate Gruneisen constant can be shown to be some complicated angular average of the logarithmic derivative with respect to the appropriate phonon strain of the *ratio* of the spin-wave velocity to the inverse susceptibility. Thus, if the apparent similarity of all the measured Gruneisen parameters applies for this case, Γ is likely to be much smaller than 20, probably closer to two or three, which is the typical variation in the Gruneisen parameters. Even with this reduction, the phonon attenuation rate will be about 1% of its frequency, which is larger than the rate estimated above from the mixing with optic spin waves even when it is *not* excluded by parity. This corresponds to an attenuation length of order 100 μm.

Because of the large spin-wave nonlinearities, the decay of phonons into four spin waves should have comparable magnitude to the two spin-wave process discussed above, once the phonon frequency is high enough that the spin waves all have momenta near the zone boundary. In addition, in a magnetic field three spin-wave decays are al-

lowed and may also play a role.

From the above discussion, it is apparent that the phonon attenuation will show a rapid increase when the phonon frequency becomes of the order of the optic spin-wave frequency because of decay into two or more spin waves. This effect should be easily observable. However, it will almost certainly mask any attempt to measure resonant mixing with optic spin waves, unless through some fluke in the spectrum in a more complicated magnetic structure than u2d2 the *even* optic mode is anomalously narrow. It is possible with certain spin-wave spectra that the two spin-wave decay rate may actually show a peak at around twice the zone boundary frequencies and decrease considerably before the four spin-wave rate takes over at higher frequencies. A peak of this kind which occurs in zero field could easily be confused with optic spin-wave mixing for a structure with three broken spin symmetries (rather than the two in the u2d2 phase) for which mixing can occur in a zero field. An interesting problem which involves questions about the extent of the quantum nature of the ordered state is the decay rate for phonons at frequencies much higher than J into many spin waves. We expect that the phonon damping rate from such processes will fall off rapidly as the frequency increases and more and more spin waves are necessary to conserve energy. Understanding the behavior in this regime should be quite a challenge. We thus expect very rich magnetoelastic behavior; however, its potential use as a probe of the ordered phase is complicated by the many competing phenomena. The best prospects are if the phase is not u2d2.

B. Hydrodynamics of coupling of phonons to acoustic spin waves

In this section we discuss the coupling of phonons to the low-frequency magnetic modes analyzed in Sec. II.A.

Phonons can mix the magnetic modes when phonon frequencies are comparable to the magnetic resonance frequency. Since this will only occur at long wavelengths, we can ignore the spatial inhomogeneity of the magnetic modes and analyze the coupling to a uniform strain in the crystal u_{ij}. As in Sec. II.A, at the low frequencies and long wavelengths of interest a hydrodynamic description will be valid.

The equations of motion for the spin and the order parameter are the same as in the unstrained case except that we must now allow for dependence of the susceptibility and dipole energy on the strain. (Note that helicoidal, or other complicated structures which have a third broken spin symmetry on which the susceptibility and dipolar anisotropy do not depend, will have an extra acoustic spin-wave mode with zero frequency in the limit of long wavelengths. However, the phonons will have no linear mixing with this extra mode, since such mixing can occur only via the susceptibility or dipolar anisotropy.) We have from Sec. II.A

$$\dot{\mathbf{S}}=\gamma\mathbf{S}\times\mathbf{H}+\hat{\mathbf{d}}\times\vec{\mathbf{A}}(u_{ij})\cdot\hat{\mathbf{d}} \tag{5.10}$$

and

$$\dot{\hat{\mathbf{d}}}=\hat{\mathbf{d}}\times[\gamma\mathbf{H}-\gamma^2\chi_0^{-1}(u_{ij})\mathbf{S}]\ . \tag{5.11}$$

These must be supplemented by an equation of motion for the displacement field u_i which has a contribution from the derivative of the magnetic energy with respect to the strain:

$$m\rho\ddot{u}_i=-\frac{\delta\mathscr{H}}{\delta u_i}=C_{ijkl}\nabla_j u_{kl}+\tfrac{1}{2}\gamma^2\mathbf{S}\cdot\nabla_j\frac{\partial\vec{\chi}^{-1}}{\partial u_{ij}}\cdot\mathbf{S}$$
$$-\tfrac{1}{2}\hat{\mathbf{d}}\cdot\nabla_j\frac{\partial\vec{\mathbf{A}}}{\partial u_{ij}}\cdot\hat{\mathbf{d}}\ , \tag{5.12}$$

where C_{ijkl} is the elastic constant tensor, $m\rho$ is the mass density, boldface denotes vectors in spin space, and the latin subscripts denote real space. Note that in general the anisotropic part of the susceptibility tensor, δ, could enter through the second term in Eq. (5.11). However, we shall be interested in small deviations about equilibrium and then the orthogonality of $\hat{\mathbf{d}}_{\rm eq}$ and $\mathbf{S}_{\rm eq}$ in the u2d2 phase will cause the dependence on δ to drop out. The linearized equations of motion about equilibrium will depend on the tensors

$$\Gamma_{ij}=\chi_0\frac{\partial\chi_0^{-1}}{\partial u_{ij}}\bigg|_{u_{ij}=0} \tag{5.13}$$

and

$$A_{\alpha\beta ij}=\frac{\partial A_{\alpha\beta}}{\partial u_{ij}}\bigg|_{u_{ij}=0}\ , \tag{5.14}$$

where the greek subscripts are spin indices. We may ignore the terms in the linearized equations of motion for the displacement which arise from second derivatives of the equilibrium magnetic energy with respect to the strain, since these will yield overall shifts in the sound velocities rather than mixing; we shall return to their effects later. Because of the spatial uniaxiality of the spin structure, the susceptibility Gruneisen tensor must have the form

$$\Gamma_{ij}=\Gamma_0\delta_{ij}+\Gamma_A l_i l_j\ . \tag{5.15}$$

The measured dependence of χ_0 on a uniform compression is given by the susceptibility Gruneisen constant

$$\gamma_\chi=\Gamma_0+\tfrac{1}{3}\Gamma_A\ , \tag{5.16}$$

which determines *one* combination of the Γ's. They are not currently known independently; however, they are both likely to be large. The dipole strain tensor $A_{\alpha\beta ij}$ has seven independent components,[12] and its effects are thus

[12]The independent components of $A_{\alpha\beta ij}$ for the uniaxial structure with a fourfold symmetry axis are, with $\hat{l}$ in the x direction, *xxxx*, *xxyy*, *yyxx*, *xyxy*, *yyyy*, *yyzz*, and *yzyz*. The last three would not be independent in a completely uniaxial structure; however, since $\hat{l}$ is only a fourfold symmetry axis, they are independent.

rather complicated. One would expect (unless perhaps the state is the SPNAF state discussed in Appendix B) that the dependence of the dipole energy on strain would be of the order of the dipole energy at zero strain. If the spins were classical, the dependence on strain would arise only from the change in the distances between the spins and would certainly be of the order of the dipole energy. As long as the quantum effects are not large enough to alter the *state*, then the logarithmic strain derivative of the dipole energy will remain of order one. We are thus probably justified in ignoring this effect all together, since it will be considerably smaller than the strain dependence of the susceptibility. In any case, we shall argue below that in certain symmetry directions the effects of the strain dependence of the dipole energy vanish.

We are interested specifically in the mixing of magnetic modes with a phonon with wave vector $\mathbf{q}$, polarization $\hat{\mathbf{e}}$, strain field $u_{ij} \propto (e_i q_j + q_i e_j)$ and velocity s. For convenience we chose a coordinate system in which $\hat{l}$ is in the $\hat{\mathbf{x}}$ direction and for simplicity restrict ourselves to the case where the magnetic field H is the x-y plane. This forces $\hat{\mathbf{d}}_{\rm eq}$ to lie in the third [100] direction $\hat{\mathbf{z}}$. Note that, as for optic modes, there will be no mixing in the absence of a field due to spin conservation. In this case, this will be true even for helicoidal structures. It can easily be shown that as long as $u_{xz} = u_{yz} = 0$, the dipole derivatives will not enter the linearized equations of motion. This condition will be satisfied, for example, for any longitudinal [100] phonon and any phonon with both $\hat{\mathbf{e}}$ and $\mathbf{q}$ in the x-y plane. Although there may be interesting information in the tensor $A_{\alpha\beta ij}$, we will restrict our attention to the cases where it drops out.

The full spectrum of the coupled spin-phonon modes is given by Eqs. (5.10)—(5.12). Near to the crossing of the bare magnetic modes with frequencies $\Omega(\mathbf{H})$ and the phonon mode with frequency sq, the frequencies of the mixed modes will be given by the usual form from degenerate perturbation theory as long as the mixing is small compared to the frequency differences between the bare magnetic modes. We thus have

$$\omega^2 = \frac{\Omega^2 + (sq)^2}{2} \pm \left[\left[\frac{\Omega^2 - (sq)^2}{2} \right]^2 + D^4 \right]^{1/2} , \quad (5.17)$$

where the minimum splitting between the modes is

$$\Delta = \frac{D^2}{\Omega} , \quad (5.18)$$

and we find

$$D^4 = (\Gamma_{ij} e_i q_j)^2 \frac{\lambda (\gamma H)^2}{m\rho} F(\theta) , \quad (5.19)$$

where λ is the anisotropy of the dipole energy given by Eq. (2.12). The function F depends on the angle θ between the magnetic field and the spatial anisotropy direction $\hat{l}$ and on the bare magnetic mode. For the two bare NMR modes with

$$\Omega^2 = \Omega_{\pm}^2 = \tfrac{1}{2}[(\gamma H)^2 + \Omega_0^2] \pm \tfrac{1}{2}\{[(\gamma H)^2 - \Omega_0^2]^2 + 4\Omega_0^2 (\gamma H)^2 \cos^2\theta\}^{1/2} , \quad (5.20)$$

F is given by

$$F_{\pm} = \tfrac{1}{2}(\gamma H)^2 \sin^2 2\theta \Omega_{\mp}^2 \{\Omega_0^4 + (\gamma H)^4 + 2\Omega_0^2 (\gamma H)^2 \cos 2\theta \pm [\Omega_0^2 + (\gamma H)^2 \cos 2\theta](\Omega_0^4 + H^4 + 2\cos 2\theta \Omega_0^2 H^2)^{1/2}\}^{-1} . \quad (5.21)$$

We quote three simple limits of this somewhat messy expression. For $H \ll \Omega_0$,

$$F_+ = \sin^2\theta , \qquad F_- = \frac{(\gamma H)^2}{\Omega_0^2} \sin^2\theta \cos^2\theta ; \quad (5.22)$$

for $H = \Omega_0$,

$$F_+ = F_- = \frac{\sin^2\theta}{2} ; \quad (5.23)$$

and for $H \gg \Omega_0$,

$$F_+ = \frac{\Omega_0^2}{(\gamma H)^2} \sin^2\theta \cos^2\theta , \qquad F_- = \sin^2\theta . \quad (5.24)$$

For $\theta = 0$ corresponding to $\mathbf{H}$ parallel to $\hat{l}$, the bare magnetic modes are at zero frequency and $[\Omega_0^2 + (\gamma H)^2]^{1/2}$. In this case the phonons do not couple to either mode (except for negligible effects involving extra powers of D^2/Ω^2). On the other hand, for $\mathbf{H}$ perpendicular to $\hat{l}$, phonons couple strongly (with $F = 1$) to the mode with frequency Ω_0 and not at all to the γH mode. Physically this is because the coupling is via the susceptibility which does not affect the pure Larmor precession mode.

Since the coupling to the low-frequency mode at Ω_0 goes up with field, this is probably the optimum place to look for the mixing of phonons with the magnetic modes. The relative splitting is given by (using $sq = \Omega_0 = \Omega$)

$$\frac{\Delta}{\Omega_0} = (\Gamma_{ij} e_i \hat{q}_j) \left[\frac{\gamma H}{\Omega_0} \right] \left[\frac{\lambda}{m\rho s^2} \right]^{1/2} F^{1/2}(\theta) , \quad (5.25)$$

which we note is independent of θ for the low-frequency mode in the high-field limit. The characteristic magnitude of the splitting is just the square root of the dipole energy per atom divided by the elastic modulus per atom $K = ms^2$, which is about 0.5×10^{-4}. The Gruneisen factor in Eq. (5.25) will depend on the relative orientation of $\hat{\mathbf{e}}$, $\hat{\mathbf{q}}$, and $\hat{l}$:

$$\Gamma_{ij} e_i \hat{q}_j = \Gamma_0 (\hat{\mathbf{e}} \cdot \hat{\mathbf{q}}) + \Gamma_A (\hat{\mathbf{e}} \cdot \hat{l})(\hat{\mathbf{q}} \cdot \hat{l}) \quad (5.26)$$

and presumably be around 20, at least for longitudinal phonons. Since $\gamma H / \Omega_0$ can be made of order 10 before

entering the high-field phase, the splitting can be made of order 1% of the frequency for the low-frequency, field-independent mode. Both the phonon and magnon line widths are small in this regime, so that a mixing of order 1% should be easily observable. From either a combination of longitudinal and transverse phonon measurements (the latter couple only via Γ_A), or from longitudinal phonons propagating parallel and perpendicular to $\hat{l}$, it should be possible to extract Γ_0 and Γ_A independently, which, as mentioned above, one hopes would yield additional clues as to the microscopic origins of the exchange processes.

We now turn to the effects of the dependence of the magnetic energy on strain which will result in shifts in the sound velocities and may yield extra symmetry information about the magnetic structure. The second derivative of the magnetic energy with respect to strain is a fourth-rank tensor Λ_{ijkl} with magnitude of order $\Gamma^2 J$, which can have isotropic parts of order 0.4 K resulting in 5% changes in the elastic constants. The interesting effects will come from the *anisotropic* parts of the magnetoelastic tensor which are likely to be somewhat smaller but still measurable. Because the magnetically ordered phase has lower spatial symmetry than the cubic paramagnetic phase, the anisotropic parts of Λ will give rise to additional anisotropies in the sound velocities.

For the u2d2 structure, the spatial symmetry is tetragonal, and so Λ will have six independent components. More complicated structures that are consistent with the known spatial symmetry, which includes a fourfold [100] axis, can generally have more nonzero magnetoelastic coefficients. In particular, structures without a mirror plane parallel to $\hat{l}$ can have an extra nonzero component $\Lambda_{zzzy}=-\Lambda_{yyyz}$. This term can in principle be absorbed into the usual tetragonal terms by rotating the $\hat{\mathbf{x}}$ and $\hat{\mathbf{y}}$ axes; however, this effect would clearly be observable. We note finally that if the SPNAF phase discussed in Appendix B existed, then the large nonlinearities needed to stabilize it would be likely to make the phonon velocities more anisotropic than the magnitude estimated above for other tetragonal phases.

C. Specific heat in a magnetic field

In the presence of a magnetic field, which we will take to be in the range $\Omega_0 \ll \gamma H \ll J$, the spin-wave spectrum deviates from linear dispersion at small k. For up-down states, i.e., those in which all $\langle \mathbf{S}_i \rangle$ are in the $\hat{\mathbf{d}}=\hat{\mathbf{z}}$ direction, the doubly degenerate acoustic spin waves in zero field correspond to the two broken spin symmetries (S^x and S^y). For the experimental case of interest for which $\chi_\perp < \chi_\parallel$, the magnetic field will always be perpendicular to $\hat{\mathbf{d}}$, say, in the $\hat{\mathbf{y}}$ direction. In nonzero field, there will hence be only one spontaneously broken symmetry, S^y, and only one linear spin-wave mode. The two low-lying branches of the spectrum will then be

$$\omega^2 = c^2(\hat{\mathbf{k}})k^2 , \qquad \omega^2 = (\gamma H)^2 + c^2(\hat{\mathbf{k}})k^2 . \tag{5.27}$$

For $\Omega_0 \ll T \ll H$, the coefficient of the low-temperature T^3 specific heat will then be decreased to half its value in zero field.

For helicoidal states with $\hat{\mathbf{d}}=\hat{\mathbf{z}}$ perpendicular to the plane of the spins (or other states with all three spin symmetries broken) but again $\chi_\perp < \chi_\parallel$ (as constrained by the experiments) the situation is somewhat different. There will be three linear spin-wave modes in zero field corresponding to the three broken spin symmetries. Two of these (S^x and S^y) will be degenerate with velocities $c_2(\hat{\mathbf{k}})$ and the third (S^z) will be distinct with velocity $c_1(\hat{\mathbf{k}})$. In a finite field in the y direction, only the S^y mode will remain gapless with $\omega^2 = c_2^2(\hat{\mathbf{k}})k^2$. The specific heat in finite field for $T \ll H$ will be

$$C_V(H) = \frac{2\pi^2}{15\hbar^3} T^3 \left\langle \frac{1}{c_2^3} \right\rangle \tag{5.28}$$

in contrast to the $H=0$ result

$$C_V(H=0) = \frac{2\pi^2}{15\hbar^3} T^3 \left[2\left\langle \frac{1}{c_2^3} \right\rangle + \left\langle \frac{1}{c_1^3} \right\rangle \right] . \tag{5.29}$$

The coefficient of T^3 for the helicoidal case in a field will thus be reduced by more than a factor of 2. Measurements of $C_V(H,T)$ at low T should provide an additional way to distinguish between an up-down structure and a helicoidal structure, the only conclusion of the general arguments from the NMR experiment in Sec II.A that relied on signs of anisotropies rather than symmetry.

Finally, we briefly discuss the high-field phase. It is clear from the above discussion that if the high field phase is a canted antiferromagnet it will still have at least one spin-wave mode with linear dispersion which will give rise to a T^3 contribution to the low-temperature specific heat. If, on the other hand, the high-field phase is a paramagnet with no broken spin symmetries, then the specific heat will be exponentially small at low temperatures. Measurements of the specific heat at sufficiently low temperatures in the high-field phase should thus differentiate between a canted antiferromagnet and a paramagnet. Note that a ferromagnetic spin structure in which the spins on one sublattice point along the field and those on the other point in the opposite direction would also have an exponentially small specific heat, since the spin rotation symmetry is unbroken, even though the structure has a broken lattice translational symmetry.

VI. CONCLUSIONS

In this paper on the magnetic properties of ^{3}He we have primarily concerned ourselves with the status of the comparison between theory and experiment. The subject is in an exciting stage of development. There exists a phenomenological spin Hamiltonian—the multiple exchange Hamiltonian of Roger, Delrieu, and Hetherington (1980a)—that shows remarkable *qualitative* agreement with a range of unusual magnetic properties of solid ^{3}He. However, this model seems to lead to large *quantitative*

disagreements and is also *conceptually* unsatisfying due to the necessity of an apparently coincidental similarity between two quite different exchange rates, a coincidence that furthermore seems to be maintained over a considerable range of densities.

It is indeed quite likely that these objections will ultimately be answered, and that a multiple-exchange Hamiltonian may provide at least a reasonable approximate description. It also seems likely, however, that reaching a consistent interpretation will advance our physical understanding of the system, and not merely represent a large computational effort.

So far, there is no definitive confrontation between theory and experiment. The only numbers which have been reliably calculated theoretically for the model are the high-field, zero-temperature transition field from the fully aligned to the canted NAF state and a few terms in the high-temperature series expansions of various thermodynamic quantities. The transition field is so far inaccessible experimentally, and there remains considerable uncertainty in the fitting of the high-temperature measurements.

The large amount of low-temperature experimental information, on the other hand (spin-wave specific-heat, susceptibilities, NMR frequencies, etc.), has so far not been very useful in restricting the parameter range of the theory due to the absence of reliable methods for theoretically treating strongly quantum spin systems. Thus we currently have a situation in which the quantitative theoretical calculations have not been stringently tested by experiment and in which quantitative experimental data cannot yet be compared with accurate theoretical predictions.

What are the prospects for improving this state of affairs?

First, from the experimental side, resolving questions about the nature of the high-field phase and the existence and nature of the phase boundary between it and the paramagnetic phase would be very useful. In particular, the absence of such a phase boundary in high fields would indicate that the high-field phase does not have a broken symmetry. On the other hand, low-temperature specific heat measurements could establish the existence of a spontaneously broken symmetry in the high-field phase. It may also be possible to indirectly excite spin waves via NMR in the presence of a magnetic field gradient (Osheroff, 1985). Furthermore, a program to establish a reliable set of high-temperature thermodynamic data could help immensely to pin down the model parameters, and should be pursued with high priority. Even the structure of the low-field antiferromagnetic phase is by no means certain. We have suggested several experiments (magneto-specific heat and phonon coupling) which might yield additional information on the symmetry and nature of this phase. However, the ideal structural probe, neutron scattering, may soon make such roundabout analysis of the structure superfluous. (See the note added in proof.)

From the theoretical side there is clearly much to be done. The most straightforward calculations are in the high-temperature paramagnetic phase. Since the zero-field transition is strongly first order, it is probable that with a few terms in high-temperature series, thermodynamic quantities could be calculated accurately down to the zero field T_c. Direct comparison with the experimental data for various quantities in the paramagnetic phase could then be made—in particular, the dramatic "hanging up" of the entropy above T_c could perhaps be compared with theory. A better phenomenological understanding of the thermodynamic anomalies above T_c may also be instructive.

More difficult, although probably more interesting and informative in the long run, would be calculations of the phase diagram and ordered phase properties *including* quantum fluctuations. This provides quite a challenge to theorists: ^{3}He should ultimately provide a nontrivial quantum system in which the microscopic (spin) Hamiltonian is well known in terms of a few interaction constants that are in turn accurately determined by (for example) high-temperature measurements. Although there has been considerable progress in quantum Monte Carlo methods recently, it is not clear that any of the methods are applicable to the ^{3}He system, and further work in this direction would clearly be useful. At low temperatures, methods might be developed for treating the apparently strongly interacting spin wave system. Other approaches such as variational or cluster methods should also be investigated.

The theoretical basis for the introduction of a phenomenological spin exchange Hamiltonian has been well addressed in the literature (Herring, 1966; McMahan, 1972). There are compelling (but no definitive) arguments for believing that a simple spin Hamiltonian should exist. We are therefore in the unusual position that accurate (and hard) quantum calculations of actual numbers may ultimately lead, if agreement with experimental data is not forthcoming, to advances in the microscopic understanding. For example, if a Hamiltonian with two, or possibly three, exchange parameters is not sufficient to fit the experiments, then we should be led to seek some microscopic physics causing many exchanges to have comparable magnitudes. Ultimately, the assumptions involved in deriving a phenomenological spin Hamiltonian might be brought into question.

This brings us to the problem of the microscopic origin of the exchange Hamiltonian.

As discussed in Sec. IV.A, reliable microscopic calculations of exchange processes at densities of interest are not yet available. Several approximate calculations, assuming very different physics, have yielded roughly the right magnitudes and ordering of exchange rates but the important physics involved in the exchange has not been elucidated. The simple scaling of the various exchanges, with a single dependence on volume observed experimentally, is also not understood at the relevant densities. This is far from being a problem for which one can, with enough effort, just use some existing machinery to crank out the answers: there are qualitative questions that are not understood. In particular, the question of whether the ex-

change is best thought of as a tunneling process through classically forbidden configurations, or is more like the hard-sphere limit for which the potential energy is relatively unimportant, is not yet resolved. It seems likely that reliable quantitative calculations on this many-body system, involving approximation techniques or advances in numerical methods, are necessary to yield new qualitative understanding of the many-body physics involved. That such progress may indeed be possible is suggested by the finite size of the clusters presumably involved (at least nonperturbatively).

Finally, given the present stage of the agreement between theory and experiment, it is still conceivable that multiple-spin exchange does not provide the correct, or perhaps the best, description of the magnetic phenomena. The field then of course becomes wide open. Neither of the alternative theories so far proposed—lattice-mediated exchange or zero-point vacancies—has been developed far enough to make quantitative predictions to be tested experimentally. Other possibilities, such as a complete breakdown of the separation (except for perturbative corrections) into a statistics-independent lattice Hamiltonian and a spin Hamiltonian to take care of the Pauli principle, have not yet even been addressed.

Understanding the processes leading to exchange, particularly if they essentially involve large numbers of atoms, should bear fruit in other quantum systems, especially electron crystals. This may even help to answer Anderson's question "when are solids solid?"

Note added in proof. Very recently, Benoit *et al.* (1985) have reported preliminary neutron scattering data showing evidence for a magnetic Bragg peak with wavevector $k=2\pi/d(\frac{1}{2},0,0)$ as expected for the principal Bragg peak of the u2d2 structure. At this stage, however, these data cannot rule out some of the other possible phases discussed in Sec. II.A. In particular a helicoidal structure with the same wave vector and umdm phases with m *even,* would also be consistent with the data. A search of other regions of the Brillouin zone could, in principle, rule out these possibilities: umdm phases will have magnetic Bragg peaks at $2\pi/d(1/m,0,0)$; the u2d2 phase will have a weak *charge* Bragg peak at $2\pi/d(1,0,0)$ due to the zone boundary lattice distortion, while the helicoidal phase will be characterized by the *absence* of any peak at this wave vector.

ACKNOWLEDGMENTS

Our understanding of solid ^{3}He has benefited from interactions with numerous colleagues. We would like especially to thank Phil Anderson, Bob Richardson, Michael Wilkinson, and most of all Doug Osheroff, for numerous stimulating discussions and elucidation of experiments and theoretical ideas.

APPENDIX A: SPIN-WAVE CALCULATIONS

In this appendix, the zero-temperature susceptibility and the thermal suppression of the dipolar anisotropy are calculated from noninteracting spin-wave theory for the u2d2 phase. Various authors (Iwahashi and Masuda, 1981; Usagawa, 1982; Roger *et al.*, 1983) have used different conventions and notation; we use a natural generalization of the notation of the paper by Harris *et al.* (1971) which has the advantage that the symmetries manifest themselves in a reasonably simple way. Because of the spin symmetry, all the spin-wave modes will be doubly degenerate and we can drop the subscript on the frequencies and spin-wave velocities which was necessary for general structures. (We shall later use a subscript on ω for the u2d2 phase to denote the acoustic and optic branches.)

The spins on the two up sublattices we label $\mathbf{S}_{i1}$ and $\mathbf{S}_{i2}$ and those on the down sublattices $\mathbf{S}_{j1}$ and $\mathbf{S}_{j2}$. We can perform a Dyson-Maleev transformation (Dyson, 1956a,1956b; Maleev, 1957) for spin-S spin operators to boson operators defined by the correspondence

$$\begin{aligned}
&S^z_{i\zeta}\rightarrow S-a^\dagger_{i\zeta}a_{i\zeta}\ ,\\
&S^+_{i\zeta}\rightarrow(2S)^{1/2}a_{i\zeta}-(2S)^{-1/2}a^\dagger_{i\zeta}a_{i\zeta}a_{i\zeta}\ ,\\
&S^-_{i\zeta}\rightarrow(2S)^{1/2}a^\dagger_{i\zeta}\ ,\\
&S^z_{j\zeta}=-S+b^\dagger_{j\zeta}b_{j\zeta}\ ,\\
&S^+_{j\zeta}=(2S)^{1/2}b^\dagger_{j\zeta}-(2S)^{-1/2}b^\dagger_{j\zeta}b^\dagger_{j\zeta}b_{j\zeta}\ ,\\
&S^-_{j\zeta}=(2S)^{1/2}b_{j\zeta}\ ,
\end{aligned}\tag{A1}$$

where $\zeta=1,2$ and we are interested in the spin-$\frac{1}{2}$ case. The Fourier transforms of the site boson operators are defined by

$$\begin{aligned}
a_\zeta(\mathbf{k})&=N_M^{-1/2}\sum_i^\zeta e^{i\mathbf{k}\cdot\mathbf{r}_{i\zeta}}a_{i\zeta}\ ,\\
b_\zeta(\mathbf{k})&=N_M^{-1/2}\sum_j^\zeta e^{i\mathbf{k}\cdot\mathbf{r}_{j\zeta}}b_{j\zeta}\ ,
\end{aligned}\tag{A2}$$

where the ζ superscript on the sum denotes a sum only over the spins of the ζth up (or down) sublattice, and N_M is the number of magnetic unit cells (equal to $\frac{1}{4}$ the number of atoms). The part of the Hamiltonian quadratic in the spin-wave operators generally has the form (ignoring additional constant terms arising from normal ordering)

$$\begin{aligned}
\mathscr{H}_2=\sum_{\zeta\eta\mathbf{k}}[\,&a_\zeta(\mathbf{k})\Gamma_{\zeta\eta}(\mathbf{k})a^\dagger_\eta(\mathbf{k})+b^\dagger_\zeta(-\mathbf{k})\Gamma_{\zeta\eta}(\mathbf{k})b_\eta(-\mathbf{k})\\
&+a_\zeta(\mathbf{k})\Delta_{\zeta\eta}(\mathbf{k})b_\eta(-\mathbf{k})+b^\dagger_\zeta(-\mathbf{k})\Delta_{\zeta\eta}(\mathbf{k})a^\dagger_\eta(\mathbf{k})]\ ,
\end{aligned}\tag{A3}$$

where $\overline{\Gamma}(\mathbf{k})$ and $\overline{\Delta}(\mathbf{k})$ are Hermitian 2×2 matrices.

This Hamiltonian can be diagonalized by a transformation of the form

$$\begin{aligned}
a^\dagger_\mu(\mathbf{k})&=l_{\mu\nu}(\mathbf{k})\alpha^\dagger_\nu(\mathbf{k})+m_{\mu\nu}(\mathbf{k})\beta_\nu(-\mathbf{k})\ ,\\
b_\mu(-\mathbf{k})&=m_{\mu\nu}(\mathbf{k})\alpha^\dagger_\nu(\mathbf{k})+l_{\mu\nu}(\mathbf{k})\beta_\nu(-\mathbf{k})\ .
\end{aligned}\tag{A4}$$

The constraint that α_ν and β_ν obey boson commutation

relation implies

$$\begin{bmatrix} \bar{\bar{l}}^{\dagger} & -\bar{\bar{m}}^{\dagger} \\ -\bar{\bar{m}}^{\dagger} & \bar{\bar{l}}^{\dagger} \end{bmatrix} \begin{bmatrix} \bar{\bar{l}} & \bar{\bar{m}} \\ \bar{\bar{m}} & \bar{\bar{l}} \end{bmatrix} = \begin{bmatrix} \bar{\bar{I}} & 0 \\ 0 & \bar{\bar{I}} \end{bmatrix}, \tag{A5}$$

where $\bar{\bar{m}}$ and $\bar{\bar{l}}$ are 2×2 matrices and $\bar{\bar{I}}$ is the identity matrix. The resulting quadratic part of the Hamiltonian takes the form

$$\mathscr{H}_2 = \sum_{\mathbf{k},\mu} \omega_\nu(\mathbf{k})[\alpha_\nu^\dagger(\mathbf{k})\alpha_\nu(\mathbf{k}) + \beta_\nu^\dagger(\mathbf{k})\beta_\nu(\mathbf{k})] + E_0 , \tag{A6}$$

where E_0 is the ground-state energy, including zero-point energy of the spin waves, and ω_ν are the spin-wave frequencies. We adopt the convention that $\omega_1(\mathbf{k})$ and $\omega_2(\mathbf{k})$ are the doubly degenerate acoustic and optic branches, respectively. These doubly degenerate modes arise from the two possible values of S^z for spin waves: the α modes carry $S^z=-1$, while the β modes carry $S^z=+1$. Their frequencies are thus the same by symmetry of the state under interchange of the up and down sublattices.

The low-temperature thermal properties of the system will depend primarily on the acoustic spin waves. In particular, the transverse susceptibility per unit volume, χ, can be written in the quadratic spin-wave approximation

$$\begin{aligned} \chi &= \frac{1}{VT} \sum_{\mathbf{R}\mathbf{R}'} \langle S^x(\mathbf{R}) S^x(\mathbf{R}') \rangle \\ &= \frac{N_M}{VT} \frac{2S}{4} \lim_{\mathbf{k}\to 0} \sum_{\zeta\eta} \langle [a_\zeta(-\mathbf{k}) + a_\zeta^\dagger(\mathbf{k}) + b_\zeta(-\mathbf{k}) + b_\zeta^\dagger(\mathbf{k})][a_\eta(\mathbf{k}) + a_\eta^\dagger(-\mathbf{k}) + b_\eta(\mathbf{k}) + b_\eta^\dagger(-\mathbf{k})] \rangle . \end{aligned} \tag{A7}$$

In terms of the diagonalized spin-wave operators this becomes

$$\begin{aligned} \chi = \frac{N_M}{TV} \frac{2S}{4} \lim_{\mathbf{k}\to 0} \sum_{\zeta\eta\nu} & [l_{\zeta\nu}(\mathbf{k}) + m_{\zeta\nu}(\mathbf{k})][l_{\eta\nu}(-\mathbf{k}) + m_{\eta\nu}(-\mathbf{k})] \\ & \times [\langle \alpha_\nu^\dagger(\mathbf{k})\alpha_\nu(\mathbf{k}) \rangle + \langle \alpha_\nu(\mathbf{k})\alpha_\nu^\dagger(\mathbf{k}) \rangle + \langle \beta_\nu^\dagger(\mathbf{k})\beta_\nu(\mathbf{k}) \rangle + \langle \beta_\nu(\mathbf{k})\beta_\nu^\dagger(\mathbf{k}) \rangle] . \end{aligned} \tag{A8}$$

In order to evaluate the susceptibility, we need to know the eigenvectors

$$\begin{bmatrix} l_{\zeta\nu} \\ m_{\zeta\nu} \end{bmatrix}$$

of the acoustic ($\nu=1$) and optic ($\nu=2$) α modes in terms of the $a^\dagger$ and b. The β modes will have eigenvectors with the up and down sublattices interchanged: i.e., with $\bar{\bar{l}}$ and $\bar{\bar{m}}$ interchanged. In fact, for the quantities we calculate we do not need to find the eigenvectors explicitly. In the limit of long wavelengths, the acoustic modes become simply rotations of the structure. The transverse components of the down spins in a small rotation point in the *opposite* direction to those of the up spins. Hence m_{11} and m_{21} corresponding to the down spins must be equal to each other and equal to minus $l_{11}=l_{21}$ corresponding to the up spins [i.e., the eigenvector is $(1,1,-1,-1)$]. The constraint Eq. (A5) that the eigenmodes satisfy boson commutation relations implies that the other modes (i.e., optic modes) must be orthogonal to the *left* eigenvector of $\mathscr{H}_2$, which is

$$(l_{\zeta 1}^* - m_{\zeta 1}^*) \propto (1111) \quad \text{for } k\to 0 . \tag{A9}$$

Therefore these modes do not couple to the total S^x, which enters the susceptibility in Eq. (A7):

$$\lim_{k\to 0} \sum_{\zeta} (l_{\zeta 2} + m_{\zeta 2}) = 0 , \tag{A10}$$

and the optic modes cannot contribute to the uniform zero-field susceptibility. This result is true for all up-down antiferromagnetic structures.

The contribution to χ from the acoustic modes would naively also be zero, since the acoustic eigenvector is proportional to $(1,1,-1,-1)$ in the limit of zero wave vectors, with components again summing to zero. However, due to the degeneracy at $k=0$, this limit must be considered more carefully. In fact, we expect the acoustic eigenvector to take the form

$$(l_{\zeta 1}, m_{\zeta 1}) = \left[\frac{\Upsilon}{\hbar\omega_1(\mathbf{k})} \right]^{1/2} [1 + a\omega_1(\mathbf{k}), 1 + b\omega_1(\mathbf{k}), -1 + c\omega_1(\mathbf{k}), -1 + d\omega_1(\mathbf{k})] + O(k^{3/2}) , \tag{A11}$$

where Υ and a,b,c,d are constants that depend on the Hamiltonian. Now the requirement that the boson commutation rules be satisfied leads to a relationship between the coefficients

$$\sum_{\zeta} [l_{\zeta 1}(\mathbf{k}) + m_{\zeta 1}(\mathbf{k})] = \left[\frac{\Upsilon}{\hbar\omega_1} \right]^{1/2} (a + b + c + d) = \frac{1}{2} \left[\frac{\hbar\omega_1(k)}{\Upsilon} \right]^{1/2} \quad \text{for } k\to 0 , \tag{A12}$$

with the *same* Υ as in the eigenvector magnitude. This combination is exactly the one appearing in the susceptibility, and leads in that expression to a nonzero value for the susceptibility at $T=0$.

The zero-temperature susceptibility per unit volume becomes, with $S=\frac{1}{2}$,

$$\chi(0)=\rho\frac{\gamma^2\hbar^2}{4}\lim_{k\to 0}\sum_{\zeta\eta}\frac{1}{\hbar\omega_1(\mathbf{k})}[l_{\zeta 1}(\mathbf{k})+m_{\zeta 1}(\mathbf{k})]\times[l^*_{\eta 1}(-\mathbf{k})+m^*_{\eta 1}(-\mathbf{k})]$$

$$=\rho\frac{\gamma^2\hbar^2}{16}\Upsilon\,, \tag{A13}$$

where we have inserted the magnetic moment factors and used Eq. (A12). Note that this quadratic spin-wave approximation is equivalent to using the classical ground state in a small field. At nonzero temperature there will be corrections to χ of relative order $(T/J)^2$.

Another useful quantity which can be calculated from spin-wave theory is the temperature dependence of the dipole energy per unit volume, Eq. (2.16):

$$E_D=-\tfrac{1}{2}d^\alpha A^{\alpha\beta}d^\beta\,. \tag{A14}$$

In particular, we are interested in the difference, $\frac{1}{2}(\lambda_3-\lambda_1)$, between the dipole energy with $\hat{\mathbf{d}}\perp\hat{\mathbf{l}}$ and that with $\hat{\mathbf{d}}\|\hat{\mathbf{l}}$. The anisotropic part of the dipole energy per volume is given by

$$E_D=-\tfrac{1}{2}\rho(\gamma\hbar)^2\sum_{\mathbf{r}}\langle S^\alpha(0)S^\beta(\mathbf{r})\rangle_{\hat{\mathbf{d}}}D^{\alpha\beta}(\mathbf{r})\,, \tag{A15}$$

where the sum runs over all sites, $\mathbf{r}$ with $D^{\alpha\beta}(\mathbf{r})=3r^\alpha r^\beta/|\mathbf{r}|^5$, and the spin expectation value is taken with a given order-parameter direction $\hat{\mathbf{d}}$. We will denote lattice vectors of the magnetic structure by $\mathbf{R}$ and the positions within one magnetic unit cell $\mathbf{r}_m$, with m running from 0 to 3 through the four [100] planes, which we take to be $\uparrow\uparrow\downarrow\downarrow$, respectively. The original Brillouin zone will be denoted by Z and the magnetic zone Z_M, with $\mathbf{G}$ the magnetic reciprocal lattice vectors. We define Fourier transforms of the spins on the mth sublattice

$$S_m(k)=\frac{1}{(N_M)^{1/2}}\sum_{\mathbf{R}}e^{-i\mathbf{k}\cdot(\mathbf{R}+\mathbf{r}_m)}S(\mathbf{R}+\mathbf{r}_m)\,. \tag{A16}$$

The dipole energy then becomes

$$E_D=\frac{-1}{2V}(\gamma\hbar)^2\sum_m\sum_{\mathbf{k}_1,\mathbf{k}_2\in Z_M}\langle S^\alpha_0(\mathbf{k}_1)S^\beta_m(\mathbf{k}_2)\rangle_{\hat{\mathbf{d}}}\times\sum_{\mathbf{G}\in Z}D^{\alpha\beta}(\mathbf{G}-\mathbf{k}_2)e^{-i\mathbf{k}_2\cdot\mathbf{r}_m}\,, \tag{A17}$$

where for $\mathbf{q}\in Z$

$$D^{\alpha\beta}(\mathbf{q})=\sum_{\mathbf{r}}D^{\alpha\beta}(\mathbf{r})e^{-i\mathbf{q}\cdot\mathbf{r}}\,. \tag{A18}$$

The depression of the dipole energy at $T=0$, $E_D(0)$, due to zero-point fluctuations will have contributions from all of the optic and acoustic modes; however, the leading low-temperature correction to $E_D(T)$ will come only from the long-wavelength acoustic modes. Thus $E_D(T)-E_D(0)$ will depend only on the dipole Fourier transform Eq. (A18) at the wave vectors $\pm\mathbf{G}_0$ of the magnetic structure, since $D^{\alpha\beta}(\mathbf{G})$ for the other $\mathbf{G}$'s in the original zone (in fact, the NAF phase $\mathbf{G}$'s) will vanish by the cubic symmetry. Furthermore, since $\cos\mathbf{G}_0\cdot\mathbf{r}_m$ is zero for $m=1$ and 3, the contribution to the leading low-T behavior from the correlations between the body-center and body-corner sublattices will vanish, as it did for the classical zero-temperature dipole energy discussed in Sec. II.A.

We want to calculate the difference between the dipole energy with $\hat{\mathbf{d}}\|\hat{\mathbf{l}}$ (note: $\hat{\mathbf{l}}=\hat{\mathbf{G}}_0$) and with $\hat{\mathbf{d}}\perp\hat{\mathbf{l}}$. Because of the uniaxiality of the dipole tensor at $\hat{\mathbf{G}}_0$ and the structure, the dipole tensor and the correlation function will have the forms

$$D^{\alpha\beta}(\mathbf{G}_0)=D_\parallel l^\alpha l^\beta+D_\perp(\delta^{\alpha\beta}-l^\alpha l^\beta) \tag{A19}$$

and

$$\langle S^\alpha_0(\mathbf{k}_1)S^\beta_m(\mathbf{k}_2)\rangle_{\hat{\mathbf{d}}}=\delta(\mathbf{k}_1+\mathbf{k}_2)[C^\parallel_m(\mathbf{k}_1)d^\alpha d^\beta+C^\perp_m(\mathbf{k}_1)(\delta^{\alpha\beta}-d^\alpha d^\beta)]\,, \tag{A20}$$

respectively.

From this it follows that the leading low-T behavior of the dipole anisotropy is given by

$$\Delta(T)=\lambda_1(T)-\lambda_3(T)-[\lambda_1(0)-\lambda_3(0)]$$

$$=\frac{(\gamma\hbar)^2}{V}\sum_{\mathbf{k}\in Z_M}2(D_\perp-D_\parallel)\{[C^\parallel_0(\mathbf{k},T)-C^\perp_0(\mathbf{k},T)-C^\parallel_2(\mathbf{k},T)+C^\perp_2(\mathbf{k},T)]-[C^\parallel_0(\mathbf{k},0)-C^\perp_0(\mathbf{k},0)-C^\parallel_2(\mathbf{k},0)+C^\perp_2(\mathbf{k},0)]\}\,, \tag{A21}$$

where the factor of 2 is from the two wave vectors $\pm\mathbf{G}_0$.

In terms of the boson operators defined in Eq. (A1), we have

$$
\begin{aligned}
C_0^{\parallel}(\mathbf{k}) &= S^2\delta(\mathbf{k}) - \delta(\mathbf{k}) \int_{\mathbf{q}\in Z_M} 2S\langle a_1^\dagger(\mathbf{q}) a_1(\mathbf{q})\rangle \ , \\
C_0^{\perp}(\mathbf{k}) &= \tfrac{1}{4}(2S)\langle [a_1(-\mathbf{k}) + a_1^\dagger(\mathbf{k})][a_1^\dagger(-\mathbf{k}) + a_1(\mathbf{k})]\rangle \ , \\
C_2^{\parallel} &= -S^2\delta(\mathbf{k}) + \delta(\mathbf{k}) \int_{\mathbf{q}\in Z_M} [S\langle b_1^\dagger(\mathbf{q}) b_1(\mathbf{q})\rangle + S\langle a_1^\dagger(\mathbf{q}) a_1(\mathbf{q})\rangle] \ , \\
C_2^{\perp} &= \tfrac{1}{4}(2S)\langle [a_1^\dagger(\mathbf{k}) + a_1(-\mathbf{k})][b_1(\mathbf{k}) + b_1^\dagger(-\mathbf{k})]\rangle \ .
\end{aligned}
\tag{A22}
$$

In terms of the diagonalized acoustic modes α_1 and β_1 with Bose occupation factor

$$
n[\omega_1(k)] = \langle \alpha_1^\dagger \alpha_1\rangle = \langle \beta_1^\dagger \beta_1\rangle \tag{A23}
$$

we have

$$
\begin{aligned}
\Delta(T) = (\gamma\hbar)^2 2(D_\perp - D_{\parallel}) \\
\times \int \frac{d^3k}{(2\pi)^3} n[\omega_1(\mathbf{k})]\{-\tfrac{5}{2}[\,|l_{11}(\mathbf{k})|^2 + |m_{11}(\mathbf{k})|^2] + \tfrac{1}{2}[l_{11}^*(\mathbf{k}) m_{11}(\mathbf{k}) + l_{11}(\mathbf{k}) m_{11}^*(\mathbf{k})]\} \ .
\end{aligned}
\tag{A24}
$$

Using

$$
l_{11} = -m_{11} = \left[\frac{\Upsilon}{\hbar\omega_1(k)}\right]^{1/2} , \tag{A25}
$$

from Eq. (A11),

$$
D_\perp - D_{\parallel} = 3\rho(2.42) \ , \tag{A26}
$$

and

$$
\begin{aligned}
\int \frac{d^3k}{(2\pi)^3} \frac{n[\omega_1(\mathbf{k})]}{\hbar\omega_1(\mathbf{k})} &= \frac{1}{\hbar^3}\left\langle \frac{1}{c^3}\right\rangle T^2 \frac{4\pi}{(2\pi)^3} \int_0^\infty \frac{x\,dx}{e^x - 1} \\
&= \frac{T^2}{12\hbar^3}\left\langle \frac{1}{c^3}\right\rangle ,
\end{aligned}
\tag{A27}
$$

we get

$$
\Delta(T) = -(7.26)(\gamma\hbar)^2 \frac{T^2\Upsilon}{\hbar^3}\rho\left\langle \frac{1}{c^3}\right\rangle . \tag{A28}
$$

Two-thirds of this suppression comes from the longitudinal spin correlations, i.e., the thermal suppression of the order parameter given by

$$
2\langle S^z(0)\rangle - 2\langle S^z(T)\rangle = \frac{4}{3}\frac{T^2\Upsilon}{\hbar^3\rho}\left\langle \frac{1}{c^3}\right\rangle , \tag{A29}
$$

where Υ is related to χ^{-1} by Eq. (A13).

For completeness, we quote some results for the RDH three- and four-spin exchange Hamiltonian Eq. (3.17) discussed in Sec. III.B. The spin-wave velocities are given by

$$
\begin{aligned}
\hbar^2 c_{\parallel}^2 a^2 &= 64\frac{J_t}{K_p}(3K_p - 4J_T)(2K_p - 3J_t) \ , \\
\hbar^2 c_{\perp}^2 a^2 &= 16(3K_p - 4J_t)(4J_t - K_p)
\end{aligned}
\tag{A30}
$$

for directions parallel and perpendicular to $\hat{l}$, respectively, and the magnetic temperature is

$$
T_m \equiv \chi^{-1}\rho\left[\frac{\gamma\hbar}{2}\right]^2 = 4\Upsilon = 8(3K_p - 4J_t) \ . \tag{A31}
$$

Roger *et al.* (1983) fit the experimental results for $\langle 1/c^3\rangle$ with

$$
\begin{aligned}
J_t &= 0.13 \text{ mK} \\
K_p &= 0.385 \text{ mK} \ ,
\end{aligned}
\tag{A32}
$$

yielding a spin-wave anisotropy

$$
\frac{c_{\parallel}}{c_{\perp}} \simeq 2.0 \tag{A33}
$$

and a magnetic temperature

$$
T_m \simeq 5.1 \text{ mK} \tag{A34}
$$

reasonably close to the measured value of 5.8 mK. Note that for $K_p \lesssim 4J_t$, $c_\perp$ is rather sensitive to the parameters but χ and $c_{\parallel}$ are much less so.

The spin-wave velocities and the susceptibility have been calculated by several authors (Iwahashi and Masuda, 1981; Usagawa, 1982; Roger *et al.*, 1983). Usagawa (1982) has calculated the temperature dependence of the dipolar anisotropy for a multispin exchange model which includes the RDH Hamiltonian. He finds that $\Delta(T)$ does *not* have the same form as the order-parameter suppression Eq. (A29). We believe this result is incorrect, although the exact origin of the error is not known.

APPENDIX B: SPIN-PEIERLS PHASE

In this appendix, we investigate the possibility of an ordered phase in which all two-spin correlations have the same *sign* as in the NAF phase but with magnitudes for different pairs which break the cubic symmetry.

A phase of this type occurs as the ground state of a one-dimensional nearest-neighbor spin-$\frac{1}{2}$ antiferromagnet coupled to static lattice distortions [Cross and Fisher (1979) and references therein]. The driving mechanism for this state is the tendency of spins to form singlets. Because of this, the magnetic energy of a dimerized chain with exchange alternating between zero and $2J$ is lower than that of a uniform chain with exchange J. The gain in magnetic energy for a small dimerization u yielding alternating exchange $(1+\Gamma u/a)J$ and $(1-\Gamma u/a)J$ is proportional to

$$\left[\frac{\Gamma u}{a}\right]^{4/3}\left[\ln\left[\frac{\Gamma u}{a}\right]\right]^{-1} J$$

(Black and Emery, 1981), while the energy cost of the lattice distortion goes only as $K(u/a)^2$, with K the appropriate elastic constant per atom and a the lattice constant. Thus the chain will dimerize at zero temperature whatever the value of the Gruneisen constant Γ. This effect is known as a spin-Peierls distortion by analogy with the Peierls instability of a one-dimensional metal, and is seen in various quasi-one-dimensional magnetic systems. We note that this effect is entirely quantum mechanical: a classical spin system at zero temperature will gain no energy from a dimerization, unless the exchanges themselves depend nonlinearly on the distortion.

How can the spin-Peierls effect manifest itself in our three-dimensional case of interest? A two-dimensional spin-$\frac{1}{2}$ antiferromagnetic will generally have lower energy per bond than a three-dimensional one because of the greater importance of quantum spin fluctuations in lower dimensions. Thus one should expect that in the presence of a small [100] zone boundary lattice distortion u, the magnetic energy will be lowered more by the increased two-dimensionality of the more strongly coupled pairs of [100] planes than by the loss of energy between different pairs. Unfortunately, this magnetic energy gain in three dimensions will behave only as $(\Gamma u/a)^2 J$, while the phonon energy cost will still be $K(u/a)^2$. It is thus not possible to lower the total energy by a small distortion unless $\eta \equiv \Gamma^2 J/K$ is greater than a number of order unity. If η is large enough, then nonlinear terms in the elastic energy will be needed to stabilize the system. On the other hand, if η is not large, then it is still possible that nonlinear dependence of the exchange constants on u—which at least naively might be more nonlinear than the elastic energy—could cause a lowering of the total energy by a relatively large distortion. We shall call this putative phase the SPNAF for spin-Peierls normal antiferromagnet, *normal* referring to the sign of the spin correlations. Unfortunately, because of the necessity of invoking a nonlinear distortion, it is hard to say much about the properties of this phase except very qualitatively.

First, it is likely that both the transitions from a SPNAF phase to a paramagnetic phase as temperature is increased and to an undistorted canted antiferromagnetic phase as the field is increased, would be strongly first order, as is observed. Second, the spin-wave velocities, which in principle are separately measurable, should be strongly anisotropic with the velocity in the direction parallel to the dimerization considerably smaller than the others. Note that this is the *opposite* sign of the anisotropy from that found in quadratic spin-wave theory for the RDH Hamiltonian: in that case the velocity parallel to the direction $\hat{l}$ is *larger* than the others.

In the classical Néel approximation, the spin correlations will be identical to the NAF phase and, except for a small effect arising from the displacement of the atoms, the dipole anisotropy would vanish for a SPNAF phase at zero temperature. However, the strong quantum fluctuations, which are presumably necessary to drive the SPNAF transition, will result in larger correlations between spins in the more strongly coupled planes than between those in weakly coupled planes, and the dipole energy will be anisotropic with the observed tetragonal symmetry. We can make a rough comparison of the dipolar anisotropy energy

$$\lambda = \tfrac{1}{2}[E_D(\hat{\mathbf{d}}\|\hat{l}) - E_D(\hat{\mathbf{d}}\perp\hat{l})] \tag{B1}$$

for the NAF, u2d2, and SPNAF phases, all of which have ferromagnetic [100] planes by writing, as in Sec. II.A, λ as the sum over the rapidly decreasing contributions from nearby planes. Following the notation of Eqs. (2.26) and (2.27), we have in classical Néel approximation

$$\lambda_{\text{u2d2}} \propto f_0 \tag{B2}$$

and

$$\lambda_{\text{NAF}} \propto f_0 - 2f_1 , \tag{B3}$$

where we have ignored the small terms from planes farther away than nearest neighbor.

For the SPNAF phase, if it exists, it is probably reasonable to assume that the order-parameter correlations fall off much more rapidly across the weak bonds than across the strong ones. If the expectation value of the order parameter is small, then we might be able to neglect the dipolar anisotropy between weakly coupled planes. Then we have simply contributions from each plane and its one strongly coupled neighboring plane

$$\lambda_{\text{SPNAF}} \propto f_0 - f_1 . \tag{B4}$$

Since $\lambda_{\text{NAF}} = 0$, $f_1 \approx \frac{1}{2} f_0$ and hence

$$\lambda_{\text{SPNAF}} \approx \tfrac{1}{2}\lambda_{\text{u2d2}} , \tag{B5}$$

i.e., the naive estimate for the SPNAF dipolar anisotropy is roughly equal to the experimental value of half the Néel estimate for the u2d2 phase. It is probable that the above estimate of λ_{SPNAF} is somewhat too large; however, we note that it would be very difficult to estimate the magnitude of the corrections, even if the effective dimerized spin Hamiltonian were known, because of the strongly quantum nature of the state.

The arguments presented above are very rough and should be treated primarily as plausibility arguments for a SPNAF phase in solid ^{3}He. It is unclear in the absence of a detailed model whether the high-temperature and high-field data could be explained in terms of nearest-neighbor coupling to phonons; probably the hardest to explain would be the near constancy of the magnetization in the high-field phase. One relevant calculation does exist, however; Varma and Nosanow (1970) have argued that the leading correction to the antiferromagnetic Curie-Weiss susceptibility at high temperatures will quite generally be *ferromagnetic* (as apparently observed in the experiments) for nearest-neighbor exchange coupled to phonons.

REFERENCES

Adams, E. D., 1984, private communication.

Adams, E. D., E. A. Schubert, G. E. Haas and D. M. Bakalyar, 1980, Phys. Rev. Lett. **44**, 789.

Anderson, P. W., 1952, Phys. Rev. **86**, 694.

Anderson, P. W., 1984, *Basic Notions of Condensed Matter Physics* (Benjamin, Menlo Park, Calif.)

Andreev, A. F., 1976, Zh. Eksp. Teor. Fiz. Pis'ma Red. **24**, 608 [JETP Lett. **24**, 564 (1976)].

Andreev, A. F., and I. M. Lifshitz, 1969, Zh. Eksp. Teor. Fiz. **56**, 2057 [Sov. Phys.—JETP **29**, 1107 (1969)].

Avilov, V. V., and S. V. Iordansky, 1982, J. Low Temp. Phys. **48**, 241.

Bak, P., and F. B. Rasmussen, 1981, *Proceedings of the 16th International Conference on Low Temperature Physics, LT-16* (Physica B + C **108**, 849).

Bakalyar, D. M., C. V. Britton, E. D. Adams, and Y. C. Huang, 1977, Phys. Lett. A **64**, 208.

Benoit, A., J. Bossy, J. Flouquet, and J. Schweizer, 1985, unpublished.

Bernat, T. P., and H. D. Cohen, 1973, Phys. Rev. A **7**, 1709.

Black, J. L., and V. J. Emery, 1981, Phys. Rev. B **23**, 429.

Brinkman, W. F., and M. C. Cross, 1978, in *Progress in Low Temperature Physics,* edited by D. F. Brewer (North-Holland, Amsterdam), Vol. VIIA, p. 105.

Brinkman, W. F., and T. M. Rice, 1970, Phys. Rev. B **2**, 1324.

Brinkman, W. F., and H. Smith, 1975, Phys. Lett. A **51**, 449.

Buttiker, M., and R. Landauer, 1982, Phys. Rev. Lett. **49**, 1739.

Castles, S. H., and E. D. Adams, 1975, J. Low Temp. Phys. **19**, 397.

Cohen, M. H., and F. Keffer, 1955, Phys. Rev. **99**, 1128.

Cross, M. C., and R. N. Bhatt, 1984, J. Low Temp. Phys. **57**, 573.

Cross, M. C., and R. N. Bhatt, 1985, unpublished.

Cross, M. C., and D. S Fisher, 1979, Phys. Rev. B **19**, 402.

Delrieu, J. M., and N. S. Sullivan, 1981, Phys. Rev. B **23**, 3197.

Devoret, M., A. S. Greenberg, D. Esteve, N. S. Sullivan, and M. Chapellier, 1982, J. Low Temp. Phys. **48**, 495.

Dundon, J. M., and J. M. Goodkind, 1974, Phys. Rev. Lett. **32**, 1343.

Dyson, F. J., 1956a, Phys. Rev. **102**, 1217.

Dyson, F. J., 1956b, Phys. Rev. **102**, 1230.

Feynman, R. P., 1953, Phys. Rev. **91**, 1291.

Fishman, F., 1982, Phys. Lett. A **89**, 203.

Goodkind, J. M., 1983, J. Low Temp. Phys. **52**, 335.

Graham, R., and H. Pleiner, 1976, J. Phys. C **9**, 279.

Greywall, D. S., 1977, Phys. Rev. B **15**, 2604.

Guyer, R. A., 1974, Phys. Rev. A **9**, 1452.

Guyer, R. A., 1978, J. Low Temp. Phys. **30**, 1.

Guyer, R. A., and P. Kumar, 1982, J. Low Temp. Phys. **47**, 321.

Halperin, B. I., and W. M. Saslow, 1977, Phys. Rev. B **16**, 2154.

Halperin, W. P., C. N. Archie, F. B. Rasmussen, R. A. Buhrman, and R. C. Richardson, 1974, Phys. Rev. Lett. **32**, 927.

Halperin, W. P., F. B. Rasmussen, C. N. Archie, and R. C. Richardson, 1978, J. Low Temp. Phys. **31**, 617.

Harris, A. B., D. Kumar, B. I. Halperin, and P. C. Hohenberg, 1971, Phys. Rev. B **3**, 961.

Hata, T., S. Yamasaki, Y. Tameka, and T. Shigi, 1981, *Proceedings of the 16th International Conference on Low Temperature Physics, LT-16* (Physica B + C **107**, 201).

Hata, T., S. Yamasaki, M. Taneda, T. Kodama, and T. Shigi, 1983, Phys. Rev. Lett. **51**, 1573.

Herring, C., 1962, Rev. Mod. Phys. **34**, 631.

Herring, C., 1966, in *Magnetism,* edited by C. I. Rado and H. Suhl (Academic, London), Vol. IIB, Chap. 1.

Hetherington, J. H., and H. L. Stipdonk, 1985, Phys. Rev. B **31**, 4684.

Holstein, T., and H. Primakoff, 1940, Phys. Rev. **58**, 1098.

Hu, C-R., and T. E. Ham, 1981, Phys. Rev. B **24**, 2478.

Iwahashi, K., and Y. Masuda, 1981, J. Phys. Soc. Jpn. **50**, 2508.

Iwahashi, K., and Y. Masuda, 1983, J. Magn. Magn. Mater. **31**, 733.

Johnson, R. T., and T. C. Wheatley, 1970, Phys. Rev. A **1**, 1836.

Kalos, M. H., D. Levesque, and L. Verlet, 1974, Phys. Rev. A **9**, 2178.

Kirk, W. P., 1983, private communication.

Kirk, W. P., and E. D. Adams, 1971, Phys. Rev. Lett. **27**, 392.

Kirk, W. P., Z. Olejniczak, P. S. Kobiela, and A. A. V. Gibson, 1984, in *Proceedings of the 17th International Conference on Low Temperature Physics, LT-17,* edited by U. Eckern, A. Schmid, W. Weber, and H. Wühl (North-Holland, Amsterdam), p. 273.

Kirk, W. P., Z. Olejniczak, P. S. Kobiela, A. A. V. Gibson, and A. Czermak, 1983, Phys. Rev. Lett. **51**, 2128.

Kirk, W. P., E. B. Osgood, and M. Garber, 1969, Phys. Rev. Lett. **23**, 833.

Kittel, C., 1971, *Introduction to Solid State Physics,* 3rd ed. (Wiley, New York).

Kubo, R., 1952, Phys. Rev. **87**, 568.

Kummer, R. B., E. D. Adams, W. P. Kirk, A. D. Greenberg, R. M. Mueller, C. V. Britton, and D. M. Lee, 1975, Phys. Rev. Lett. **34**, 517.

Lieb, E. H., and D. S. Fisher, 1981, unpublished.

Maleev, S. V., 1957, Zh. Eksp. Teor. Fiz. **33**, 1010 [Sov. Phys.—JETP **6**, 776 (1958)].

Mamiya, T., A. Sawada, H. Fukuyama, Y. Hirao, and Y. Masuda, 1981, *Proceedings of the 16th International Conference on Low Temperature Physics, LT-16* (Physica B + C **108**, 847).

McMahan, A. K., 1972, J. Low Temp. Phys. **8**, 115.

McMahan, A. K., and J. W. Wilkins, 1975, Phys. Rev. Lett. **35**, 376.

Montambaux, G., M. Heritier, and P. Lederer, 1982, J. Low Temp. Phys. **47**, 39.

Morii, Y., K. Ichikawa, T. Hata, C. Kanamori, H. Hokamoto, T. Kodama, and T. Shigi, 1978, in *Physics of Ultralow Temperatures,* edited by T. Sugawara (Physical Society of Japan, Kyoto), p. 196.

Nagaoka, Y., 1966, Phys. Rev. **147**, 392.

Osheroff, D. D., 1982, *Proceedings of the 16th International Conference on Low Temperature Physics, LT-16* (Physica B + C **109-110**, 1461).

Osheroff, D. D., 1985, private communication.

Osheroff, D. D., M. C. Cross, and D. S. Fisher, 1980, Phys. Rev. Lett. **44**, 792.

Osheroff, D. D., and C. Yu, 1980, Phys. Lett. A **77**, 458.

Panczyk, M. F., and E. D. Adams, 1970, Phys. Rev. A **1**, 1356.

Prewitt, T. C., and J. M. Goodkind, 1977, Phys. Rev. Lett. **39**, 1283.

Prewitt, T. C., and J. M. Goodkind, 1980, Phys. Rev. Lett. **44**, 1699.

Roger, M., 1984, Phys. Rev. B **30**, 6432.

Roger, M., and J. M. Delrieu, 1981, *Proceedings of the 16th International Conference on Low Temperature Physics, LT-16* (Physica B + C **108**, 857).

Roger, M., J. M. Delrieu, and J. H. Hetherington, 1980a, Phys. Rev. Lett. **45**, 137.

Roger, M., J. M. Delrieu, and J. H. Hetherington, 1980b, J. Phys. (Paris) Lett. **41**, L139.

Roger, M., J. H. Hetherington, and J. M. Delrieu, 1983, Rev. Mod. Phys. **55**, 1.

Shigi, T., T. Hata, S. Yamasaki, and T. Kodama, 1983, *Quantum Fluids and Solids—1983 (Sanibel Island, Florida),* edited by E. D. Adams and G. G. Ihas (AIP, New York), p. 47.

Sites, J. R., D. D. Osheroff, R. C. Richardson, and D. M. Lee, 1969, Phys. Rev. Lett. **23**, 836.

Thouless, D. J., 1965, Proc. Phys. Soc. London **86**, 893.

Uhlig, K., E. D. Adams, G. E. Haas, R. Rosenbaum, Y. Morii, and S. F. Kral, 1984, in *Proceedings of the 17th International Conference on Low Temperature Physics, LT-17,* edited by U. Eckern, A. Schmid, W. Weber, and H. Wühl (North-Holland, Amsterdam), p. 279; and private communication from E. D. Adams.

Usagawa, T., 1982, J. Low Temp. Phys. **49**, 43.

Van Degrift, C. T., W. T. Bowers, P. B. Pipes, and D. F. McQueeny, 1982, Phys. Rev. Lett. **49**, 149.

Varma, C. M., 1970, Phys. Rev. Lett. **24**, 203.

Varma, C. M. and L. H. Nosanow, 1970, Phys. Rev. A **1**, 133.

Varma, C. M., and N. R. Werthamer, 1976, in *The Physics of Liquid and Solid Helium, Part 1,* edited by K. H. Benneman and J. B. Ketterson (Wiley, New York), p. 503.

Yosida, K., 1980, Prog. Theor. Phys. Suppl. **69**, 475.